ESSAYS ON OPTIMAL REINSURANCE DESIGN, SOLVENCY ANALYSIS OF DEFERRED ANNUITIES AND PENSION BUY-OUTS

Khadija Gasimova

A thesis submitted in fulfilment of the requirements

for the degree of

Doctor of Philosophy

CASS
BUSINESS SCHOOL
CITY, UNIVERSITY OF LONDON
EST 1894

Supervisors: Prof. Steven Haberman

Dr. Pietro Millossovich

Faculty of Actuarial Science and Insurance

City, University of London

London, United Kingdom

2021

Acknowledgements

First and foremost, I would like to thank my supervisors Professor Steven Haberman and Dr. Pietro Millossovich for their constant support throughout these years and for their patience in overcoming obstacles I have been facing through my research.

I am thankful to Professor Vali Asimit for his contribution to the first chapter of my thesis.

Finally, I am deeply indebted to my parents, Nazim and Sakina, my sister, Jamila and my husband, Samir, for their love and support.

Declaration

I hereby grant powers of discretion to the University Librarian of the Business School, City, University of London, to allow the thesis to be copied in whole or in part without further reference to the author.

Khadija Gasimova

Dedicated to the memory of my loving father ...

Abstract

This thesis is a collection of three essays on optimal reinsurance design, solvency analysis of deferred annuities and pension buy-outs. Two approaches to the optimal reinsurance strategy are investigated in the first essay. First approach demonstrates an optimal reinsurance model from insurer's viewpoint whereas the second approach discusses an optimal reinsurance model using Pareto optimality principle. Depending on how the reinsurance premium is calculated, several optimal reinsurance problems are formulated for the first and second approaches and Second Order Conic Programming is applied to solve them. The second essay analyses the effect of stochastic mortality and interest rates in the solvency analysis of a portfolio of simple deferred annuity contracts and compares the results for deterministic and stochastic models. The analysis consist of three risk scenarios: the benchmark case where mortality rates and interest rates are both deterministic, the second case where only mortality rates are stochastic and the last case where mortality rates and interest rates are both stochastic. The third essay evaluates model risk associated with pricing pension buy-outs using different stochastic mortality models. We use numerical examples to demonstrate that changes in various model parameters have a significant effect in the pricing of pension-buyouts.

Contents

List of Figures

List of Tables

Chapter 1

Introduction

An effective reinsurance strategy is critical for managing and mitigating an insurer's risk exposure. Insurers purchase reinsurance contracts to protect themselves from large losses. Reinsurers receive premiums from the insurers and earn profits by undertaking risks. Optimal reinsurance strategy enables risks of loss to be spread more widely across companies, limit liability on a specific risk, stabilize loss experience, and to protect against catastrophic events. Therefore, reinsurance helps insurance companies to restrict the loss in their balance sheets helps them to stay solvent. Without reinsurance insurers would have been unable to accept a risk beyond their financial strength or resources for that class of business. Consequently, insurers' service to the public would also have been limited. For this reason, the insurance industry and academia are constantly researching optimal reinsurance strategies. Many optimal reinsurance models have been proposed so far and in chapter 2 we discuss some of them and suggest some new approaches to this problem. Two main approaches to the optimal reinsurance strategy are investigated in the chapter 2. Risk margins for these purposes are defined based on the principles of the Solvency II regulations, which developed a methodology applied to all insurance and reinsurance companies described in Quantitative Impact Studies (QIS 5) (see QIS [2010]) Solvency II determines quantitative requirements, such as the rules to value assets and liabilities (in particular, technical provisions), to calculate capital requirements and to identify eligible own funds to cover those requirements. Capital requirements are determined on the basis of a 99.5% value-at-risk measure over one year and depend on diversification between different sources of risk.

The first approach to the optimal reinsurance strategy demonstrates an optimal reinsurance model from the point of view of an insurer who wants to minimise the sum of its technical provisions and reinsurance premium. The second approach discusses an optimal reinsurance model using Pareto optimality principle and aims to minimise the single-objective optimisation function of the liabilities of insurer and reinsurer. The number of claims in both methods is assumed to be random and individual claims are mutually independent. Our optimisation problem is an infinite dimensional problem and a standard solution is to assume that all random variables are discrete, which reduces the infinite dimensional problem to a finite dimensional optimisation problem. This can be achieved by sampling from a parametric risk model or from claim history if it is available to the decision-maker. The resulting optimisation models are convex and Second Order Conic Programming is applied to solve them. Numerical examples demonstrate that different types of reinsurance models are optimal under expected value and standard deviation premium principle. Namely, quota-share reinsurance appears to be optimal for expected value premium principle and capped stop loss reinsurance is optimal when standard deviation premium principle is in place.

Annuity products are used as protection from longevity risk, providing minimum guaranteed income for policyholders and reducing the risk of outliving their retirement assets. Insurers and regulators, therefore, try to better understand solvency characteristics of annuity products due to the fact that systematic longevity risk substantially affects annuity providers' solvency. While solvency characteristics of immediate life annuities have been studied thoroughly, the role of deferred annuity liabilities in the portfolios of annuity providers has not been widely discussed in the literature. Chapter 3 estimates the importance and effect of stochastic mortality rates in the solvency analysis of a portfolio of simple deferred annuity contracts comparing the results for deterministic and stochastic mortality models. Moreover, we conduct a solvency analysis assuming a stochastic model for the interest rates and estimate the combined effect of stochastic mortality and interest rates for solvency analysis. Our analysis contains three risk scenarios: the benchmark case where mortality rates and interest rates are both deterministic, the second case where only mortality rates are stochastic and the last case where mortality rates and interest rates are both stochastic. The results demonstrate the dramatic importance of the mortality models on evaluation of solvency margins for life annuities and the fact that model risk is a prevalent issue when forecasting solvency margins. This also has significant effect on the increase of solvency margins depending on deferred periods which is caused by the extra longevity risk and the greater uncertainty about numbers of future survivors.

Pension buy-ins and buy-outs are tools used by defined benefit pension schemes for buying bulk annuities from insurance companies. Buy-outs and buy-ins transfer some or all of the longevity and investment risk of a pension scheme to an insurance company and cover a subset of the liabilities allowing partial de-risking. The financial crisis in 2007 - 2009 and the subsequent reduction in discount rates and the continuing increases in life expectancy have led to substantially increased deficits of the pension funds. Nowadays pension schemes increasingly hold buy-in and buy-out products as part of their de-risking plan which is driven by pension deficits due to market downturns, low interest rate environments, increased life expectancy of retirees and new pension accounting standards. In response to these challenges and in order to off-load risks capital markets have developed solutions for defined benefit pensions plans such as pension buy-ins and pension buy-outs. According to LCP [2020], 2019 was a record-breaking year for pension buy-out and buy-in deals , with both transaction sizes and volumes sizes increasing dramatically. The total value of transactions completed exceeded £43.8 billions. There were five transactions over £3 billions in 2019 compared with only one such transaction ever occurring in prior years. For example, in September 2019, the Allied Domecq Pension Fund completed a £3.8 billions buy-in covering over 27000 members, including 10000 deferred pensioners. Another example is Legal & General completing a £4.6 billion pounds partial buy-out with the Rolls-Royce UK Pension Fund in June 2019. According to LCP [2020], the largest transaction in 2018 was £4.4 billion British Airways Pensioner buy-in contact. LCP [2020] discusses how the buy-in and buy-out market has performed in 2020, which has been one of the most challenging periods of market volatility on record and conclude that the buy-in market has been remarkably resilient. The survey looks at the proportion of transactions that have been paused in the wake of the Covid-19 crisis and the impact on target volumes for the year and conclusion was that significant activity has continued throughout the crisis, and lockdowns did not impact the ability of the insurers to operate or to write transactions. 2019 is the most recent year for which data for buy-ins and buy-outs is available in the report, but LCP estimated that buy-in and buy-out volumes will be £20bn−£25bn in 2020 making it one of the busiest years ever. Conversion of longevity swaps to buy-ins has become an established model and over 20% of longevity swaps have been successfully converted to buy-ins up to date. 2020 has also provided opportunities for small schemes to de-risk with a 25% increase in transactions. The main difference between pension buy-outs and pension buy-ins arises from credit risk. By using pension buy-outs firms sponsoring defined benefit pension plans can take pension liabilities off balance sheets and can eliminate counter-party risk. However,in the case of pension buy-ins the obligations of buy-in insurers are usually not fully collateralised and guaranteed by third parties, and therefore credit risk arises.

In chapter 4 we choose different stochastic mortality models to be representative of different model types and conduct sensitivity analysis in order to evaluate model risk associated with pricing pension buy-outs. Calculation of the s-year survival probabilities associated with using these models involves calculation of conditional expectations that usually have no closed form. When we simulate the probability out to some future horizon period T, we then need to obtain the future time-T probabilities and annuity values contingent on the value of the state variables at time T. If stochastic simulation is applied to solve this, we will need to implement ”simulations within simulations”, i.e. nested simulations. To avoid nested simulations technique which is computationally expensive we use the methods proposed by Cairns [2011] and we extend it to Lee-Carter and Plat stochastic mortality models. This pricing framework is then used to determine the prices of the pension buy-outs and assess sensitivity of buyout premiums to choice of stochastic mortality model. We use the method described by Lin et al. [2017b] for assessing the longevity risk premium of a buy-out bulk annuity and the risk-neutral price of the buy-outs. Our sensitivity analysis and numerical examples illustrate that changes in the various parameters have a significant effect in the pricing of pension-buyouts.

Chapter 5 summarises the thesis and discusses potential future research work.

Chapter 2

Optimal reinsurance for the classical risk model

2.1 Introduction

An appropriate reinsurance strategy is an effective tool for managing and mitigating an insurer's risk exposure. Therefore, practitioners and academics are constantly looking for optimal reinsurance strategies. Different optimal reinsurance models have been proposed and we discuss some of them in this chapter. Some models are based on optimal criterion and derive an optimal reinsurance strategy from the point of view of insurer under such criterion. Therefore, the insurer is the active part whereas the reinsurer is the passive counterpart in these models. Even if such optimal reinsurance treaty is not available in the market, these insurer-oriented type models can be a good guideline for the insurer. Another category of models discusses an optimal reinsurance from the reinsurer's point of view under a certain optimal criterion. Also, some authors attempted to construct optimal models by combining different reinsurance strategies, which is also very informative.

The first studies of optimal reinsurance were conducted by Borch [1960] and Arrow

[1963] and they caused great interest in this field. Borch [1960] proved that the stop-loss reinsurance is optimal, by minimising the variance of insurer's loss and making an assumption that the reinsurance premium is calculated using expected value of reinsurer's losses. Arrow [1963] demonstrated that a stop-loss reinsurance is optimal by maximising the expected utility of insurer's final wealth and also computed the reinsurer's premium using the expected value principle. These classical works have been then extended to models with default risks or to multiple-risk models. Dayananda [1970] discusses development of "risk theory" which led to research concerning the probability of 'ruin' of an insurance company. Hesselager [1990] discusses optimal reinsurance structures when the ceding insurer, and the reinsurer, seek to minimize the probability of eventual ruin. Cai and Weng [2016] constructed optimal reinsurance portfolio from the insurer's perspective using sum of actuarial reserves and risk margins to define the risk exposure of the insurer. To measure the risk margins expectile function was used in the latter paper. Chi and Meng [2014] investigated optimal reinsurance model with multiple reinsurers. Cai et al. [2008], Cheung et al. [2014], Chi and Tan [2011] and Lu et al. [2014] used VaR and conditional VaR as risk measures. Guerra and Centeno [2008] show that excess of loss reinsurance is not the optimal form of reinsurance if the premium loadings of the reinsurer are not proportional to the expected ceded claims; it also explored the relationship between maximising the expected utility of wealth and maximising the adjustment coefficient. Kaluszka [2004] demonstrates that both stop loss and quota share models can be optimal depending on different assumptions for the constraints. Centeno and Guerra [2010] further extended the results of Guerra and Centeno [2008] to the case where number of risks in the portfolio are dependent. Asimit et al. [2013], Bernard and Ludkovski [2012] and Biffis and Millossovich [2012] created optimisation models where the counterparty default risk is taken into account. An empirical approach to optimal reinsurance design was investigated by Tan and Weng [2014]. More extensions of optimisation models were developed depending on different decision criteria, such as Verlaak and Beirlant [2003], Kaluszka and Okolewski [2008], Ludkovski and Young [2009] etc.

The aim of this chapter is to introduce two approaches to optimal reinsurance modelling taking into account randomness of the number of claims. First approach investigates optimal reinsurance model from insurer's point of view depending on how risk measure corresponding to reinsurance premium is calculated. We define risk margins based on principles of Solvency II regulations, which developed a methodology applied to all insurance and reinsurance companies in the European Union. Quantitative Impact Studies (QIS 5) (see QIS [2010]) determines the principles and calculation basics for implementation of Solvency II. The second approach demonstrates Pareto optimal reinsurance model based on different risk measure calculation principles. Borch [1962] investigated Pareto optimal risk sharing in a reinsurance market, but monotonicity condition of the utility function was omitted in this work. DuMouchel [1968] extended Pareto optimal risk sharing model, adding the condition of monotonicity of the utility function. With the introduction of coherent and convex risk measures by Artzner et al. [1999] further analysis of the problem of optimal sharing and allocation of risk developed. Using Pareto optimality principle and coherent and convex risk measures, Barrieu and El Karoui [2005] developed a methodology to minimise the risk of the issuer under the constraint established by a buyer who enters the transaction only if his risk level remains below a given threshold. Acciaio and Svindland [2009] study the existence of Pareto optimal risk allocations for the agents with different (subjective) reference probability measures. We introduce a coherent risk measure in this chapter to construct Pareto optimal reinsurance model applied to aggregate losses and assuming random number of claims. Zeng and Luo [2013] apply stochastic control theory to Pareto-optimal reinsurance games. By maximising a weighted sum of two utilities which is an arithmetic Brownian motion they demonstrate that the Pareto-optimal contracts can be classified into either proportional/quota-share functions or excess of loss functions based on standard deviation or expected value premium principles respectively. Our numerical results show that proportional reinsurance is optimal when reinsurance premium is calculated under expected value principle and the objective is to minimise the sum of technical provisions under Solvency II and resinurance premium. On the other hand, when standard deviation principle is in place, optimality in our model is obtained when reinsurance model gets the form functional form $\sum R = \sum X \wedge c$, where c is a constant, X is loss amount and R is loss of the reinsurer. This can be considered a special case of capped stop loss reinsurance. Same applies when one-sided moments introduced by Fischer [2003] are used to calculate reinsurance premium.

This chapter is organised as follows: Section 4.2 describes the main functions that are used in this chapter to build optimal resinurance models, i.e. risk margins, risk measures etc. Section 2.3 describes the process of constructing of optimal reinsurance models and is divided into two parts. The first subsection discusses an optimal reinsurance model from insurer's viewpoint, whereas the second subsection demonstrates an optimal reinsurance model using Pareto optimality principle. Section 2.4 provides numerical illustrations related to the optimisation models in the section 2.3. Section 2.5 concludes this chapter. The proofs of the propositions from the Section 2.3 are relegated to Section 2.6.

2.2 Background

The current section determines risk margins, risk measures and other functions that are needed to construct optimal reinsurance models for the purposes of this chapter.

Different methods have been proposed in the literature to determine the risk margin. For the purposes of this thesis we define risk margin based on Solvency II principles. Let X be a generic random risk X that is paid in full by an insurer, i.e. net of reinsurance. According to the QIS5 specifications, the *Risk Margin*(RM) for the *Underwriting Risk*

(UwR) is given by

$$RM_{UwR}(X) := g\Big(a_1 \cdot P_{net}, b_1 \cdot \mathbb{E}(X)\Big), \tag{2.1}$$

where P_{net} is the net premium retained by the insurer. In addition, $g(x,y) := \sqrt{x^2+y^2+xy}$,

$$\begin{aligned} a_1 &:= \delta\left(\frac{\exp\left\{\Phi^{-1}(p)\sqrt{\log(1+\sigma^2_{PR})}\right\}}{\sqrt{1+\sigma^2_{PR}}} - 1\right) \\ b_1 &:= \delta\left(\frac{\exp\left\{\Phi^{-1}(p)\sqrt{\log(1+\sigma^2_{RR})}\right\}}{\sqrt{1+\sigma^2_{RR}}} - 1\right). \end{aligned} \tag{2.2}$$

Moreover, $p = 99.5\%$, $\Phi^{-1}(\cdot)$ is the quantile function of the standard Normal distribution and δ is the adjusted Cost-of-Capital-rate. Note that σ^2_{PR} and σ^2_{RR} are standard deviations for the premium risk (PR) and reserve risk (RR) respectively. The QIS5 recommendations have shown that σ_{PR} and σ_{RR} estimates are within $(5\%, 21.5\%)$.

The next source of risk is the *Unavoidable Market Risk*, for which the corresponding RM is given by

$$RM_{UMR}(X) := c \cdot \mathbb{E}(X), \tag{2.3}$$

where $c = CoC \times (d-n)(d-n+1)\Delta_n$ and CoC is the Cost-of-Capital rate and d is the modified duration of the insurer's net liability. In addition, n represents the longest duration of available risk-free financial instruments to cover X, and Δ_n is the absolute decrease of the risk-free interest for maturity n under the downward stress scenario of the interest rate risk sub-module.

Now, assume that in fact the random risk $X = X_I + X_R$ is shared between the insurer and one reinsurer, where X_I and X_R are the amounts paid in full by the insurer and reinsurer, respectively. Consequently, the RM corresponding to another source of risk, namely *Counterparty Default Risk*, is measured as follows

$$RM_{CDR}\left(X_R\right) := g\left(a_2 \cdot P_{Reins}, b_2 \cdot \mathbb{E}(X_R)\right), \tag{2.4}$$

where P_{Reins} is the reinsurance premium. In addition,

$$a_2 := \delta(1 - RecR)l\sqrt{q(1-q)} \times \left(\frac{\Phi\Big(\sqrt{\log(1+\sigma_{PR}^2)} - \Phi^{-1}(p)\Big)}{1-p} - \frac{\exp\Big\{\Phi^{-1}(p)\sqrt{\log(1+\sigma_{PR}^2)}\Big\}}{\sqrt{1+\sigma_{PR}^2}} \right) \tag{2.5}$$

and

$$b_2 := \delta(1 - RecR)l\sqrt{q(1-q)} \times \left(\frac{\Phi\Big(\sqrt{\log(1+\sigma_{RR}^2)} - \Phi^{-1}(p)\Big)}{1-p} - \frac{\exp\Big\{\Phi^{-1}(p)\sqrt{\log(1+\sigma_{RR}^2)}\Big\}}{\sqrt{1+\sigma_{RR}^2}} \right). \tag{2.6}$$

where q and $RecR$ are the reinsurer's one-year probability of default and recovery rate, respectively, and l is a constant and usually, $3 < l < 5$.

To assess insurer's risk exposure we use risk margins of the insurer and expected value of its losses. As mentioned above, such a risk margin-based approach is justified by Solvency II regulations. Moreover, reinsurance optimisation in this chapter is applied to independent and identically distributed claims.

Let us assume that the claim amounts $X_i, i = 1, 2, \ldots$ are non-negative independent and identically distributed (i.i.d.) random variables and the number of claims N arising in one period is random. The reinsurer agrees to pay $R[X_i]$, the amount by which the entire loss exceeds the insurer's amount, $I[X_i]$, and therefore $I[X_i] + R[X_i] = X_i$. The functions $I(\cdot)$ and $R(\cdot)$ are called the retained loss function and ceded loss function, respectively. To prevent moral hazard in a reinsurance contract, both $I(\cdot)$ and $R(\cdot)$ are assumed to be non-decreasing and therefore, Lipschitz continuous and we have that

$$I, R \in \mathcal{F} := \Big\{ f : 0 \le f(x) \le x \;\text{ and }\; x - f(x) \;\text{ are non-decreasing functions} \Big\} \tag{2.7}$$

For practical prospectives, our risk model assumes that actual number of risks is random, as explained earlier, and the insurer's risk includes its reserves (expected claim payments and their variability that is measured by the risk margins) and the reinsurance premium. Specifically, the insurer measures the "common" risk, known as the *best estimate*, as $(1 + \rho_1)\mathbb{E}(\cdot)$ and it can be seen as an insurer's cost to set up the reserves in normal circumstances with ρ_1 being marginal cost per risk exposure. According to QIS5 best estimate can be calculated either net or gross of reinsurance. For the purposes of this chapter we calculate it net of reinsurance. Moreover, the reinsurer premium, denoted as π, is charged for the entire risk portfolio ans should be less than P, the premium charged by the insurer. Therefore, one needs to make further assumptions. There is a variety of risk-based premium calculations, but two common *premium principles* known in practice are:

i) *Expected value principle:* $\pi(\cdot) = (1 + \lambda)\mathbb{E}(\cdot)$;

ii) *Standard deviation principle:* $\pi(\cdot) = \mathbb{E}(\cdot) + \lambda \operatorname{Sd}(\cdot)$.

Moreover, we demonstrate Pareto optimal models using parametric class of non-comonotone coherent risk measures that are not comonotone from Fischer [2003]

$$\pi(\cdot; e, d) = \mathbb{E}(\cdot) + e\bigg(\mathbb{E}\left(\cdot - \mathbb{E}(\cdot)\right)_+^d\bigg)^{1/d} \quad \text{with} \quad 0 \leq e \leq 1,\ 1 \leq d \leq \infty, \tag{2.8}$$

where, $x_+ = max(x, 0)$, therefore the above formula represents the right-end point of the sample space.

2.3 Main results

This section discusses the main optimisation models for the purposes of this chapter. It is divided into two parts. The first subsection demonstrates an optimal reinsurance model from insurer's point of view, while the second subsection analyses an optimal reinsurance strategies using Pareto optimality principle.

2.3.1 Optimal reinsurance model from insurer's viewpoint

The current subsection demonstrates the scope of optimal reinsurance from insurer's point of view. In this case our aim is to minimise the insurer's liabilities and reinsurance premium. In other words, we need to minimise the sum of risk margins, best estimate and reinsurance premium. Considering all the mentioned in the previous section, a plausible optimisation problem can be formulated as follows:

$$\min_{(I,R)\in\mathcal{F}} H(I,R), \quad \text{where} \tag{2.9}$$

$$\begin{aligned} H(I,R) \quad &:= \quad RM_{UwR}\left(I\sum_{i=1}^{N}X_i\right) + RM_{UMR}\left(I\sum_{i=1}^{N}X_i\right) + RM_{CDR}\left(R\sum_{i=1}^{N}X_i\right) \\ &\quad +(1+\rho_1)\mathbb{E}\left(I\sum_{i=1}^{N}X_i\right) + \pi\left(R\sum_{i=1}^{N}X_i\right), \\ &= \quad g\left(a_1\left(P-\pi\left(R\sum_{i=1}^{N}X_i\right)\right), b_1\cdot\mathbb{E}\left(I\sum_{i=1}^{N}X_i\right)\right) + (1+\rho_1+c_1)\cdot\mathbb{E}\left(I\sum_{i=1}^{N}X_i\right) \\ &\quad +g\left(a_2\cdot\pi\left(R\sum_{i=1}^{N}X_i\right), b_2\cdot\mathbb{E}\left(R\sum_{i=1}^{N}X_i\right)\right) + \pi\left(R\sum_{i=1}^{N}X_i\right). \end{aligned} \tag{2.10}$$

Clearly, we need to ensure that the insurer premium P is larger than the reinsurer's charges and therefore, our optimisation problem is now given by

$$\min_{(I,R)\in\mathcal{F}} H(I,R), \quad \text{s.t.} \quad \pi\left(R\sum_{i=1}^{N}X_i\right) \le P \quad \text{and} \quad I(\cdot)+R(\cdot)=\cdot, \tag{2.11}$$

which is the main aim of this subsection.

The optimisation problem displayed in (2.11) is an infinite dimensional problem due to the function variable R, which is a very difficult problem to solve. A standard solution is to assume that all random variables are discrete, which reduces to solving a finite dimensional optimisation problem. This can be achieved by sampling from a parametric risk model or from claim history if it is available to the decision-maker. That is, let $(n_1, n_2, \ldots, n_m)$ be the "observed" number of claims sample. For each scenario, the claim sizes are $\mathbf{x}_k = (x_{k1}, x_{k2}, \ldots, x_{kr})^T$, where $1 \le k \le m$ and $r := \max\{n_k,\ 1 \le k \le m\}$.

Note that $x_{ki} = 0$ for all $n_k \leq i \leq r$ and we make this choice in order to make our numerical implementations possible. If one needs to sample from a parametric model, then the threshold r is chosen such that $\Pr(N > r)$ is very small. Further, a claim size sample $\mathbf{t}_k = (t_{k1}, t_{k2}, \ldots, t_{kr})^T$ is drawn for the k^{th} scenario and the actual claim size sample becomes $\mathbf{x}_k = (x_{k1}, x_{k2}, \ldots, x_{kr})^T$ with $x_{ki} = t_{ki} I_{i \leq n_k}$ for all $1 \leq i \leq r$, where by definition, 1_A represents the indicator operator corresponding to set A that equals to 1 if A is true and 0 otherwise.

Next, a portion of each loss x_{ki} is paid by the reinsurance company, denoted as z_{ki}, while the remaining amount $y_{ki} := x_{ki} - z_{ki}$ is paid by the insurance company. Consequently, the decision variables in (2.11) are now given by $2r \times m$ decision variables, $\mathbf{Y} = \Big(\mathbf{y}_1, \mathbf{y}_2, \ldots, \mathbf{y}_m\Big)$ and $\mathbf{Z} = \Big(\mathbf{z}_1, \ldots, \mathbf{z}_m\Big)$. The moral hazard constraints are replaced by

$$\mathbf{A}\mathbf{y}_k \leq \mathbf{A}\mathbf{x}_k, \quad \mathbf{A}\mathbf{z}_k \leq \mathbf{A}\mathbf{x}_k \;\text{ and }\; \mathbf{y}_k + \mathbf{z}_k = \mathbf{x}_k \;\text{ for all }\; 1 \leq k \leq m, \tag{2.12}$$

where the $r \times r$ matrix $\mathbf{A}$ is given by

$$\begin{pmatrix} 1 & 0 & \ldots & 0 \\ -1 & 1 & \ldots & 0 \\ & \ddots & \ddots & \\ 0 & 0 & \ldots & 1 \end{pmatrix}. \tag{2.13}$$

Finally, the RMs and reinsurer's premium in (2.11) are replaced by their sample estimators. The reinsurance premium based on the Expected value principle and the given sample becomes

$$\frac{1+\lambda}{m} \sum_{k=1}^{m} \mathbf{1}^T \mathbf{z}_k = \frac{1+\lambda}{m} \mathbf{1}^T \Big(\mathbf{1}^T \mathbf{z}_1, \ldots, \mathbf{1}^T \mathbf{z}_m\Big), \tag{2.14}$$

where $\mathbf{1}$ is a column vector of ones. For the second case where the Standard deviation principle is used for premium calculations, the reinsurance premium is given by

$$\frac{1}{m} \mathbf{1}^T \Big(\mathbf{1}^T \mathbf{z}_1, \ldots, \mathbf{1}^T \mathbf{z}_m\Big) + \lambda \frac{\Big\| \mathbf{Q}\Big(\mathbf{1}^T \mathbf{z}_1, \ldots, \mathbf{1}^T \mathbf{z}_m\Big) \Big\|}{\sqrt{m-1}}, \tag{2.15}$$

where the matrix $\mathbf{Q}$ is defined as

$$\begin{pmatrix} 1-\frac{1}{m} & -\frac{1}{m} & \dots & -\frac{1}{m} \\ -\frac{1}{m} & 1-\frac{1}{m} & \dots & -\frac{1}{m} \\ \vdots & \vdots & \ddots & \vdots \\ -\frac{1}{m} & -\frac{1}{m} & \dots & 1-\frac{1}{m} \end{pmatrix} \tag{2.16}$$

and $\|\cdot\|$ represents the *Euclidean distance*, i.e. $\|\mathbf{x}\| := \left(\sum_{i=1}^{n} x_i^2\right)^{1/2}$. Recall that for larger sample, one may use the biased estimator, i.e. divide by m instead of $m-1$ in the standard deviation estimator (for details, see Asimit et al. [2018])

We are now ready to state the first finite dimensional optimisation problem where the Expected value principle is in place.

Problem 2.3.1 *Assume that the optimisation problem from* (2.11) *is defined under the Expected value principle assumption, i.e.* $\pi(\cdot) = (1+\lambda)\mathbb{E}(\cdot)$. *Therefore, the following has to be solved:*

$$\begin{aligned} \min_{\substack{(\boldsymbol{Y},\boldsymbol{Z})\in \\ \Re^{r\times m}\times\Re^{r\times m}}} \quad & \left\{ g\left(a_1 P - \frac{a_1(1+\lambda)}{m} \sum_{k=1}^{m} \boldsymbol{1}^T \boldsymbol{z}_k, \frac{b_1}{m} \sum_{k=1}^{m} \boldsymbol{1}^T \boldsymbol{y}_k \right) + c_3 \sum_{k=1}^{m} \boldsymbol{1}^T \boldsymbol{y}_k \right\} \\ s.t. \quad & \frac{1+\lambda}{m} \sum_{k=1}^{m} \boldsymbol{1}^T \boldsymbol{z}_k \leq P, \\ & \boldsymbol{A}\boldsymbol{y}_k \leq \boldsymbol{A}\boldsymbol{x}_k,\ \boldsymbol{A}\boldsymbol{z}_k \leq \boldsymbol{A}\boldsymbol{x}_k,\ \boldsymbol{y}_k + \boldsymbol{z}_k = \boldsymbol{x}_k \ \ \textit{for all}\ \ 1 \leq k \leq m, \end{aligned} \tag{2.17}$$

where $c_3 := \Big(\rho_1 + c_1 - \lambda - g\big(a_2(1+\lambda), b_2\big)\Big)/m$.

Recall that Problem 2.3.1 is a non-linear and convex optimisation problem that is almost linear, except of the terms that involve the g function. Various algorithms are available for solving such problems and some algorithms are more efficient than others. The non-linearity is a big issue, but some formulation are efficiently solved even for high dimensional problems. For example, it is well-known that *Second Order Conic Programming* (SOCP) type problems are implementable in fairly large dimensions. Specifically, computations are possible if the number of decision variables is very large, even for a couple of millions. The SOCP-type problems have the following representation

$$\min_{\mathbf{x}} \left\{ \mathbf{a}_1^T \mathbf{x} \right\} \quad \text{s.t.} \;\; \|\mathbf{B}_l \mathbf{x} + \mathbf{b}_l\| \le \mathbf{c}_l^T \mathbf{x} + \mathbf{d}_l, \; l = 1, \ldots, L, \;\; \mathbf{B}\mathbf{x} = \mathbf{a}_2, \tag{2.18}$$

where $\mathbf{B}$ and $\mathbf{B}_l$ ($\mathbf{a}_1$, $\mathbf{a}_2$, $\mathbf{b}_l$, $\mathbf{c}_l$ and $\mathbf{c}_l$) are matrices (column vectors) of appropriate dimensions. We are now able to show that the instance displayed in (2.17) is SOCP representable as given in Proposition 2.3.1 and its proof is relegated to Section 2.6.

Proposition 2.3.1 *The Problem 2.3.1 is solved by the following SOCP:*

$$\begin{aligned}
\min_{\substack{(\boldsymbol{Y},\boldsymbol{Z},u)\in\\ \Re^{r\times m}\times\Re^{r\times m}\times\Re}} \quad & \left\{ u + c_3 \sum_{k=1}^m \boldsymbol{1}^T \boldsymbol{y}_k \right\} \\
s.t. \quad & \left\| \boldsymbol{B} \left(a_1 P - \frac{a_1(1+\lambda)}{m} \sum_{k=1}^m \boldsymbol{1}^T \boldsymbol{z}_k, \frac{b_1}{m} \sum_{k=1}^m \boldsymbol{1}^T \boldsymbol{y}_k \right) \right\| \le u, \frac{1+\lambda}{m} \sum_{k=1}^m \boldsymbol{1}^T \boldsymbol{z}_k \le P, \\
& \boldsymbol{A}\boldsymbol{y}_k \le \boldsymbol{A}\boldsymbol{x}_k, \boldsymbol{A}\boldsymbol{z}_k \le \boldsymbol{A}\boldsymbol{x}_k, \boldsymbol{y}_k + \boldsymbol{z}_k = \boldsymbol{x}_k, \;\; \textit{for all} \;\; 1 \le k \le m,
\end{aligned} \tag{2.19}$$

where $\boldsymbol{B} := \begin{pmatrix} 1 & 1/2 \\ 0 & \sqrt{3}/2 \end{pmatrix}$.

Next, we solve the second finite dimensional optimisation problem under the Standard deviation principle assumption, which is stated as Problem 2.3.2.

Problem 2.3.2 *Assume that the optimisation problem from* (2.11) *is made under the Standard deviation principle assumption, i.e.* $\pi(\cdot) = \mathbb{E}(\cdot) + \lambda \; \mathrm{Sd}(\cdot)$. *Therefore, the following optimisation problem has to be solved*

$$\begin{aligned}
\min_{\substack{(\boldsymbol{Y},\boldsymbol{Z})\in\\ \Re^{r\times m}\times\Re^{r\times m}}} \quad & \Bigg\{ g\left(a_1 P - \frac{a_1}{m} \sum_{k=1}^m \boldsymbol{1}^T \boldsymbol{z}_k - a_1 \lambda \frac{\left\| \boldsymbol{Q}\left(\boldsymbol{1}^T \boldsymbol{z}_1, \ldots, \boldsymbol{1}^T \boldsymbol{z}_m \right) \right\|}{\sqrt{m-1}}, \frac{b_1}{m} \sum_{k=1}^m \boldsymbol{1}^T \boldsymbol{y}_k \right) \\
& + g\left(\frac{a_2}{m} \sum_{k=1}^m \boldsymbol{1}^T \boldsymbol{z}_k + a_2 \lambda \frac{\left\| \boldsymbol{Q}\left(\boldsymbol{1}^T \boldsymbol{z}_1, \ldots, \boldsymbol{1}^T \boldsymbol{z}_m \right) \right\|}{\sqrt{m-1}}, \frac{b_2}{m} \sum_{k=1}^m \boldsymbol{1}^T \boldsymbol{z}_k \right) + c_4 \sum_{k=1}^m \boldsymbol{1}^T \boldsymbol{y}_k \\
& + \frac{1}{m} \sum_{k=1}^m \boldsymbol{1}^T \boldsymbol{z}_k + \lambda \frac{\left\| \boldsymbol{Q}\left(\boldsymbol{1}^T \boldsymbol{z}_1, \ldots, \boldsymbol{1}^T \boldsymbol{z}_m \right) \right\|}{\sqrt{m-1}} \Bigg\} \qquad (2.20) \\
s.t. \quad & \frac{1}{m} \sum_{k=1}^m \boldsymbol{1}^T \boldsymbol{z}_k + \lambda \frac{\left\| \boldsymbol{Q}\left(\boldsymbol{1}^T \boldsymbol{z}_1, \ldots, \boldsymbol{1}^T \boldsymbol{z}_m \right) \right\|}{\sqrt{m-1}} \le P, \\
& \boldsymbol{A}\boldsymbol{y}_k \le \boldsymbol{A}\boldsymbol{x}_k, \boldsymbol{A}\boldsymbol{z}_k \le \boldsymbol{A}\boldsymbol{x}_k, \boldsymbol{y}_k + \boldsymbol{z}_k = \boldsymbol{x}_k \;\; \textit{for all} \;\; 1 \le k \le m,
\end{aligned}$$

where $c_4 := \Big(1+\rho_1+c_1\Big)/m$

As before, Problem 2.20 could be efficiently solved if one could rewrite the optimisation problem in a SOCP form, which is shown in Proposition 2.3.2.

Proposition 2.3.2 *If the function* $g(a_1P - a_1x, y) + g(a_2x, z) + x$ *is non-decreasing in* x *for all* $x \in [0, P]$ *and any given* y, z*, then the Problem 2.3.2 is solved by the following SOCP:*

$$\begin{aligned}
&\min_{\substack{(\boldsymbol{Y},\boldsymbol{Z},u,v,w)\in \\ \Re^{r\times m}\times\Re^{r\times m}\times\Re\times\Re\times\Re}} && \left\{u+v+w+c_4\sum_{k=1}^{m}\boldsymbol{1}^T\boldsymbol{y}_k\right\} \\
&\quad s.t. && \left\|\boldsymbol{B}\left(a_1P-a_1w,\frac{b_1}{m}\sum_{k=1}^{m}\boldsymbol{1}^T\boldsymbol{y}_k\right)\right\|\le u,\ \left\|\boldsymbol{B}\left(a_2w,\frac{b_2}{m}\sum_{k=1}^{m}\boldsymbol{1}^T\boldsymbol{y}_k\right)\right\|\le v, \\
& && \left\|\boldsymbol{Q}\Big(\boldsymbol{1}^T\boldsymbol{z}_1,\ldots,\boldsymbol{1}^T\boldsymbol{z}_m\Big)\right\|\le\frac{\sqrt{m-1}}{\lambda}\left(P-\frac{1}{m}\sum_{k=1}^{m}\boldsymbol{1}^T\boldsymbol{z}_k\right), \\
& && \left\|\boldsymbol{Q}\Big(\boldsymbol{1}^T\boldsymbol{z}_1,\ldots,\boldsymbol{1}^T\boldsymbol{z}_m\Big)\right\|\le\frac{\sqrt{m-1}}{\lambda}\left(w-\frac{1}{m}\sum_{k=1}^{m}\boldsymbol{1}^T\boldsymbol{z}_k\right), \\
& && \boldsymbol{A}\boldsymbol{y}_k\le\boldsymbol{A}\boldsymbol{x}_k,\ \boldsymbol{A}\boldsymbol{z}_k\le\boldsymbol{A}\boldsymbol{x}_k,\ \boldsymbol{y}_k+\boldsymbol{z}_k=\boldsymbol{x}_k\ \text{ for all }\ 1\le k\le m.
\end{aligned} \tag{2.21}$$

Remark 2.3.1 *Note that the non-decreasing property of function* $g(a_1P - a_1\cdot, y) + g(a_2\cdot, z) + \cdot$ *is clearly satisfied if* $-1 \le a_1, a_2 \le 1$*, since the derivatives of* $g(\cdot, y)$ *with respect to the first variable is less than 1 for any* y*. One may verify that* $0 \le a_1, b_1 \le 1$ *is true for all recommended values and market-wide estimates of* σ_{PR} *and* σ_{RR}*, respectively.*

A more general way of writing (2.11) is as follows:

$$\begin{aligned}
&\min_{(I,R,t)\in\mathcal{F}\times\Re} H(I,R,t), \quad \text{s.t.}\quad \pi\left(\sum_{i=1}^{N}R[X_i]\right)\le t\le P \quad\text{and}\quad I(\cdot)+R(\cdot)=\cdot, \quad\text{where} \\
&H(I,R,t) := g\left(a_1(P-t), b_1\cdot\mathbb{E}\left(\sum_{i=1}^{N}I\Big[X_i\Big]\right)\right)+mc_4\cdot\mathbb{E}\left(\sum_{i=1}^{N}I\Big[X_i\Big]\right)+ \\
&g\left(a_2t, b_2\cdot\mathbb{E}\left(\sum_{i=1}^{N}R[X_i]\right)\right)+t.
\end{aligned} \tag{2.22}$$

provided that $H(I, R, t)$ is non-decreasing in t.

Now, the premium calculation based on π for a generic risk X, discrete distributed with a state space $\Omega = \Big\{x_1, \ldots, x_m\Big\}$, is given by $\pi\Big(\mathbf{x}\Big)$. Therefore, the finite dimensional optimisation problem becomes

$$\begin{aligned} \min_{\substack{(\mathbf{Y},\mathbf{Z},t)\in \\ \Re^{r\times m}\times\Re^{r\times m}\times\Re}} \quad & \left\{g\left(a_1P - a_1t, \frac{b_1}{m}\sum_{k=1}^{m}\mathbf{1}^T\mathbf{y}_k\right) + g\left(a_2t, \frac{b_2}{m}\sum_{k=1}^{m}\mathbf{1}^T\mathbf{z}_k\right) + c_4\sum_{k=1}^{m}\mathbf{1}^T\mathbf{y}_k + t\right\} \\ \text{s.t.} \quad & \pi\Big(\mathbf{1}^T\mathbf{z}_1, \ldots, \mathbf{1}^T\mathbf{z}_m\Big) \le t \le P, \\ & \mathbf{A}\mathbf{y}_k \le \mathbf{A}\mathbf{x}_k, \mathbf{A}\mathbf{z}_k \le \mathbf{A}\mathbf{x}_k, \mathbf{y}_k + \mathbf{z}_k = \mathbf{x}_k \ \text{ for all } \ 1 \le k \le m. \end{aligned} \tag{2.23}$$

Similar arguments to those used in the proof of Proposition 2.3.2, one may show that the above is equivalent to solving the following optimisation problem:

$$\begin{aligned} \min_{\substack{(\mathbf{Y},\mathbf{Z},u,v,t)\in \\ \Re^{r\times m}\times\Re^{r\times m}\times\Re\times\Re\times\Re}} \quad & \left\{u + v + t + c_4\sum_{k=1}^{m}\mathbf{1}^T\mathbf{y}_k\right\} \\ \text{s.t.} \quad & \left\|\mathbf{B}\left(a_1P - a_1t, \frac{b_1}{m}\sum_{k=1}^{m}\mathbf{1}^T\mathbf{y}_k\right)\right\| \le u, \left\|\mathbf{B}\left(a_2t, \frac{b_2}{m}\sum_{k=1}^{m}\mathbf{1}^T\mathbf{z}_k\right)\right\| \le v, \\ & \pi\Big(\mathbf{1}^T\mathbf{z}_1, \ldots, \mathbf{1}^T\mathbf{z}_m\Big) \le t \le P, \\ & \mathbf{A}\mathbf{y}_k \le \mathbf{A}\mathbf{x}_k, \mathbf{A}\mathbf{z}_k \le \mathbf{A}\mathbf{x}_k, \mathbf{y}_k + \mathbf{z}_k = \mathbf{x}_k \ \text{ for all } \ 1 \le k \le m. \end{aligned} \tag{2.24}$$

provided that $g(a_1P–a_1x, y)+g(a_2x, z)+x$ is non-decreasing function in x for all $x \in [0, P]$ and any given y, z. Recall that Remark 2.3.1 explains why the latter sufficient condition is not restrictive. Clearly, (2.21) is SOCP-representable as long as $\pi\Big(\mathbf{1}^T\mathbf{z}_1, \ldots, \mathbf{1}^T\mathbf{z}_m\Big) \le t$ is SOCP-representable. It is shown in Asimit et al. [2018]) that many common risk measure choices for π leads to SOCP representations.

2.3.2 Pareto optimal reinsurance model

All the optimisation problems that we have been investigated by now are from the insurer's point of view. Since the risk transfer is possible if both parties of the bilateral insurance contract are incentivised to accept the transfer, finding the Pareto optimal contracts would also be informative. The aim of using Pareto optimality principle here is to construct contracts such that no further changes in the contact can make insurer or reinsurer better off without making other party worse off. We introduce another coherent risk measure for reinsurance premium principle in this subsection for construction of Pareto optimal reinsurance model.

Note, that to avoid confusion in this subsection we use G_1 and G_2 for insurer and reinsurer respectively. Moreover, for the sake of simplicity, we use same notation for a_1, a_2, b_1, b_2 for insurer and reisurer. In practice, these coefficients may differ. c_2 and ρ_2 are the reinsurer's model parameters with equivalent definitions of c_1 and ρ_1. Let us assume that the insurer seeks to minimise its risk, $G_1(I,R) := H(I,R)$, while the reinsurer aims to reduce its risk

$$\begin{aligned} G_2(I,R) := g\left(a_1 \cdot \pi\left(R\sum_{i=1}^{N} X_i\right), b_1 \cdot \mathbb{E}\left(R\sum_{i=1}^{N} X_i\right)\right) \\ + \left(1+\rho_2+c_2\right) \cdot \mathbb{E}\left(R\sum_{i=1}^{N} X_i\right) - \pi\left(R\sum_{i=1}^{N} X_i\right) \end{aligned} \tag{2.25}$$

subject to $\pi\left(R\sum_{i=1}^{N} X_i\right) \leq P$ and $I(\cdot)+R(\cdot) = \cdot$. Therefore, we call a contract $(I^*, R^*) \in \mathcal{F}$ satisfying the constraints of (2.11) and (2.25) feasible. As we can see, conflicting objectives arise amongst the insurer and the reisurer and we use the concept Pareto optimality. The contract profile $(I^*, R^*) \in \mathcal{F}$ is called *Pareto Optimal* if there is no other feasible contract profile $(\tilde{I}, \tilde{R}) \in \mathcal{F}$ such that $G_1(\tilde{I}, \tilde{R}) \leq G_1(I^*, R^*)$ and $G_2(\tilde{I}, \tilde{R}) \leq G_2(I^*, R^*)$ with at least one strict inequality.

Finding all Pareto optimal contracts is a much more difficult problem and the difficulty here lies in the necessity of considering two or more objective functions. This involves standard multi-objective optimisation methods that could be reduced to a weighted sum scalarisation of the concurrent objectives as long as all objective functions are convex. The main idea behind multi-objective optimisation is that there are several conflicting objectives $f_1(x), f_2(x), ..., f_n(x)$ that need to be simultaneously optimised. An optimal solution to the MOP is a solution where there exists no other feasible solution that improves the value of at least one objective function without making any other objective function worse off. This is the concept of Pareto optimality. That is, a vector $x^* \in S$ is Pareto optimal for a multi-objective optimisation problem if all vectors $x \in S$ have a greater value for at least one of the objective functions f_i, where $i = 1, \ldots, n$ or have the same value for all the objective functions. Generally, a decision vector $x^* \in S$ is considered to be Pareto optimal if there does not exist $x \in S$ such that $f_i(x) < f_i(x^*)$ and $f_j(x) < f_j(x^*)$ for at least one index j. The vector of objective functions is said to be Pareto optimal if the corresponding decision vector x is Pareto optimal. Scalarisation method formulates a single-objective optimisation problem by aggregating all the objective functions of a multi-objective optimisation problem into a single function , such that optimal solutions to the single-objective optimisation problem are Pareto optimal solutions to the MOP. Particularly, a single objective optimisation problem is defined related to the multi-objective optimisation using a real-valued scalarising function, normally being a function of the objective functions, auxiliary scalar or vector variables, and/or scalar or vector parameters.

Linear scalarisation generates efficient solutions if the objective functions are convex. Thus, the weighted sum scalarisation method minimises a positively weighted sum of the objectives, which represents a standard optimisation problem. In particular, scalarisation-based multi-objective optimisation methods formulate a scalarised function F from the objective functions $f_1, \ldots, f_N$ of the multi-objective optimisation problem (MOP) with certain non negative weights $\gamma_1, \ldots, \gamma_N \geq 0$ and minimise F. They solve the following single-objective optimisation problem :

$$\min_{x \in S} F(x, \gamma), \gamma \in \Omega^+ \tag{2.26}$$

where

$$F(x,\gamma) = \sum_{n=1}^{N} \gamma_n f_n(x), \tag{2.27}$$

$$\Omega^+ = \left\{ \gamma \middle| \sum_{n=1}^{N} \gamma = 1, \gamma \geq 0, n = 1, ..., N \right\} \tag{2.28}$$

Here, $\boldsymbol{\gamma} = [\gamma_1, ..., \gamma_N]^T$ denotes weight vector and Ω^+ is the set of normalized weight vectors whose sum of elements is equal to one. Under the convexity assumptions, the solution to this single objective optimisation problem is Pareto optimal. If the problem is strictly convex, the solution $x^* \in S$ is also unique.

Thus, having two objective functions $G_1(I,R)$ and $G_2(I,R)$ we are now able to formulate our optimisation problem using weighted sum scalarisation method as follows:

$$\min_{(I,R)\in\mathcal{F}} \gamma G_1(I,R) + (1-\gamma)G_2(I,R), \quad \text{s.t.} \quad \pi\left(R\sum_{i=1}^{N} X_i\right) \leq P$$
$$\text{and} \quad I(\cdot) + R(\cdot) = \cdot, \tag{2.29}$$

where $\gamma \in (0,1)$. If functions G_1 and G_2 are convex, their affine combination (2.29) is also convex. Thus, we can present (2.29) in the following form

$$\min_{(I,R,t)\in\mathcal{F}\times\mathbb{R}} \gamma G_1(I,R,t) + (1-\gamma)G_2(I,R,t),$$
$$\text{s.t.} \quad \pi\left(R\sum_{i=1}^{N} X_i\right) \leq t \leq P \quad \text{and} \quad I(\cdot)+R(\cdot) = \cdot \tag{2.30}$$

where $G_1(I,R,t) = H_1(I,R,t)$ and $G_2(I,R,t) = g\left(a_1 \cdot t, b_1 \cdot \mathbb{E}\left(R\sum_{i=1}^{N} X_i\right)\right) + \left(1+\rho_2+c_2\right) \cdot \mathbb{E}\left(R\sum_{i=1}^{N} X_i\right) - t.$

Again, in order to be able to solve this problem using SOCP we need to discretise it and ensure that the constraint involving π is convex. Thus, the Pareto optimal contracts could be found via a finite dimensional optimisation problem and is given Problem 2.3.3.

Problem 2.3.3 *Assume that π is a convex risk measure. Therefore, the multi-objective* *problem is reduced to the following convex optimisation instance:*

$$\begin{aligned}
\min_{\substack{(\boldsymbol{Y},\boldsymbol{Z},t)\in\\ \Re^{r\times m}\times\Re^{r\times m}\times\Re}} & \Bigg\{\gamma g\left(a_1P-a_1t,\frac{b_1}{m}\sum_{k=1}^{m}\boldsymbol{1}^T\boldsymbol{y}_k\right)+\gamma g\left(a_2t,\frac{b_2}{m}\sum_{k=1}^{m}\boldsymbol{1}^T\boldsymbol{z}_k\right).\\
& +(1-\gamma)g\left(a_1t,\frac{b_1}{m}\sum_{k=1}^{m}\boldsymbol{1}^T\boldsymbol{z}_k\right)\\
& +c_5\sum_{k=1}^{m}\boldsymbol{1}^T\boldsymbol{y}_k+(2\gamma-1)t\Bigg\} \qquad (2.31)\\
s.t. \quad & \pi\Big(\boldsymbol{1}^T\boldsymbol{z}_1,\ldots,\boldsymbol{1}^T\boldsymbol{z}_m\Big)\le t\le P,\\
& \boldsymbol{A}\boldsymbol{y}_k\le\boldsymbol{A}\boldsymbol{x}_k,\ \boldsymbol{A}\boldsymbol{z}_k\le\boldsymbol{A}\boldsymbol{x}_k,\ \boldsymbol{y}_k+\boldsymbol{z}_k=\boldsymbol{x}_k\ \textit{ for all }\ 1\le k\le m,
\end{aligned}$$

where $\gamma\in[0,1]$ *is a given parameter and* $c_5:=\Big(\gamma\big(1+\rho_1+c_1\big)-(1-\gamma)\big(1+\rho_2+c_2\big)\Big)/m.$

As before, Problem 2.3.3 could be rewritten in a more convenient form, as shown in Proposition 2.3.3.

Proposition 2.3.3 *If* $\gamma\ge\frac{1}{2-a_1}$ *the Problem 2.3.3 is solved by the following optimisation problem:*

$$\begin{aligned}
\min_{\substack{(\boldsymbol{Y},\boldsymbol{Z},t,u,v,w)\in\\ \Re^{r\times m}\times\Re^{r\times m}\times\Re\times\Re\times\Re\times\Re}} & \left\{\gamma(u+v)+(1-\gamma)w+(2\gamma-1)t+c_5\sum_{k=1}^{m}\boldsymbol{1}^T\boldsymbol{y}_k\right\}\\
s.t. \quad & \left\|\boldsymbol{B}\left(a_1P-a_1t,\frac{b_1}{m}\sum_{k=1}^{m}\boldsymbol{1}^T\boldsymbol{y}_k\right)\right\|\le u,\ \left\|\boldsymbol{B}\left(a_2t,\frac{b_2}{m}\sum_{k=1}^{m}\boldsymbol{1}^T\boldsymbol{z}_k\right)\right\|\le v,\\
& \left\|\boldsymbol{B}\left(a_1t,\frac{b_1}{m}\sum_{k=1}^{m}\boldsymbol{1}^T\boldsymbol{z}_k\right)\right\|\le w, \qquad (2.32)\\
& \pi\Big(\boldsymbol{1}^T\boldsymbol{z}_1,\ldots,\boldsymbol{1}^T\boldsymbol{z}_m\Big)\le t\le P,\\
& \boldsymbol{A}\boldsymbol{y}_k\le\boldsymbol{A}\boldsymbol{x}_k,\ \boldsymbol{A}\boldsymbol{z}_k\le\boldsymbol{A}\boldsymbol{x}_k,\ \boldsymbol{y}_k+\boldsymbol{z}_k=\boldsymbol{x}_k\ \textit{ for all }\ 1\le k\le m.
\end{aligned}$$

We can show that 2.32 is SOCP-representable as long as $\pi\Big(\mathbf{1}^T\mathbf{z}_1,\ldots,\mathbf{1}^T\mathbf{z}_m\Big)\le t$ is SOCP-representable. As mentioned before, it is shown in Asimit et al. [2018]) that many common risk measure choices for π lead to SOCP representations.

Lemma 2.3.1 *Let us assume that the optimisation Problem 2.3.3 is made under the Expected value assumption i.e* $\pi(\cdot)=(1+\lambda)\mathbb{E}(\cdot)$. *Then 2.32 is equivalent to solving the* *following problem*

$$\begin{aligned}
\min_{\substack{(\boldsymbol{Y},\boldsymbol{Z},t,u,v,w)\in \\ \Re^{r\times m}\times\Re^{r\times m}\times\Re\times\Re\times\Re\times\Re}} \quad & \left\{\gamma(u+v)+(1-\gamma)w+(2\gamma-1)t+c_5\sum_{k=1}^{m}\boldsymbol{1}^T\boldsymbol{y}_k\right\} \\
s.t. \quad & \left\|\boldsymbol{B}\left(a_1P-a_1t,\frac{b_1}{m}\sum_{k=1}^{m}\boldsymbol{1}^T\boldsymbol{y}_k\right)\right\|\leq u, \left\|\boldsymbol{B}\left(a_2t,\frac{b_2}{m}\sum_{k=1}^{m}\boldsymbol{1}^T\boldsymbol{z}_k\right)\right\|\leq v, \\
& \left\|\boldsymbol{B}\left(a_1t,\frac{b_1}{m}\sum_{k=1}^{m}\boldsymbol{1}^T\boldsymbol{z}_k\right)\right\|\leq w, \\
& \left\|\frac{(1+\lambda)}{m}\sum_{k=1}^{m}\boldsymbol{1}^T\boldsymbol{z}_k\right\|\leq t\leq P \\
& \boldsymbol{A}\boldsymbol{y}_k\leq\boldsymbol{A}\boldsymbol{x}_k, \boldsymbol{A}\boldsymbol{z}_k\leq\boldsymbol{A}\boldsymbol{x}_k, \boldsymbol{y}_k+\boldsymbol{z}_k=\boldsymbol{x}_k \text{ for all } 1\leq k\leq m.
\end{aligned} \tag{2.33}$$

Lemma 2.3.2 *Assume that the optimisation problem 2.3.3 is defined under the Standard deviation principle assumption, i.e.* $\pi(\cdot)=\mathbb{E}(\cdot)+\lambda\,\mathrm{Sd}(\cdot)$. *Then* (2.32) *is equivalent to solving the following problem*

$$\begin{aligned}
\min_{\substack{(\boldsymbol{Y},\boldsymbol{Z},t,u,v,w)\in \\ \Re^{r\times m}\times\Re^{r\times m}\times\Re\times\Re\times\Re\times\Re}} \quad & \left\{\gamma(u+v)+(1-\gamma)w+(2\gamma-1)t+c_5\sum_{k=1}^{m}\boldsymbol{1}^T\boldsymbol{y}_k\right\} \\
s.t. \quad & \left\|\boldsymbol{B}\left(a_1P-a_1t,\frac{b_1}{m}\sum_{k=1}^{m}\boldsymbol{1}^T\boldsymbol{y}_k\right)\right\|\leq u, \left\|\boldsymbol{B}\left(a_2t,\frac{b_2}{m}\sum_{k=1}^{m}\boldsymbol{1}^T\boldsymbol{z}_k\right)\right\|\leq v, \\
& \left\|\boldsymbol{B}\left(a_1t,\frac{b_1}{m}\sum_{k=1}^{m}\boldsymbol{1}^T\boldsymbol{z}_k\right)\right\|\leq w, \\
& \left\|\boldsymbol{Q}\Big(\boldsymbol{1}^T\boldsymbol{z}_1,\ldots,\boldsymbol{1}^T\boldsymbol{z}_m\Big)\right\|\leq\frac{\sqrt{m-1}}{\lambda}\left(t-\frac{1}{m}\sum_{k=1}^{m}\boldsymbol{1}^T\boldsymbol{z}_k\right), t\leq P, \\
& \boldsymbol{A}\boldsymbol{y}_k\leq\boldsymbol{A}\boldsymbol{x}_k, \boldsymbol{A}\boldsymbol{z}_k\leq\boldsymbol{A}\boldsymbol{x}_k, \boldsymbol{y}_k+\boldsymbol{z}_k=\boldsymbol{x}_k \text{ for all } 1\leq k\leq m.
\end{aligned} \tag{2.34}$$

Proposition 2.3.4 *Let us assume that the risk measure in the optimisation Problem 2.3.3 is defined as*

$$\pi(\boldsymbol{Z},e,d):=\frac{1}{m}\sum_{k=1}^{m}\boldsymbol{1}^T\boldsymbol{z}_k+e\left(\frac{1}{m}\sum_{k=1}^{m}\left(\boldsymbol{1}^T\boldsymbol{z}_k-\frac{1}{m}\sum_{k=1}^{m}\boldsymbol{1}^T\boldsymbol{z}_k\right)_+^d\right)^{1/d} \tag{2.35}$$

Problems (2.32) *and* (2.36) *are equivalent, where*

$$\begin{aligned}
\min_{\substack{(\boldsymbol{Y},\boldsymbol{Z},\boldsymbol{\tau},u,v,w,r,t)\in\\ \Re^{r\times m}\times\Re^{r\times m}\times\Re^{m}\times\Re\times\Re\times\Re\times\Re\times\Re}} \quad & \left\{\gamma(u+v)+(1-\gamma)w+(2\gamma-1)t+c_5\sum_{k=1}^{m}\boldsymbol{1}^T\boldsymbol{y}_k\right\}\\
s.t. \quad & \left\|\boldsymbol{B}\left(a_1P-a_1t,\frac{b_1}{m}\sum_{k=1}^{m}\boldsymbol{1}^T\boldsymbol{y}_k\right)\right\|\le u, \left\|\boldsymbol{B}\left(a_2t,\frac{b_2}{m}\sum_{k=1}^{m}\boldsymbol{1}^T\boldsymbol{z}_k\right)\right\|\le v,\\
& \left\|\boldsymbol{B}\left(a_1t,\frac{b_1}{m}\sum_{k=1}^{m}\boldsymbol{1}^T\boldsymbol{z}_k\right)\right\|\le w, \qquad (2.36)\\
& \boldsymbol{Z}^T\boldsymbol{1}-r\boldsymbol{1}\le\boldsymbol{\tau},\boldsymbol{0}\le\boldsymbol{\tau}\\
& r+e_1\left(\sum_{k=1}^{m}\tau_k^d\right)^{1/d}\le t, t\le P\\
& \boldsymbol{A}\boldsymbol{y}_k\le\boldsymbol{A}\boldsymbol{x}_k, \boldsymbol{A}\boldsymbol{z}_k\le\boldsymbol{A}\boldsymbol{x}_k, \boldsymbol{y}_k+\boldsymbol{z}_k=\boldsymbol{x}_k, \frac{1}{m}\sum_{k=1}^{m}\boldsymbol{1}^T\boldsymbol{z}_k=r\\
& \textit{for all } \ 1\le k\le m.
\end{aligned}$$

where $e_1 := e(1/m)^{1/d}$.

The above formulation is almost written in a SOCP form, but the risk measure function requires more work.

Lemma 2.3.3 *If* $d \in \{1, +\infty\}$, *then* (2.36) *is SOCP-representable without any change and the case when* $d = 2$ *has the following form:*

$$\begin{aligned}
\min_{\substack{(\mathbf{Y},\mathbf{Z},\boldsymbol{\tau},u,v,w,r,t,\epsilon)\in\\ \Re^{r\times m}\times\Re^{r\times m}\times\Re^{m}\times\Re\times\Re\times\Re\times\Re\times\Re\times\Re}} \quad & \left\{\gamma(u+v)+(1-\gamma)w+(2\gamma-1)t+c_5\sum_{k=1}^{m}\mathbf{1}^T\mathbf{y}_k\right\}\\
\text{s.t.} \quad & \left\|\mathbf{B}\left(a_1P-a_1t,\frac{b_1}{m}\sum_{k=1}^{m}\mathbf{1}^T\mathbf{y}_k\right)\right\|\le u, \left\|\mathbf{B}\left(a_2t,\frac{b_2}{m}\sum_{k=1}^{m}\mathbf{1}^T\mathbf{z}_k\right)\right\|\le v,\\
& \left\|\mathbf{B}\left(a_1t,\frac{b_1}{m}\sum_{k=1}^{m}\mathbf{1}^T\mathbf{z}_k\right)\right\|\le w, \qquad (2.37)\\
& \frac{1}{m}\sum_{k=1}^{m}\mathbf{1}^T\mathbf{z}_k=r, \mathbf{Z}^T\mathbf{1}-r\mathbf{1}\le\boldsymbol{\tau},\mathbf{0}\le\boldsymbol{\tau},\|\boldsymbol{\tau}\|\le\epsilon\\
& \|\epsilon\|\le\frac{1}{e_1}(t-r), t\le P\\
& \mathbf{A}\mathbf{y}_k\le\mathbf{A}\mathbf{x}_k, \mathbf{A}\mathbf{z}_k\le\mathbf{A}\mathbf{x}_k, \mathbf{y}_k+\mathbf{z}_k=\mathbf{x}_k \ \text{ for all } \ 1\le k\le m.
\end{aligned}$$

According to Morenko et al. (2013), $\left(\sum_{k=1}^{m}\tau^d\right)^{1/d} \leq \epsilon$ is SOCP-representable, therefore we can discuss the cases when d is a rational number. For example, if $d = 3$, then the constraints in the (2.36) could be rewritten as follows:

$$\mathbf{1}^T\boldsymbol{\xi} \leq \epsilon, \mathbf{0} \leq \boldsymbol{\xi}, \mathbf{0} \leq \boldsymbol{\delta}, \tau_k^2 \leq \epsilon\delta_k, \delta_k^2 \leq \tau_k\xi_k, 1 \leq k \leq m \tag{2.38}$$

Lemma 2.3.4 *If $d = 3$, the SOCP reformulation of (2.36) is given by:*

$$\begin{aligned}
\min_{\substack{(\mathbf{Y},\mathbf{Z},\boldsymbol{\tau},\boldsymbol{\xi},\boldsymbol{\delta},u,v,w,r,\epsilon,t)\in\\ \Re^{r\times m}\times\Re^{r\times m}\times\Re^m\times\Re^m\times\Re^m\times\Re\times\Re\times\Re\times\Re\times\Re\times\Re}} \quad & \left\{\gamma(u+v) + (1-\gamma)w + (2\gamma-1)t + c_5\sum_{k=1}^{m}\mathbf{1}^T\mathbf{y}_k\right\} \\
\text{s.t.} \quad & \left\|\mathbf{B}\left(a_1P - a_1t, \frac{b_1}{m}\sum_{k=1}^{m}\mathbf{1}^T\mathbf{y}_k\right)\right\| \leq u, \left\|\mathbf{B}\left(a_2t, \frac{b_2}{m}\sum_{k=1}^{m}\mathbf{1}^T\mathbf{z}_k\right)\right\| \leq v, \\
& \left\|\mathbf{B}\left(a_1t, \frac{b_1}{m}\sum_{k=1}^{m}\mathbf{1}^T\mathbf{z}_k\right)\right\| \leq w, \\
& \frac{1}{m}\sum_{k=1}^{m}\mathbf{1}^T\mathbf{z}_k = r, \mathbf{Z}^T\mathbf{1} - r\mathbf{1} \leq \boldsymbol{\tau}, \mathbf{0} \leq \boldsymbol{\tau}, \\
& \mathbf{1}^T\boldsymbol{\xi} \leq \epsilon, \mathbf{0} \leq \boldsymbol{\xi}, \mathbf{0} \leq \boldsymbol{\delta}, \\
& \|\ 2\tau_k, \epsilon - \delta_k\| \leq \epsilon + \delta_k, \|\ 2\delta_k, \tau_k - \xi_k\| \leq \tau_k + \xi_k, 1 \leq k \leq m \\
& \|\epsilon\| \leq \frac{1}{e_1}\left(t - r\right), t \leq P \\
& \mathbf{A}\mathbf{y}_k \leq \mathbf{A}\mathbf{x}_k, \mathbf{A}\mathbf{z}_k \leq \mathbf{A}\mathbf{x}_k, \mathbf{y}_k + \mathbf{z}_k = \mathbf{x}_k \text{ for all } 1 \leq k \leq m.
\end{aligned} \tag{2.39}$$

2.4 Numerical Illustrations

This section provides numerical illustrations to give some intuitive interpretation of optimisation problems from section 2.3. We demonstrate that different types of reinsurance contract are optimal when using different principles for the risk measure.

Results are illustrated using four different distributions for claim amounts. First distribution is Log-Normal with parameters $\mu = 6.7084$ and $\sigma = 0.6315$. The second one is exponential distribution with expected value of 1000. The third distribution is Pareto distribution with the shape parameter 0, scale parameter 700 and location parameter 300. Finally, the last distribution is Gamma with the shape parameter 2.041 and scale parameter 490. The parameters are chosen such that the four distributions have the same expected value of 1000 and three of the distributions, namely, Log-Normal, Pareto and Gamma have the same standard deviation of 700. We also choose $\lambda = CoC/1.04$, $CoC = 6\%$, $\sigma_{PR} = 0.1$ and $\sigma_{RR} = 0.095$, while $n = 1$ and $\Delta_n = 3\%$ as suggested in Asimit et al. (2015). We set $RecR = 50\%$, which is the benchmark value used in Solvency II, and q = 6.04% that represents the one-year default probability of a B-rating reinsurer calibrated in QIS5. Finally, it is also assumed that $\rho_1 = \rho_2 = 0.17$, $d_1 = d_2 = 2.53$, and $l = 3$. Number of scenarios m in our numerical example is 50 for all four distributions since we have experienced computational difficulties for scenario numbers larger than 50 and we trust that this number of scenarios is sufficiently informative for the purposes of this chapter.

In the first example we consider four different distributions for aggregate losses in Proposition 2.3.1, where we discuss optimisation problem from insurer's point of view, with expected value principle for the reinsurance premium. The Figure 2.4.1 contains the plots of individual losses to reinsurer's share in individual losses. We can see that the individual losses mimic the functional form $z_{kr} = ax_{kr}$, where $a \leq 1$ is a constant.

We use linear regression to find a and adjusted R-squared and Normalised Root-mean-square deviation (NRMSD) in order to assess goodness of fit.

Adjusted R-squired is greater than 99% and NRMSD is less that 5% for all distributions. Thus, evidence provided by the Table 2.4.1 is enough to accept functional form $z_{kr} = ax_{kr}$ in this model. We can conclude that proportional reinsurance, specifically,

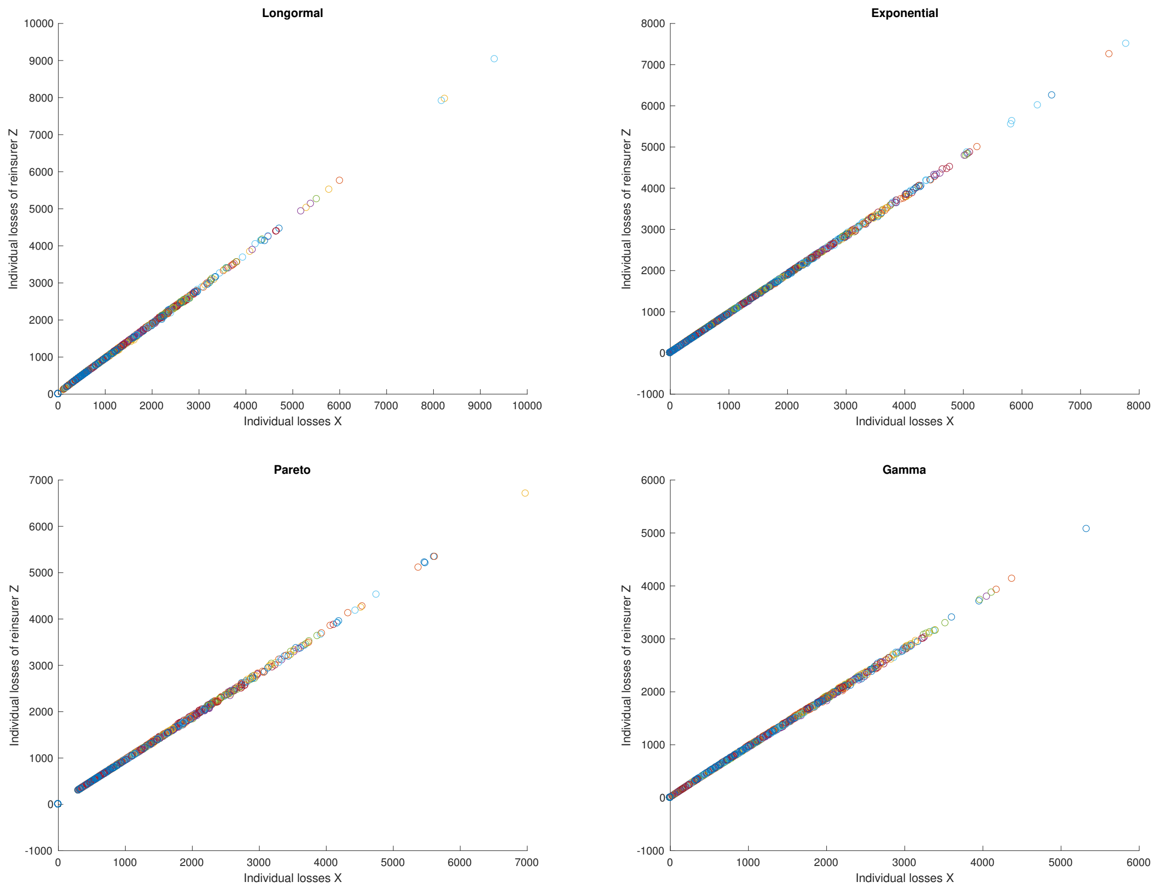

Figure 2.4.1: Empirical solutions of $z_{kr}, 1 \leq k \leq m$ for proposition 2.3.1 for different distributions.

quota-share is optimal here. The share of the reinsurer seems to be very high, but this, apparently, happens due to the choice of parameters at the beginning of this section. This value changes significantly with the change of parameters.

Next, we plot the Figure 2.4.2 of aggregate losses to reinsurer's share in aggregate losses for Proposition 2.3.2, where we discuss optimisation problem from insurer's point of view, with standard deviation principle based reinsurance premium. Choice of the parameters is the same as in the previous example.

In this example optimal reinsurance contact mimics the functional form $\mathbf{1}^T\mathbf{z}_k = \mathbf{1}^T\mathbf{x}_k \wedge c$, where c is a constant. This means that the reinsurer should cover aggregate portfolio losses up to amount c, and if aggregate losses are higher than c, insurer pays the rest and

Table 2.4.1: Linear regression results for individual losses

Distribution	a (share of the reinsurer)	Adj R-squared	NRMSD
Lognormal	0.9484	0.995	0.0047
Exponential	0.9485	0.9995	0.0056
Gamma	0.9483	0.9993	0.0063
Pareto	0.9483	0.9996	0.0041

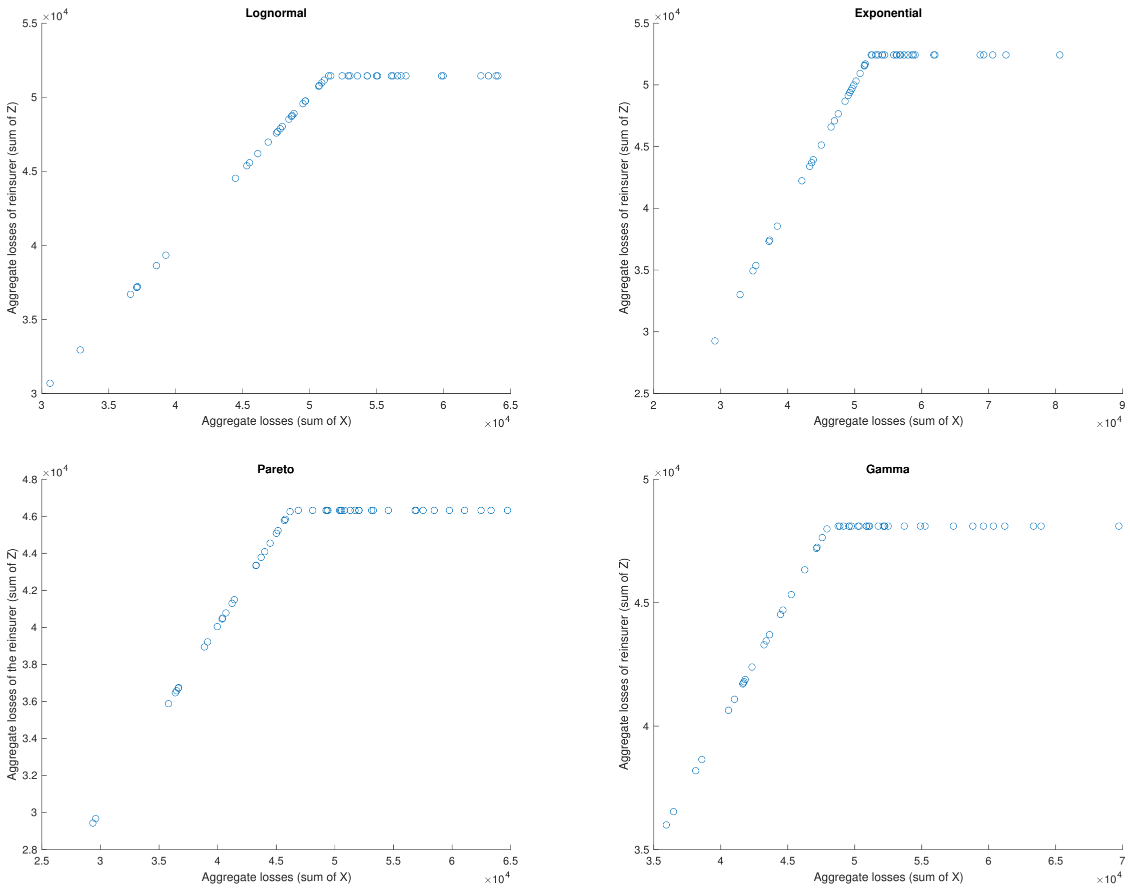

Figure 2.4.2: Empirical solutions of $\mathbf{1}^T\mathbf{z}_k, 1 \leq k \leq m$ for proposition 2.3.2 for different distributions.

keeps the heavy tailed risks. In order to explain the limit on aggregate losses we need to define a slightly different problem which allows risk transfer to control not only individual but also aggregate losses. That is, we need to add additional constraints to our problem and formulate the below infinite-dimensional optimisation model, where minimisation is taken with respect to all possible ceded and retained loss functions for aggregate claims:

$$\min_{I,R,s,g} H\left(I,R\right), \quad \text{s.t.} \quad \pi\left(\sum_{i=1}^{N} R[X_i]\right) \leq P, \quad I(\cdot)+R(\cdot)=\cdot, \\ s\left(\sum_{i=1}^{N} X_i\right)+g\left(\sum_{i=1}^{N} X_i\right)=\sum_{i=1}^{N} X_i \tag{2.40}$$

In order to avoid moral hazard the set of feasible solutions of I, R, s and g must satisfy

$$I, R, s, g := \Big\{f : 0 \leq f(x) \leq x \ \text{ and } \ x - f(x) \ \text{ are non-decreasing in } x\Big\} \tag{2.41}$$

Now we can formulate the discretised version of the above problem

$$\begin{aligned} \min_{\substack{(\mathbf{Y},\mathbf{Z},u,v,w)\in \\ \Re^{r\times m}\times\Re^{r\times m}\times\Re\times\Re\times\Re}} \quad & \left\{u+v+w+c_4\sum_{k=1}^{m}\mathbf{1}^T\mathbf{y}_k\right\} \\ \text{s.t.} \quad & \left\|\mathbf{B}\left(a_1P-a_1w,\frac{b_1}{m}\sum_{k=1}^{m}\mathbf{1}^T\mathbf{y}_k\right)\right\|\leq u, \left\|\mathbf{B}\left(a_2w,\frac{b_2}{m}\sum_{k=1}^{m}\mathbf{1}^T\mathbf{y}_k\right)\right\|\leq v, \\ & \left\|\mathbf{Q}\Big(\mathbf{1}^T\mathbf{z}_1,\ldots,\mathbf{1}^T\mathbf{z}_m\Big)\right\| \leq \frac{\sqrt{m-1}}{\lambda}\left(P-\frac{1}{m}\sum_{k=1}^{m}\mathbf{1}^T\mathbf{z}_k\right), \\ & \left\|\mathbf{Q}\Big(\mathbf{1}^T\mathbf{z}_1,\ldots,\mathbf{1}^T\mathbf{z}_m\Big)\right\| \leq \frac{\sqrt{m-1}}{\lambda}\left(w-\frac{1}{m}\sum_{k=1}^{m}\mathbf{1}^T\mathbf{z}_k\right), \\ & \mathbf{Y1}\leq\mathbf{X1}, \mathbf{Z1}\leq\mathbf{X1}, \mathbf{A}\mathbf{y}_k\leq\mathbf{A}\mathbf{x}_k, \mathbf{A}\mathbf{z}_k\leq\mathbf{A}\mathbf{x}_k, \mathbf{y}_k+\mathbf{z}_k=\mathbf{x}_k \\ & \text{for all } \ 1\leq k\leq m. \end{aligned} \tag{2.42}$$

We can fit $b(\mathbf{1}^T\mathbf{x}_k - c_1)_+ \wedge b(c_2 - c_1)$ for all $k = 1, ..., m$ and estimate parameters by introducing Ordinary Least Square (OLS) regression method. Moreover, admissibility criterion is used to test goodness of fit. The estimates of the parameters $(\tilde{b}, \tilde{c_1}, \tilde{c_2})$ are admissible whenever

$$\left|\mathbf{1}^T\mathbf{z}_k^* - \tilde{b}(\mathbf{1}^T\mathbf{x}_k - \tilde{c}_1)_+ \wedge \tilde{b}(\tilde{c}_2 - \tilde{c}_1)\right| < \epsilon \tag{2.43}$$

Our results are based on 1000 independent replications of the code, that is we draw 1000 random samples from X for each distribution and estimate the parameters b, c_1, c_2. Table (2.4.2) provides numerical results for the parameters for different distributions.

The values of ϵ are quite small comparing to average total loss of around $50,000$. Thus,

Table 2.4.2: Results of admissibility test for aggregate losses

Distribution	Admissibility		mean (stdev) of $\tilde{b}$	mean (stdev) of $\tilde{c_1}$	mean (stdev) of $\tilde{c_2}$
	$\epsilon = 1$	$\epsilon = 10$			
Lognormal	98.2%	100%	1 (0)	0.05199 (0.1075)	49,018 (1,627)
Exponential	98%	100%	1 (0)	0.04314 (0.092)	48,672 (1,858)
Gamma	98.3%	100%	1 (0)	0.0538 (0.1167)	48,969 (1,602)
Pareto	98.7%	100%	1 (0)	0.0437 (0.0755)	49,024 (1,567)

in percentage terms $\epsilon \approx \frac{1}{50{,}000} = 0.002\%$ and $\epsilon \approx \frac{10}{50{,}000} = 0.02\%$. We notice that when $\epsilon \approx 0.002\%$ the admissibility is around 98%, and when $\epsilon \approx 0.02\%$ it is 100%. The estimate of $\tilde{b}$ is 1 and $\tilde{c_1}$ is close to 0, which is in line with graphical illustrations. Thus, we can conclude that our empirical results confirm the functional form of $\mathbf{1}^T \mathbf{z}_k = \mathbf{1}^T \mathbf{x}_k \wedge c$.

In the next example we consider four different distributions for individual losses for Lemma 2.3.1 which is made under the expected value assumption for reinsurance premium and using Pareto optimality principle. The parameter for weighted sum scalarisation in Pareto optimal model is $\gamma = \frac{1}{2-a_1} + \epsilon$ and the choice of other parameters is the same as in the previous examples.

Table providing results for linear regression is demonstrated below. We notice that, as in the case with the first example, evidence provided by the Table 2.4.3 Pareto optimal model is enough to accept functional form $z_{kr} = ax_{kr}$ for this model. Notice, that when Pareto optimality principle is in place the share of the reinsurer a is less. Thus, from the Figure 2.4.3 and Table 2.4.3 we can see that the functional form of the optimal reinsurance

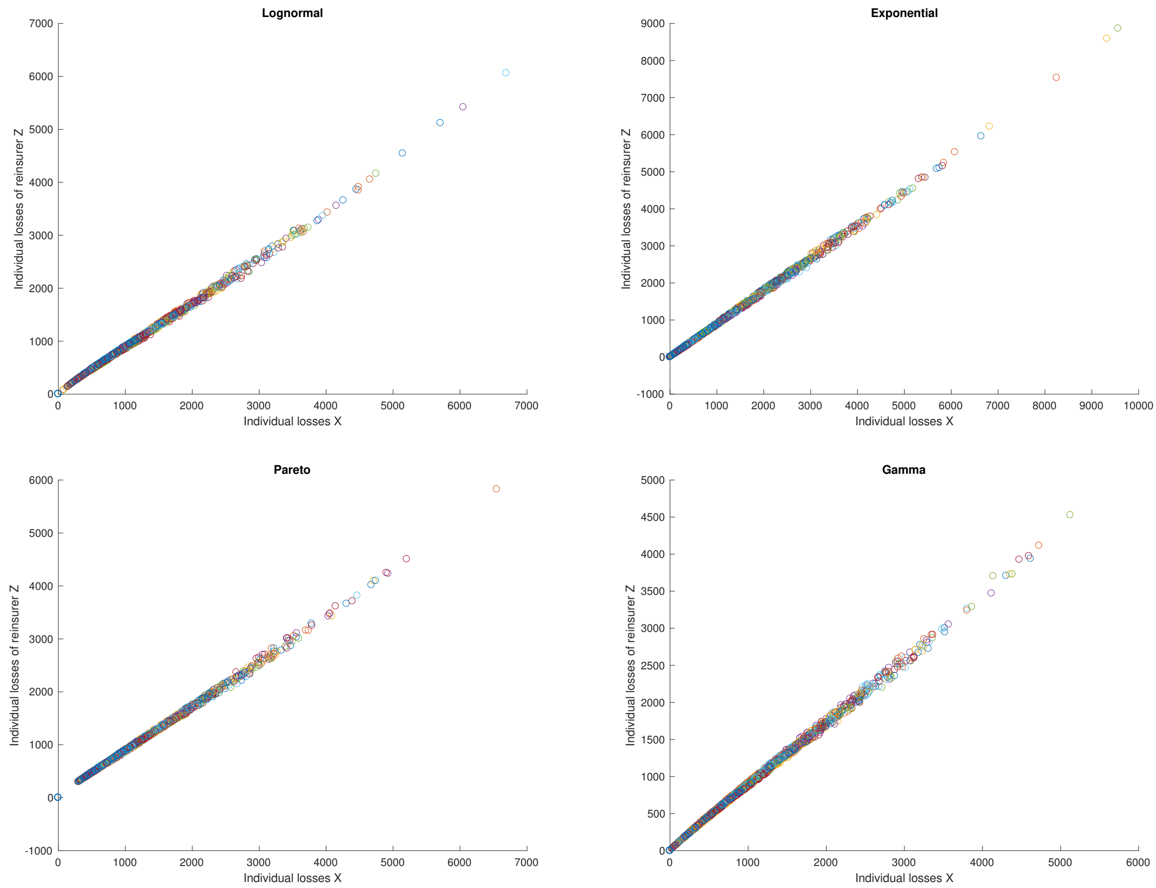

Figure 2.4.3: Empirical solutions of $z_{kr}, 1 \leq k \leq m$ for Lemma 2.3.1 for different distributions.

model is proportional.

Next, we plot the graphs of aggregate losses to reinsurer's share in aggregate losses for Lemma 2.3.2, where the optimisation problem is defined under the Standard deviation principle assumption and using Pareto optimality. Similarly, we plot graphs for Lemma 2.3.3.

Graphical illustrations 2.4.4 and 2.4.5 demonstrate that in the last two cases, optimality is obtained when the function of aggregate losses takes the form $\mathbf{1}^T\mathbf{z}_k = \mathbf{1}^T\mathbf{x}_k \wedge c$. Here again, we need to define a slightly different problem which allows risk transfer to control not only individual but also aggregate losses in order to explain the limit on aggregate

Table 2.4.3: Linear regression results for individual losses for Pareto optimal model

Distribution	a (share of the reinsurer)	Adj R-squared	NRMSD
Lognormal	0.8772	0.9971	0.0124
Exponential	0.8787	0.9943	0.0165
Gamma	0.8778	0.9971	0.013
Pareto	0.8772	0.9982	0.0099

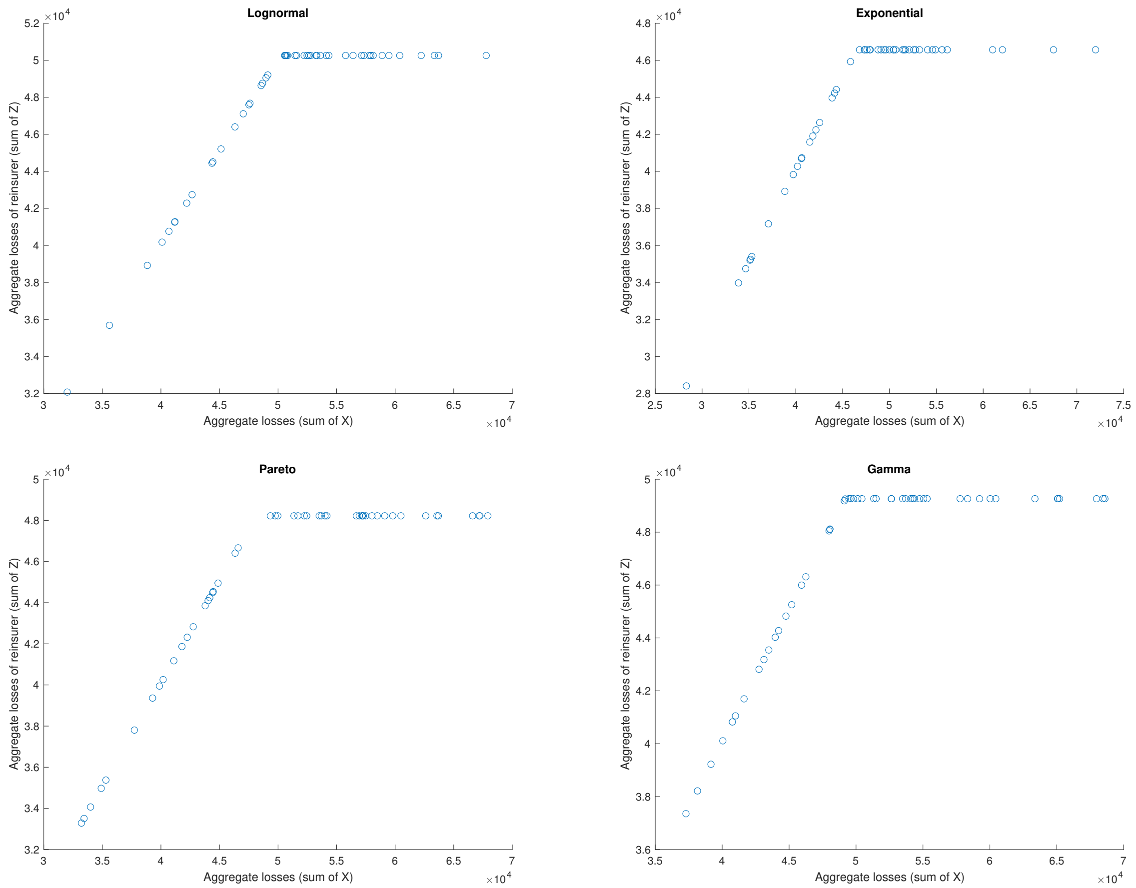

Figure 2.4.4: Empirical solutions of $\mathbf{1}^T\mathbf{z}_k, 1 \leq k \leq m$ for Lemma 2.3.2 for different distributions.

losses.

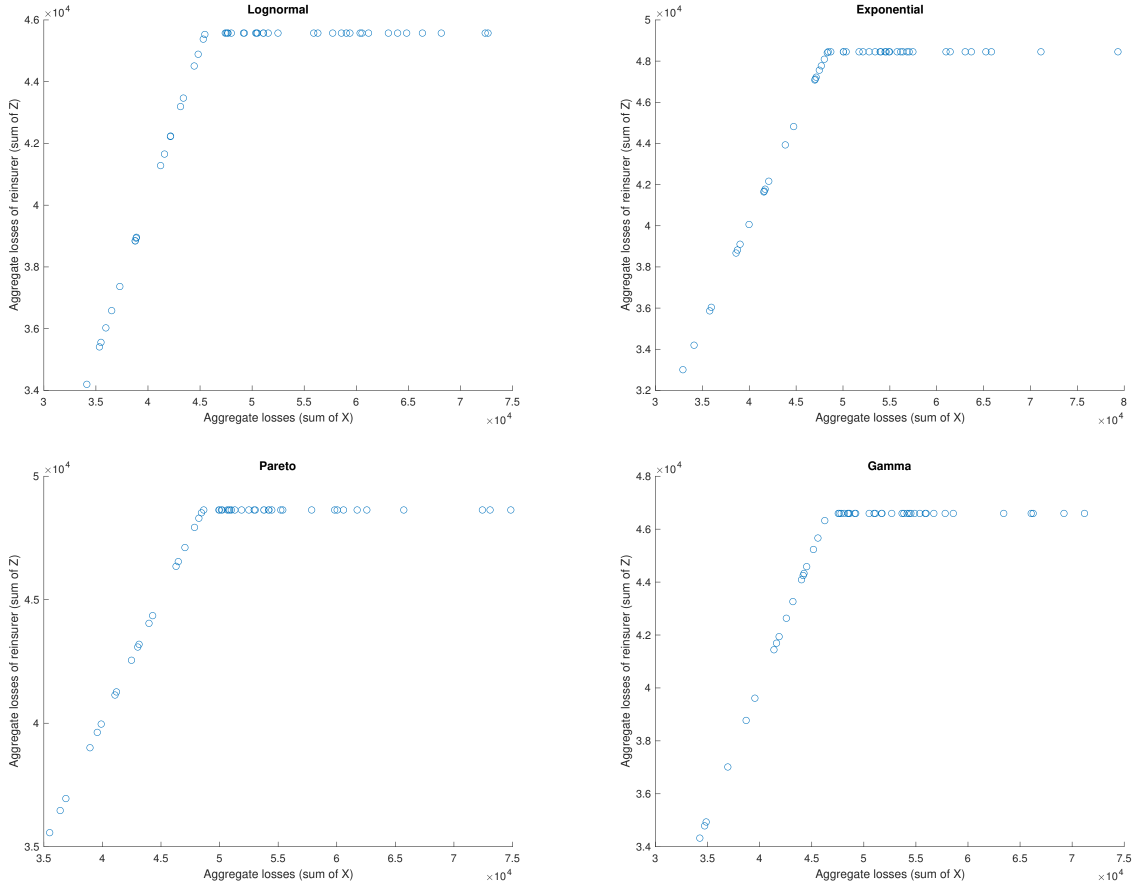

Figure 2.4.5: Empirical solutions of $\mathbf{1}^T \mathbf{z}_k, 1 \leq k \leq m$ for Lemma 2.3.3 for different distributions.

$$\min_{I,R,s,g} \gamma G_1(I,R)+(1-\gamma)G_2(I,R), \quad \text{s.t.} \quad \pi\left(\sum_{i=1}^{N} R[X_i]\right) \leq P, \quad I(\cdot)+R(\cdot)=\cdot,$$
$$s\left(\sum_{i=1}^{N} X_i\right)+g\left(\sum_{i=1}^{N} X_i\right)=\sum_{i=1}^{N} X_i \tag{2.44}$$

where

$$I,R,s,g := \Big\{f : 0 \leq f(x) \leq x \;\text{ and }\; x - f(x) \;\text{ are non-decreasing in } x\Big\} \tag{2.45}$$

Discretised form of the optimisation problem is as follows

$$\begin{aligned}
\min_{\substack{(\mathbf{Y},\mathbf{Z},t,u,v,w)\in\\ \Re^{r\times m}\times\Re^{r\times m}\times\Re\times\Re\times\Re\times\Re}} \quad & \left\{\gamma(u+v)+(1-\gamma)w+(2\gamma-1)t+c_5\sum_{k=1}^{m}\mathbf{1}^T\mathbf{y}_k\right\} \\
\text{s.t.} \quad & \left\|\mathbf{B}\left(a_1P-a_1t,\frac{b_1}{m}\sum_{k=1}^{m}\mathbf{1}^T\mathbf{y}_k\right)\right\|\le u, \left\|\mathbf{B}\left(a_2t,\frac{b_2}{m}\sum_{k=1}^{m}\mathbf{1}^T\mathbf{z}_k\right)\right\|\le v, \\
& \left\|\mathbf{B}\left(a_1t,\frac{b_1}{m}\sum_{k=1}^{m}\mathbf{1}^T\mathbf{z}_k\right)\right\|\le w, \qquad (2.46)\\
& \left\|\mathbf{Q}\Big(\mathbf{1}^T\mathbf{z}_1,\dots,\mathbf{1}^T\mathbf{z}_m\Big)\right\|\le\frac{\sqrt{m-1}}{\lambda}\left(t-\frac{1}{m}\sum_{k=1}^{m}\mathbf{1}^T\mathbf{z}_k\right), t\le P, \\
& \mathbf{Y1}\le\mathbf{X1}, \mathbf{Z1}\le\mathbf{X1}, \mathbf{A}\mathbf{y}_k\le\mathbf{A}\mathbf{x}_k, \mathbf{A}\mathbf{z}_k\le\mathbf{A}\mathbf{x}_k, \mathbf{y}_k+\mathbf{z}_k=\mathbf{x}_k \\
& \text{for all } \ 1\le k\le m.
\end{aligned}$$

In the Table 2.4.4 we present the results of the OLS test. As we can see the limit on the losses of reinsurer c_2 is considerably smaller when Pareto optimality principles is in place. It is around $40,000$ whereas we observed the values around $50,000$ for the optimisation problem from insurer's point of view. This result is consistent with Pareto optimality principle which involves also the objective function of the reinsurer who aims at minimising its own losses.

Table 2.4.4: Results of admissibility test for aggregate losses for Pareto optimality princile

Distribution	Admissibility $\epsilon=1$	Admissibility $\epsilon=10$	mean (stdev) of $\tilde{b}$	mean (stdev) of $\tilde{c_1}$	mean (stdev) of $\tilde{c_2}$
Lognormal	99.2%	100%	1 (0)	0.08825 (0.3009)	41,213 (1,676)
Exponential	98.7%	100%	1 (0)	0.0542 (0.194)	39,982 (1,451)
Gamma	98.1%	100%	1 (0)	0.0642 (0.1284)	40,982 (1,582)
Pareto	99.1%	100%	1 (0)	0.0769 (0.0634)	41,128 (1,522)

2.5 Conclusion

We analyse two approaches to optimal reinsurance in this chapter and demonstrate numerical examples related to each of them. First approach discussed optimal reinsurance model from insurer's point of view, and the second approach demonstrated a model which uses Pareto optimality principle. We use different premium principles for each approach and solve optimality problems for each premium principles using Second Order Conic Programming. Numerical illustrations demonstrate that proportional reinsurance is optimal when risk measure follows expected value principle. When standard deviation principle and one-sided moments are used for calculation of reinsurance premium, optimality is obtained when the model takes the form functional form $\sum R = \sum X \wedge c$, where c is a constant, X is loss amount and R is loss of the reinsurer. This is a special case of capped stop loss reinsurance. Thus, the shape of optimal ceded loss function can vary for different types of reinsurance premium principles. Our results demonstrate that the functional form of optimal reinsurance contact depends on the adopted reinsurance premium principle and hence emphasize the important role of the premium principle in the determination of the optimal design. Moreover, we observed that the limit on the aggregate losses of reinsurer is considerably smaller when Pareto optimality principle is in place, provided that all the parameters in the numerical examples are the same for both problems. Similarly, for expected value premium principle the share of the reinsurer in quota-share reinsurance contract is less for Pareto optimal models. This result is intuitive, due to the fact that the Pareto optimality principle involves objective function of the reinsurer who aims at minimising its own losses.

As the next step, this research can be extended to the cases when there is a dependence among individual risks, different lines of business or claim sizes and numbers which can be modelled using multivariate distributions and copula functions, and this can increase or decrease the share of the insurer/reinsurer in the losses subject to this correlation being positive or negative. Interdependency of the risks is real and therefore it is of great interest to have a better understanding on how the shape of the optimal reinsurance contract would be affected under this assumption. Dependence among risks of different lines of business can strongly affect the overall risk of the company. Moreover, there are many cases within one line of business when the assumption about the independence among risks is violated, for example, the remaining life-times of a group life policies for employees of one company (i.e. oilfield offshore companies) can be considered to have some positive dependency. Several concepts of dependencies in insurance have appeared in the actuarial literature up to now. According to Shi et al. [2015] claims for different business lines are not independent. Krämer et al. [2013] demonstrate that claim securities are not independent of the claim frequencies and provide a model to capture this dependency. Frees and Valdez [1998] provide introduction to the theory of copulas for the application in actuarial science and investigate some of the practical applications of copulas including reinsurance pricing. The paper also demonstrates that simulation of multivariate outcomes can be accomplished when the distribution is expressed as a copula. This can be very useful when solving the optimisation problem numerically. Given the distribution functions for each line of business or for individual risks, the effect of change in the dependency assumption on the functional form of reinsurance contracts can be investigated. Another objective can be the use of the joint distribution of losses or different lines of business to determine optimal reinsurance contract by minimising Conditional Tail Expectation. For this purpose applicable functional forms of copulas to be used in the optimisation model can be chosen or estimated from given data using maximum likelihood method and then multivariate distribution for the losses can be derived.It is also possible to add some *probabilistic constraints*, such as a guarantee of a minimum level of expected profit with some probability, to the optimisation problems. Furthermore, this research can be extended to applying stochastic optimal control theory to solve optimal reinsurance problems for life insurance.

2.6 Appendix

Proof of Proposition 2.3.1 Recall that the objective function (2.19) is increasing and continuous in u and therefore, the first inequality constraint of the SOCP reformulation becomes identity constraint when the optimal solution is attained. Moreover, it is not difficult to find that

$$g(x,y) = \sqrt{x^2+y^2+xy} = \sqrt{\Big(x+y/2\Big)^2 + \Big(\sqrt{3}y/2\Big)^2} = \|\mathbf{B}\ (x,y)\|. \tag{2.47}$$

Putting these two facts together, it becomes now clear why the optimisation problems from (2.17) and (2.19) are equivalent.

Proof of Proposition 2.3.2 Recall that $x \mapsto g(a_1P - a_1x, y) + g(a_2x, z) + x$ is non-decreasing, which implies that solving (2.20) is equivalent to solving the following surrogate optimisation problem

$$\begin{aligned}
\min_{\substack{(\mathbf{Y},\mathbf{Z},w)\in \\ \Re^{r\times m}\times\Re^{r\times m}\times\Re}} \quad & \left\{ g\left(a_1P - a_1w, \frac{b_1}{m}\sum_{k=1}^m \mathbf{1}^T\mathbf{y}_k\right) + g\left(a_2w, \frac{b_2}{m}\sum_{k=1}^m \mathbf{1}^T\mathbf{z}_k\right) + w + c_4\sum_{k=1}^m \mathbf{1}^T\mathbf{y}_k \right\} \\
\text{s.t.} \quad & \frac{1}{m}\sum_{k=1}^m \mathbf{1}^T\mathbf{z}_k + \frac{b}{\sqrt{m-1}}\|\mathbf{Q}\Big(\mathbf{1}^T\mathbf{z}_1, \mathbf{1}^T\mathbf{z}_2, \ldots, \mathbf{1}^T\mathbf{z}_m\Big)\| \le P, \\
& \frac{1}{m}\sum_{k=1}^m \mathbf{1}^T\mathbf{z}_k + \frac{b}{\sqrt{m-1}}\|\mathbf{Q}\Big(\mathbf{1}^T\mathbf{z}_1, \mathbf{1}^T\mathbf{z}_2, \ldots, \mathbf{1}^T\mathbf{z}_m\Big)\| \le w, \\
& \mathbf{A}\mathbf{y}_k \le \mathbf{A}\mathbf{x}_k, \mathbf{A}\mathbf{z}_k \le \mathbf{A}\mathbf{x}_k, \mathbf{y}_k + \mathbf{z}_k = \mathbf{x}_k \ \text{ for all } \ 1 \le k \le m.
\end{aligned} \tag{2.48}$$

As previously mentioned in the proof of Proposition 2.3.1, $g(x,y) = \|\mathbf{B}\ (x,y)\|$, which allows one to reformulate (2.48) in an epigraph form as displayed in (2.21). Therefore, any optimal solution of (2.48) solves (2.21), which in turn solves (2.20). The proof is now complete.

Proof of Proposition 2.3.3 It is not difficult to find that the derivative of the objective function (2.31) of the generic form $\gamma g(a_1 P - a_1 x, y) + \gamma g(a_2 x, z) + (1-\gamma) g(a_1 x, z) + (2\gamma - 1)x$ with respect to x is

$$\frac{\gamma a_2(2a_2x+z)}{2\sqrt{a_2^2x^2+a_2zx+z^2}} + \frac{(1-\gamma)a_1(2a_1x+z)}{2\sqrt{a_1^2x^2+a_1zx+z^2}} - \frac{\gamma a_1(2a_1(P-x)+y)}{2\sqrt{a_1y(P-x)+a_1^2(P-x)^2+y^2}} + 2\gamma - 1 \geq -\gamma a_1 + 2\gamma - 1$$

Thus, if $\gamma \geq \frac{1}{2-a_1}$, the above is non-negative and therefore, the objective function is non-decreasing. Since the objective function of (2.31) is non-decreasing in $x \in [0, P]$ and, as previously mentioned, $g(x, y) = \|\mathbf{B}\ (x, y)\|$, then the first three inequality constraints of (2.32) become identity constraints, where the optimal solution is attained. Therefore, any optimal solution of (2.32) solves (2.31). The proof is now complete.

Proof of Proposition 2.3.4 If $(\mathbf{Y}^*, \mathbf{Z}^*, \boldsymbol{\tau}, u^*, v^*, w^*, r^*, t^*)$ solves (2.36), then $(\mathbf{Y}^*, \mathbf{Z}^*, u^*, v^*, w^*, t^*)$ solves (2.32).

Assume that $(\mathbf{Y}^*, \mathbf{Z}^*, \boldsymbol{\tau}, u^*, v^*, w^*, r^*, t^*)$ solves (2.36), but $(\mathbf{Y}^*, \mathbf{Z}^*, u^*, v^*, w^*, t^*)$ does not solve (2.32). That is, there exists $(\mathbf{Y}, \mathbf{Z}, u, v, w, t) \in \Re^{r\times m} \times \Re^{r\times m} \times \Re \times \Re \times \Re \times \Re$ feasible to (2.32), i.e.

$$\pi(\mathbf{Z}, e, d) := \frac{1}{m}\sum_{k=1}^{m} \mathbf{1}^T\mathbf{z}_k + e\left(\frac{1}{m}\sum_{k=1}^{m}\left(\mathbf{1}^T\mathbf{z}_k - \frac{1}{m}\sum_{k=1}^{m}\mathbf{1}^T\mathbf{z}_k\right)_+^d\right)^{1/d} \leq t, \tag{2.49}$$

such that $t < t^*$. Recall that $(\mathbf{Y}^*, \mathbf{Z}^*, \boldsymbol{\tau}, u^*, v^*, w^*, r^*, t^*)$ is feasible to (2.36), i.e.

$$r^* + e_1\left(\sum_{k=1}^{m}\tau_k^{*d}\right)^{1/d} \leq t, \mathbf{Z}^{*T}\mathbf{1} - r^*\mathbf{1} \leq \boldsymbol{\tau}^*, \mathbf{0} \leq \boldsymbol{\tau}^*. (2.50)$$

Note that, $(\mathbf{Y}, \mathbf{Z}, \boldsymbol{\tau}, u, v, w, r, t)$ is feasible to (2.36), where

$$\boldsymbol{\tau} = \left(\mathbf{1}^T\mathbf{z}_k - \frac{1}{m}\sum_{k=1}^{m}\mathbf{1}^T\mathbf{z}_k\right)_+, \tag{2.51}$$

since

$$r + e_1\left(\sum_{k=1}^{m}\tau_k^{**d}\right)^{1/d} = \frac{1}{m}\sum_{k=1}^{m}\mathbf{1}^T\mathbf{z}_k + e\left(\frac{1}{m}\sum_{k=1}^{m}\left(\mathbf{1}^T\mathbf{z}_k - \frac{1}{m}\sum_{k=1}^{m}\mathbf{1}^T\mathbf{z}_k\right)_+^d\right)^{1/d} \leq t, \tag{2.52}$$

$$\boldsymbol{\tau} = \left(\mathbf{1}^T\mathbf{z}_k - \frac{1}{m}\sum_{k=1}^{m}\mathbf{1}^T\mathbf{z}_k\right)_+ \geq \mathbf{0}, \tag{2.53}$$

$$\boldsymbol{\tau} = \left(\mathbf{1}^T\mathbf{z}_k - \frac{1}{m}\sum_{k=1}^{m}\mathbf{1}^T\mathbf{z}_k\right)_+ \geq \mathbf{1}^T\mathbf{z}_k - \frac{1}{m}\sum_{k=1}^{m}\mathbf{1}^T\mathbf{z}_k \tag{2.54}$$

And since $t < t^*$ we get contradiction to our assumption.

If $(\mathbf{Y}^*, \mathbf{Z}^*, u^*, v^*, w^*, t^*)$ solves (2.32), then $(\mathbf{Y}^*, \mathbf{Z}^*, \boldsymbol{\tau}^*, u^*, v^*, w^*, r^*, t^*)$ solves (2.36), where

$$\boldsymbol{\tau} = \left(\mathbf{1}^T\mathbf{z}_k - \frac{1}{m}\sum_{k=1}^{m}\mathbf{1}^T\mathbf{z}_k\right)_+ \tag{2.55}$$

Assume that $(\mathbf{Y}^*, \mathbf{Z}^*, u^*, v^*, w^*, t^*)$ solves (2.32), but there exists $(\mathbf{Y}, \mathbf{Z}, \boldsymbol{\tau}^*, u, v, w, r, t) \in \Re^{r\times m} \times \Re^{r\times m} \times \Re^m \times \Re \times \Re \times \Re \times \Re \times \Re$ feasible to (2.36), i.e.

$$r + e_1\left(\sum_{k=1}^{m}\tau_k^{**d}\right)^{1/d} \leq t, \mathbf{0} \leq \boldsymbol{\tau}, \mathbf{Z}^{**T}\mathbf{1} - r\mathbf{1} \leq \boldsymbol{\tau} \tag{2.56}$$

such that $t < t^*$.

As before, it is sufficient to show that $(\mathbf{Y}, \mathbf{Z}, u, v, w, t)$ is feasible to (2.32).

$$r + e_1\left(\sum_{k=1}^{m}\tau_k^{**d}\right)^{1/d} \geq \frac{1}{m}\sum_{k=1}^{m}\mathbf{1}^T\mathbf{z}_k + e\left(\frac{1}{m}\sum_{k=1}^{m}\left(\mathbf{1}^T\mathbf{z}_k - \frac{1}{m}\sum_{k=1}^{m}\mathbf{1}^T\mathbf{z}_k\right)_+^d\right)^{1/d}, \tag{2.57}$$

since

$$r + e_1\left(\sum_{k=1}^{m}\tau_k^{**d}\right)^{1/d} \leq t, \mathbf{0} \leq \boldsymbol{\tau}, \mathbf{Z}^{**T}\mathbf{1} - r\mathbf{1} \leq \boldsymbol{\tau} \tag{2.58}$$

and the fact that the objective function is non-decreasing in each argument. If

$$\frac{1}{m}\sum_{k=1}^{m}\mathbf{1}^T\mathbf{z}_k + e\left(\frac{1}{m}\sum_{k=1}^{m}\left(\mathbf{1}^T\mathbf{z}_k - \frac{1}{m}\sum_{k=1}^{m}\mathbf{1}^T\mathbf{z}_k\right)_+^d\right)^{1/d} \leq r + e_1\left(\sum_{k=1}^{m}\tau_k^{**d}\right)^{1/d} \leq t, \tag{2.59}$$

then $(\mathbf{Y}, \mathbf{Z}, u, v, w, t)$ is feasible to (2.32). The proof is now complete.

Chapter 3

Solvency analysis of deferred annuities

3.1 Introduction

Annuity products play a significant role in protecting policyholders from longevity risk, providing minimum guaranteed income and reducing the risk of outliving their retirement assets. Regulators therefore have a strong incentive to better understand the solvency characteristics of annuity products due to the fact that substantial systematic longevity risk seriously affects annuity providers' solvency. While the solvency characteristics of immediate life annuities have been studied to a large extent, the role of deferred annuity liabilities in the portfolios of annuity providers has not been considered thoroughly in the literature.

Yaari [1965] demonstrates that a risk averse person should convert all their assets to an immediate annuity due to the fact that people who die earlier subsidise those who live longer. However, the evidence shows that retirees are reluctant to convert retirement savings into annuities voluntarily. This effect is called the ”annuity puzzle” and many authors have attempted to research it. The main reasons proposed to explain this low demand for annuities include the mortality risk-sharing among family members (Brown and Poterba [1999], the possibility of health care expenditure shocks at an old age (Davidoff [2009]) and the existence of provision through social security and DB pension scheme membership (Dushi and Webb [2004]). Davidoff et al. [2005] conclude that due to psychological or behavioral biases limited annuity purchases are feasible.

As a result of the discounting effect and the possibility that the annuitant may not live until benefit payments start, a deferred annuity is much cheaper than an immediate annuity with identical benefits and therefore could play an important role in households' portfolios. Hu and Scott [2007] apply Cumulative Prospect Theory (CPT) to the analysis of annuities and demonstrate that CPT can explain the low demand for immediate annuities purchased at retirement and higher preference for deferred annuities. Chen et al. [2019] extend this analysis and show that immediate annuities are not attractive for retirees at all ages due to loss aversion and that preferences for deferred annuities increase with the deferred period. Chen et al. [2018] demonstrates that a hyperbolic discount model can explain the low demand of immediate annuities at retirement and the greater attractiveness of long-term deferred annuities. In this section we analyse solvency characteristics of deferred annuities using different assumptions and scenarios for longevity and investment risk.

Assumptions about underlying mortality and interest rate dynamics play an important role in pricing and solvency assessment of life annuity contracts. Comparing the results for deterministic and stochastic mortality models we estimate the importance and effect of random changes in the mortality for solvency analysis. The systematic risk component is analysed in Coppola et al. [2000], Coppola et al. [2002], Olivieri [2001], or Pitacco [2004]. In Olivieri and Pitacco [2003] instead of stochastic realisations the authors use a finite range of mortality scenarios and differentiate between pooling and non-pooling risks. In contrast, De Waegenaere et al. [2010] examine pension annuities in a generalized Lee-Carter model. A stochastic Gompertz-model is used in Christiansen and Helwich [2008] both for temporary life and pure endowment insurance. Bauer and Weber [2008] and Hari et al. [2008] calculate the VaR and the expected shortfall for immediate starting life annuities using different static hedging scenarios and analyse solvency aspects. Artzner et al. [1999] present a unified framework for the analysis, construction, and implementation of different measures of risk such as VaR and expected shortfall. Artzner et al. [1999] and McNeil et al. [2005] describe the theoretical grounds and advantages of using expected shortfall measure.

There is indeed a big choice of stochastic mortality models in the literature. Booth and Tickle [2008] provides a comparison between different stochastic mortality models such as two-factor models, regression-based (GLM) methods and three-factor methods. According to this paper two-factor Lee–Carter method, and, in particular, its variants, have been successful in terms of accuracy of goodness of fit and forecasting. However, regression based models have been less successful, due to nonlinearities in time. Haberman and Renshaw [2011] compares different stochastic mortality models using England and Wales mortality experience and conducts detailed comparisons at pensioner ages. Furthermore, the model is extended to include the England and Wales female data and USA mortality experiences over a wider age range including the working ages. Similarly, Cairns et al. [2009] provides a quantitative review of some of the most commonly used ones in practice. The choice of a model requires significant judgement by the analyst and a change in the model can significantly impact solvency margins and the best-estimate reserves [Richards and Currie, 2009]. Therefore, the notion of model risk is particularly important, and it requires the use of more than one stochastic mortality model when estimating longevity risk.

We use the solvency analysis method from Olivieri and Pitacco [2003] for immediate annuities in order to compare solvency margins to deferred annuities given a range of deferred periods. This approach is based on Solvency II principles. In general, Solvency

II is a directive in European Union law that harmonises the EU insurance regulation and outlines the amount of capital that EU insurance companies must hold to reduce the risk of insolvency. Deferred life annuities are policies which provide life-long payments to the annuitants after a certain period of time conditional on survival. Exposure to the longevity risk and interest rate risk is an important issue for an insurance company particularly in the case of deferred annuities when the payments are postponed.

Moreover, the contributions and benefits are highly exposed to interest rate risk because of the long term nature of the contracts. Therefore, in this chapter we aim to contribute to the exsisting literature on deferred annuities by conducting a solvency analysis allowing for stochastic nature of the interest rates and estimating the combined effects of stochastic mortality and interest rates for solvency analysis.

The results of the stochastic models are compared to the results of deterministic counterpart model which allows us to analyse the effects of different degrees of randomness. Essentially, our analysis contains three risk scenarios: the benchmark case where mortality rates and interest rates are both deterministic, second case where only mortality rates are stochastic and the last case where mortality rates and interest rates are both stochastic.

Since pension annuities are particularly affected by longevity and investment risk, for the purposes of this thesis we focus on these risks only, disregarding expense, and economic risks, such as inflation.

We observe that the risk of random fluctuations in mortality decrease with increasing cohort size because fluctuations are smoothed in large homogeneous portfolios. Our results show the importance of systematic risk in comparison to the risk of random fluctuations. Moreover, the chapter outlines the dramatic importance of model risk and deferred period in the estimation of solvency margins. This also has a significant effect on solvency margins with increasing deferred periods which is caused by the extra longevity risk and the greater uncertainty about numbers of future survivors.

The structure of this chapter is as follows: Section 3.2 describes the general model for the calculation of solvency margins. We continue in Section 3.3 with discussing the model from Olivieri and Pitacco [2003] and our adjustment to the method by using CMI working paper [CMI, 2016] and fitting it to deferred annuities. Section 3.4 discusses different stochastic mortality models and calculation of solvency margins for these models with deterministic interest rates, while Section 3.5 considers the improvement of the chosen models by introducing stochastic interest rates. Section 3.6 considers some possible extensions to this chapter and Section 3.7 concludes the chapter.

3.2 General model for solvency margins

We consider a portfolio of N_0 identical deferred life annuities with annual payment R starting at $d \geq 0$ as long as the insured is living and until the contract expiration $\omega - x_0$ where x_0 is the initial age of the insureds and ω denotes the biological age limit. The single premium for group of lives P is paid in advance at the launch of the contract. The remaining lifetimes of the insureds which are independent and identically distributed and are described with some mortality law to be specified.

Let N_t denote the random number of insureds alive at time t at age $x_0 + t$. Thus, the random number of people dying in the time interval $(t, t+1)$ can be expressed as $D_t = N_t - N_{t+1}$.

Several quantities in this chapter, such as the total benefits to policyholders R_t during the year t, portfolio reserve $\mathcal{V}_t$, are functions of the random numbers D_t and N_t. Specifically, the portfolio reserve is random due to the fact that it is the sum of a random number of individual reserves:

$$\mathcal{V}_t = N_t V_t, \quad t = 0, ..., \omega - x_0, \tag{3.1}$$

where V_t is the individual reserve, calculated with a given (conservative) basis.

Using the retrospective approach, the random portfolio fund at time t, denoted Z_t, also depends on the random number of policyholder alive

$$Z_0 = P + C, \tag{3.2}$$

$$Z_t = Z_{t-1}(1+i) - R_t, \quad t = 1, 2, ..., \omega - x_0, \tag{3.3}$$

where i is the rate of return earned by the fund and C is the initial capital. In practice, C can equivalently be partially financed by an additional premium loading. The variable $Z_t - \mathcal{V}_t$ is called the *free portfolio fund*.

One of the possible ways to assess solvency of the fund described in Olivieri and Pitacco [2003] is described below. The insurance company is considered solvent at a given time t if the free portfolio fund is positive,

$$Z_t - \mathcal{V}_t \geq 0. \tag{3.4}$$

The aim of this section is to determine the solvency margin required at time 0 such that one of the following conditions is satisfied:

$$Pr\left\{\bigwedge_{t=1}^{T}(Z_t - \mathcal{V}_t \geq 0)\right\} = 1 - \epsilon \tag{3.5}$$

or

$$Pr\left\{Z_T - \mathcal{V}_T \geq 0\right\} = 1 - \epsilon, \tag{3.6}$$

where T is the time horizon and ϵ is the ruin probability.

The *Solvency Margin* is based on VaR principle and is the additional capital $Z_0 - V_0$ needed at time $t = 0$ so that one of the conditions (3.5) and (3.6) is satisfied. For the purposes of analysis in this chapter we will be using condition (3.6) in order to assess solvency margins. Note that since by definition the initial reserve V_0 is equal to the single premium, the solvency margin at time 0 is $Z_0 - V_0 = Z_0 - P = C$ and must be financed with shareholders' funds, i.e. initial capital or additional premium loading. For the purposes of this chapter we consider a portfolio of immediate or deferred annuities and adopt a run-off approach. In addition, in the case of full stochastic mortality models we investigate the results for expected shortfall (ES). This risk measure is widely used in some countries for solvency purposes and in Basel Committee on Banking Supervision's accords. It quantifies the amount of tail risk a portfolio has. Expected shortfall is derived by taking a weighted average of the "extreme" losses in the tail of the distribution of possible losses, beyond the value at risk (VaR) cutoff point. This metrics focuses on the expected size of a loss assuming that a given p-value has been breached or, in other words, it is the expected loss of the portfolio in the worst $p\%$ of cases. It has a number of theoretical and practical advantages. When losses are not normally distributed, which is mostly the case in practice, expected shortfall produces higher results for solvency margins than VAR. Moreover, expected shortfall is a coherent risk measure meaning that if several portfolios are combined, the total expected shortfall decreases, hence reflecting the advantages of diversification, whereas VAR can increase. VaR and ES results are related and can be calculated from the same set of simulated losses.

3.3 Model for projection of survival rates and its results for solvency margins

In this section we discuss the model used to project mortality rates and the results of our projections for solvency margins. In general, we assume that there are two sources of uncertainty, one due to process risk (random fluctuations risk), related to the individual times of deaths, and another one due to systematic risk (longevity risk) linked to the uncertainty in future death rates. Therefore, we model the evolution of the number of survivors through

$$D_t|N_t, q_{x_0+t} \sim Bin(N_t, q_{x_0+t}). \tag{3.7}$$

Depending on the modelling approach chosen in sections 3.3 and 3.4, the future death rates q_{x_0+t} will be modelled as deterministic quantities or as random quantities chosen in a finite set of scenarios (section 3.3) or resulting from a full stochastic mortality model (section 3.4).

The stochastic approach discussed in this section is implemented with a set of projected mortality functions. This approach allows for both the random fluctuation risk and the longevity risk. A "degree of belief" is assigned to each mortality function. The results of this stochastic approach with several scenarios are then compared to the results obtained from a set of full stochastic mortality models in section 3.4.
For the methods outlined above, we choose three projected mortality functions, denoted by $q^{[min]}$, $q^{[med]}$ and $q^{[max]}$ which express a small, a medium and a high mortality respectively. Only $q^{[med]}$ function is used in the deterministic approach. The stochastic approach exploits all three functions, applying "degree of belief" to each of them. For the purposes of this chapter we determine $q^{[min]}$, $q^{[med]}$ and $q^{[max]}$ functions using the CMI Mortality Projections Model [CMI, 2016] developed by IFOA's Mortality Projections Committee. We consider England and Wales mortality data for the period 1965-2011 for ages $0-100$ which contain age-specific deaths and exposures for England and Wales from the Human Mortality Database and use quadratic interpolation to close the life table and obtain death rates for ages $101-120$. We observed that during this period the maximum, medium and minimum levels of annual mortality improvements across all ages were 4.16%, 2.34% and 0.16% respectively. Note that we have excluded negative mortality improvement rates. When we use these exact improvement rates the difference in solvency margins between deterministic and stochastic models is not stable. Therefore, also considering the fact that according to current trends mortality improvements in the future are likely to be lower, we apply a 20% decrease to the maximum mortality improvement rate and use the obtained rates as inputs for CMI model in order to project $q^{[min]}$ for the future. Thus,

20% decrease is applied to $q^{[min]}$ and the improvement rate of 4.16% per annum.

One of the portfolios we are analysing consists of identical immediate annuities, paid to policyholder's of initial age $x_0 = 65$, with annual amount $R = 100$. The other portfolio consists of identical deferred annuities with deferred period $d > 0$. The constant annual interest rate for calculation of the premium and the reserves is $i = 0.03$. The single premium which is paid at the launch of the contract and individual reserves are calculated according to the survival function $S^{[med]}(x)$.

The only source of uncertainty in the deterministic model is the time of death, because the probability distribution of the future lifetime of each insured is predefined. As mentioned above, we first produce results for the benchmark case when the deferred period is $d = 0$, and then compare it to $d = 5, 10, 15, 20$ in order to inspect the behaviour of the required solvency margin with respect to the corresponding deferred period. The corresponding solvency margins for are reported in Table 3.3.1 for two time horizons, $T = \omega - x_0 = n$ and $T = 5$. Solvency margins are higher for the longer time horizons reflecting the higher uncertainty (risk). As far as the size of the portfolio is concerned, Table 3.3.1 demonstrates that the required margin decreases as N_0 increases. This is due to the fact that in a deterministic approach, the insurance company is only exposed to a diversifiable pooling risk, which is the result of an insufficiently large insurance cohort. These results are similar both for immediate and deferred annuities. However, we can observe from the table that the relative solvency margins $\frac{Z_0 - \mathcal{V}_0}{\mathcal{V}_0}$ are higher for the deferred annuities. Clearly, there are fewer benefit payments during the same time horizon in the case of the deferred annuities due to the postponed payment time, and therefore lower reserves are required to be held. However, the relative solvency margins are higher due to the riskiness and uncertainty associated with the postponed time of the benefit payments.

Table 3.3.2 demonstrates the dependence of solvency margins on ruin probabilities. As we can see, the lower the ruin probability ϵ is the higher is the required solvency margin.

Table 3.3.1: Required absolute and relative solvency margins for immediate and deferred annuities for $\epsilon = 0.025$. Deterministic model.

	Immediate annuities				Deferred annuities ($d = 5$)			
	$T = n$		$T = 5$		$T = n$		$T = 5$	
N_0	$Z_0 - \mathcal{V}_0$	$\frac{Z_0 - \mathcal{V}_0}{\mathcal{V}_0}$	$Z_0 - \mathcal{V}_0$	$\frac{Z_0 - \mathcal{V}_0}{\mathcal{V}_0}$	$Z_0 - \mathcal{V}_0$	$\frac{Z_0 - \mathcal{V}_0}{\mathcal{V}_0}$	$Z_0 - \mathcal{V}_0$	$\frac{Z_0 - \mathcal{V}_0}{\mathcal{V}_0}$
100	10335	7.47%	6302	4.55%	9646	10.21%	4948	5.24%
1,000	33031	2.39%	21305	1.54%	30757	3.26%	17384	1.84%
10,000	106548	0.77%	69087	0.50%	98906	1.05%	56838	0.60%
100,000	334160	0.24%	218185	0.16%	309699	0.33%	180114	0.19%
1,000,000	1054597	0.08%	697866	0.05%	981717	0.10%	578354	0.06%

Table 3.3.2: Required relative solvency margins for $d = 5$ for different ϵ's. Deterministic model.

	$T = n$			$T = 5$		
N_0	$\epsilon = 0.01$	$\epsilon = 0.025$	$\epsilon = 0.05$	$\epsilon = 0.01$	$\epsilon = 0.025$	$\epsilon = 0.05$
100	12.12%	10.21%	8.61%	6.34%	5.24%	5.11%
1,000	3.85%	3.26%	2.74%	2.17%	1.84%	1.62%
10,000	1.24%	1.05%	0.88%	0.71%	0.60%	0.51%
100,000	0.39%	0.33%	0.28%	0.23%	0.19%	0.16%
1,000,000	0.12%	0.10%	0.09%	0.07%	0.06%	0.05%

Table 3.3.3 demonstrated the dependence of solvency margins on different deferred periods d for different initial portfolio sizes N_0 and time horizons T. We notice that the bigger the deferred period is the higher are the relative solvency margins. We also notice that solvency margins are equal for the all the cases where $d \geq T$. This is because the deferred period does not play any role if the time horizon for which we are analysing solvency margins is less than or equal to the deferred period. This result is intuitive considering the fact that in all these cases there are no payments before time T, therefore, at the launch of the contact in all the cases where $d \geq T$ the company needs to hold the same relative solvency margins in order to be solvent at the time T regardless of the time in future after time T when the first payment is going to take place.

With the deterministic approach, the insurance company is only exposed to a diversifiable pooling risk. In reality, there exists also a non-pooling risk which cannot be

Table 3.3.3: Required relative solvency margins for different deferred periods d, time horizons T and portfolio sizes N when $\epsilon = 0.025$. Deterministic model

	$N_0 = 100$			$N_0 = 10,000$			$N_0 = 1,000,000$		
d	$T = n$	$T = 10$	$T = 5$	$T = n$	$T = 10$	$T = 5$	$T = n$	$T = 10$	$T = 5$
0	7.47%	6.02%	4.55%	0.77%	0.64%	0.50%	0.08%	0.06%	0.05%
5	10.21%	7.95%	5.24%	1.05%	0.83%	0.60%	0.10%	0.08%	0.06%
10	13.60%	8.88%	5.24%	1.39%	0.96%	0.60%	0.14%	0.10%	0.06%
20	18.22%	8.88%	5.24%	1.84%	0.96%	0.60%	0.18%	0.10%	0.06%
30	39.54%	8.88%	5.24%	3.81%	0.96%	0.60%	0.38%	0.10%	0.06%

diversified due to the fact that it affects each individual's mortality in the same manner. Therefore, stochastic mortality models need to be introduced. In the stochastic model, solvency margins are evaluated considering not only uncertainty about the time of death of each insured but also uncertainty in future mortality trends and the actual distribution of the future lifetimes. It is assumed that each of the three mortality functions $q^{[min]}$, $q^{[med]}$ and $q^{[max]}$ can be a possible distribution of the future lifetime in the cohort. The single premium and individual reserve are still calculated using the function $q^{[med]}$ and the interest rate $i = 0.03$. We assign weights $\rho^{[min]} = 0.2$, $\rho^{[med]} = 0.6$ and $\rho^{[max]} = 0.2$ representing the "degree of belief" for the three survival functions respectively and choose the survival function through simulation. Then the actual number of surviving policyholders is simulated assuming that under a given mortality function the policyholders are independent risks. Changes in parameters ρ and i might strongly affect the results, therefore as a next step in our research we are going to use different stochastic models for i in section 3.4 and mortality rates in order to analyse solvency in section 3.5.

Table 3.3.4 compares the results for solvency margins for immediate and deferred annuities for the stochastic model. The comparison between the stochastic and deterministic case demonstrates a strong increase of the required solvency margin in the former both for immediate and deferred annuities. This is due to the fact that the stochastic model allows us to analyse not only the risk of random fluctuations in the number of survived policyholders, but also systematic deviations, i.e. the longevity risk which is a non-pooling risk.

Table 3.3.4: Required absolute and relative solvency margins for immediate and deferred annuities for $\epsilon = 0.025$. Stochastic model.

	Immediate annuities				Deferred annuities ($d = 5$)			
	$T = n$		$T = 5$		$T = n$		$T = 5$	
N_0	$Z_0 - \mathcal{V}_0$	$\frac{Z_0 - \mathcal{V}_0}{\mathcal{V}_0}$	$Z_0 - \mathcal{V}_0$	$\frac{Z_0 - \mathcal{V}_0}{\mathcal{V}_0}$	$Z_0 - \mathcal{V}_0$	$\frac{Z_0 - \mathcal{V}_0}{\mathcal{V}_0}$	$Z_0 - \mathcal{V}_0$	$\frac{Z_0 - \mathcal{V}_0}{\mathcal{V}_0}$
100	11854	8.56%	6574	4.75%	11123	11.78%	6024	6.38%
1,000	69226	5.00%	29663	2.14%	64816	6.86%	24631	2.61%
10,000	558634	4.04%	211851	1.53%	525365	5.56%	175908	1.86%
100,000	5179169	3.74%	1861356	1.34%	4874397	5.16%	1548893	1.64%
1,000,000	50479496	3.65%	17790597	1.29%	47519369	5.03%	14807651	1.57%

Table 3.3.5: Required relative solvency margins for $d = 5$ for different ϵ's. Stochastic model.

	$T = n$			$T = 5$		
N_0	$\epsilon = 0.01$	$\epsilon = 0.025$	$\epsilon = 0.05$	$\epsilon = 0.01$	$\epsilon = 0.025$	$\epsilon = 0.05$
100	13.81%	11.78%	9.92%	7.04%	6.38%	6.27%
1,000	7.70%	6.86%	6.09%	3.05%	2.61%	2.28%
10,000	5.81%	5.56%	5.32%	2.00%	1.86%	1.73%
100,000	5.24%	5.16%	5.08%	1.68%	1.64%	1.60%
1,000,000	5.06%	5.03%	5.01%	1.58%	1.57%	1.55%

Similar to the deterministic case we can observe from the table that the relative solvency margins $\frac{Z_0 - \mathcal{V}_0}{\mathcal{V}_0}$ are higher for the deferred annuities whereas absolute solvency margins $Z_0 - \mathcal{V}_0$ are lower. Moreover, time horizon $T = 5$ leads to a solvency margin significantly lower than for $T = n$ which again outlines the effect of higher riskiness of longer time horizons.

Table 3.3.5 demonstrates dependence of solvency margins on different ruin probabilities ϵ for the stochastic model. As in the case with the deterministic approach Table 3.3.6 shows that solvency margins are higher for longer deferred periods.

Systematic risk has a substantial impact on the solvency requirements. By comparing Table 3.3.1 with Table 3.3.4, and Table 3.3.2 with Table 3.3.5, we can see that the trends in the stochastic approach are quite similar to the trends in the deterministic approach, however the magnitude of solvency margins in the stochastic model is much greater. This is due to the fact that stochastic framework allows us to take into consideration not only

Table 3.3.6: Required relative solvency margins for different deferred periods d, time horizons T and portfolio sizes N when $\epsilon = 0.025$. Stochastic model

	$N_0 = 100$			$N_0 = 10,000$			$N_0 = 1,000,000$		
d	$T = n$	$T = 10$	$T = 5$	$T = n$	$T = 10$	$T = 5$	$T = n$	$T = 10$	$T = 5$
0	8.56%	6.51%	4.75%	4.04%	2.69%	1.53%	3.65%	2.37%	1.29%
5	11.78%	8.58%	5.24%	5.56%	3.57%	1.86%	5.03%	3.16%	1.57%
10	15.72%	10.12%	5.24%	7.31%	4.13%	1.86%	6.61%	3.66%	1.57%
20	21.66%	10.12%	5.24%	8.99%	4.13%	1.86%	8.04%	3.66%	1.57%
30	41.70%	10.12%	5.24%	12.74%	4.13%	1.86%	10.61%	3.66%	1.57%

risk of random fluctuations in deaths but also non-pooling systematic risk.

3.4 Full stochastic mortality models

It is quite clear that the figures quoted so far strongly depend on the assumed choices, in particular the mortality models, survival functions and relevant weights. The projection of mortality rates is an important part of pension liabilities valuation and the choice of stochastic projection model plays significant role here. To a large extent the stochastic framework discussed above gives a general perspective of the severity of longevity risk. However, this model is static and does not account for systematic time trends. Therefore, analysis of solvency margins based on different stochastic mortality models is introduced below. Particular attention is given to the differences in the magnitude of solvency margins for different mortality models and how insurance regulators and practitioners might use them.

Generalised age-period-cohort (GAPC) stochastic mortality models as introduced by Hunt and Blake [2020] have four components, such as the random component, the systematic component, the link function and the set of parameter constraints. Consistently with the choice made in section 3.2, the number of deaths at age x and calendar year t

in the general population is considered to follow Binomial distribution.

$$D_{xt} \sim Bin(E^0_{xt}, q_{x,t}) \tag{3.8}$$

where $q_{x,t}$ is the death rate and E^0_{xt} is the initial exposed to risk. The link function of $q_{x,t}$ is the logit, given by $log\frac{q_{x,t}}{1-q_{x,t}} = \eta_{xt}$, where η_{xt} is the predictor. As described in Millossovich et al. [2015], the *systematic component* captures the effects of age x, calendar year t and cohort $c = t - x$ through the *predictor* η_{xt}

$$\eta_{xt} = \alpha_x + \sum_{i=1}^{N} \beta_x^{(i)} k_t^{(i)} + \beta_x^{(0)} \gamma_{t-x} \tag{3.9}$$

where α_x is the static age function capturing the general shape of mortality by age, $N \geq 0$ an integer indicating the number of age-period terms describing the mortality trends, with each time index
$k_t^{(i)}, i = 1, ..., N$ and the term γ_{t-x} accounts for the cohort effect with $\beta_x^{(0)}$ modulating its effect across ages.

There are many stochastic mortality models but for the purposes of this chapter we use 6 main representative models which have distinct features depending on whether they have cohort term, age modulating term and whether age is treated as quantitative variable or categorical variable.

One of the models discussed in this section is the stochastic mortality model by Lee and Carter [1992] which assumes that the predictor is given by:

$$\eta_{xt} = \alpha_x + \beta_x^{(1)} k_t^{(1)}. \tag{3.10}$$

The next model we discuss in this chapter is the stochastic mortality model by Renshaw and Haberman [2006] which generalises the Lee-Carter model by incorporating a cohort effect to obtain the predictor:

$$\eta_{xt} = \alpha_x + \beta_x^{(1)} k_t^{(1)} + \beta_x^{(0)} \gamma_{t-x}. \tag{3.11}$$

Independence between the period and the cohort effects is assumed in this model and time series forecasts of the estimated $k_t^{(1)}$ and γ_{t-x} are used to derive mortality projections.

Haberman and Renshaw [2011] also discussed a substructure of this model when $\beta_x^{(0)} = 1$ which is a simpler model and eliminates some stability issues from the original model.

$$\eta_{xt} = \alpha_x + \beta_x^{(1)} k_t^{(1)} + \gamma_{t-x}. \tag{3.12}$$

The age-period-cohort (APC) model is another substructure of the Renshaw and Haberman model, when $\beta_x^{(1)} = 1$, $\beta_x^{(0)} = 1$,

$$\eta_{xt} = \alpha_x + k_t^{(1)} + \gamma_{t-x}. \tag{3.13}$$

The Cairns et al. [2006] model (M5) proposes a predictor structure with two age-period terms with pre-specified age-modulating parameters $\beta_x^{(1)} = 1$, $\beta_x^{(2)} = x - \bar{x}$, no static age function and no cohort effect. Therefore, the predictor of the M5 model is:

$$\eta_{xt} = k_t^{(1)} + (x - \bar{x}) k_t^{(2)}, \tag{3.14}$$

where $\bar{x}$ is the average age in the data.

Another model that we use in this chapter is the so-called M7 model, which is a quadratic CBD model with cohort effects. The original CBD model (M5) was expanded in Cairns et al. [2009] by cohort effect and a quadratic age effect to obtain the predictor:

$$\eta_{xt} = k_t^{(1)} + (x - \bar{x}) k_t^{(2)} + ((x - \bar{x})^2 - \hat{\sigma}_x^2) k_t^{(3)} + \gamma_{t-x}, \tag{3.15}$$

where $\hat{\sigma}_x^2$ is the average value of $(x - \bar{x})^2$.

There are also other members of CBD model family, such as M6, M8 and M9 but as mentioned before we restrict this chapter to a range of models to cover a set of distinct

characteristics depending on whether they have cohort term, age modulating term and whether age is treated as quantitative variable or categorical.
The last model that we use is model by Plat [2009] where the CBD model is combined with some features of the Lee-Carter model. Plat model is suitable for full age ranges and also captures the cohort effect. The predictor in this model is given by

$$\eta_{xt} = \alpha_x + k_t^{(1)} + (x - \bar{x})k_t^{(2)} + (x - \bar{x})^+ k_t^{(3)} + \gamma_{t-x}, \tag{3.16}$$

where α_x is a static age function. There are three age period terms with pre-specified age-modulating parameters $\beta_x^{(1)} = 1$, $\beta_x^{(1)} = \bar{x} - x$, $\beta_x^{(3)} = (x - \bar{x})^+ = \max(0, x - \bar{x})$.
In general, the force of mortality μ is targeted with the logit *link* and the parameters of the model are estimated using the binomial distribution for the number of deaths.

ARIMA processes, under the assumption of independence between the period and the cohort effects are used to model and forecast k_t and γ_{t-x} in order to project mortality and, consistently with the prevailing literature, a multivariate random walk with drift is adopted to provide a reasonable fit for the k terms and ARIMA(1,1,0) for γ.

First, we implement a goodness-of fit test which is typically analysed by inspecting the residuals of the fitted models. Regular patterns in the residuals demonstrate the inability of the model to describe all the features of the data appropriately. We assess scaled deviance residuals in order to see if there are regular patterns in them:

$$r_{xt} = \mathrm{sign}(d_{xt} - \hat{d}_{xt})\sqrt{\frac{\mathrm{dev}(x,t)}{\hat{\phi}}}, \qquad \hat{\phi} = \frac{D(d_{xt}, \hat{d}_{xt})}{K - \nu}, \tag{3.17}$$

where

$$\mathrm{dev}(x,t) = 2\left[d_{xt}\log\left(\frac{d_{xt}}{\hat{d}_{xt}}\right) - (E_{xt}^0 - d_{xt})\log\left(\frac{E_{xt}^0 - d_{xt}}{E_{xt}^0 - \hat{d}_{xt}}\right)\right] \tag{3.18}$$

Furthermore,

$$D(d_{xt}, \hat{d}_{xt}) = \sum_x \sum_t \omega_{xt} \mathrm{dev}(x,t) \tag{3.19}$$

is the total deviance of the model, $K = \sum_x \sum_t \omega_{xt}$ is the number of observations in the data and ν is the effective number of parameters in the model. ω_{xt} are weights taking the value 0 if a particular (x,t) data cell is omitted or 1 if the cell is included. d_{xt} denotes the observed number of deaths.

$$\hat{d}_{xt} = E_{xt} g^{-1}\left(\alpha_x - \sum_{i=1}^{N} \beta_x^{(i)} k_t^{(i)} + \beta_x^{(0)} \gamma_{(t-x)}\right) \tag{3.20}$$

is the expected number of deaths predicted by the model, with g^{-1} denoting the inverse of the link function g.

Heat-maps of the deviance residuals for the all the six discussed models fitted to England and Wales male mortality data for the years 1965-2011 are demonstrated. The data is for ages $0 - 100$ and contains age-specific deaths and exposures for England and Wales from the Human Mortality Database. From the Figure 3.4.1 we see that models LC, CBD and APC display strong residual patterns while the residuals of models RH, M7 and PLAT look reasonably random. The APC model shows a strong clustering of residuals due to its inability to allow for varying improvement rates with age. The LC and CBD models, which do not have a cohort effect, demonstrate very marked diagonals patterns illustrating the inability of these models to capture the well-known cohort effect observed in the England and Wales population. The right panels in Figure 3.4.2 and 3.4.6 clearly show that the LC and CBD models are unable to capture the cohort effect. In addition, the left panel in Figure 3.4.6 reveals some strong patterns by age, reflecting the lack of a quadratic age term in the CBD which may be necessary to capture the commonly observed curvature of the mortality rates in a logit scale. When evaluating the goodness-of-fit of different models, it is generally anticipated that models with more parameters provide a better fit to the data.

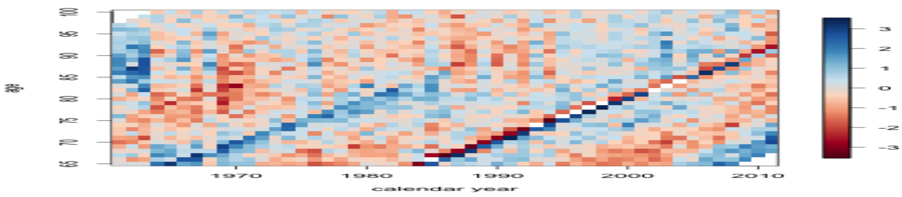

LC

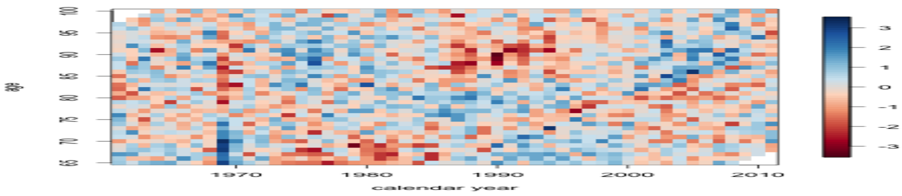

RH

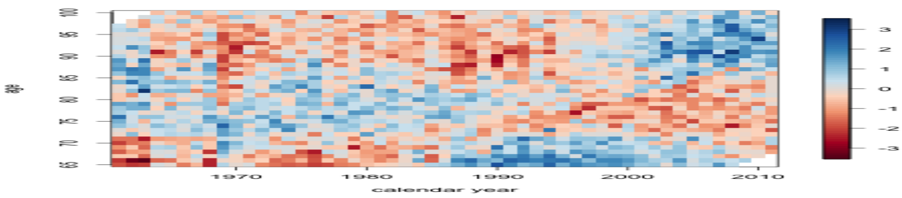

APC

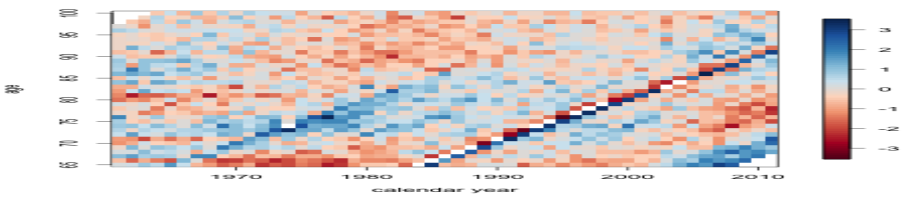

CBD

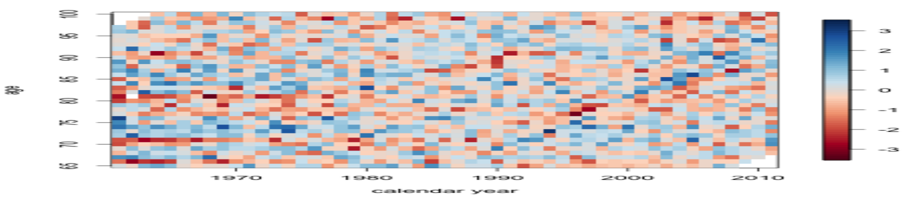

M7

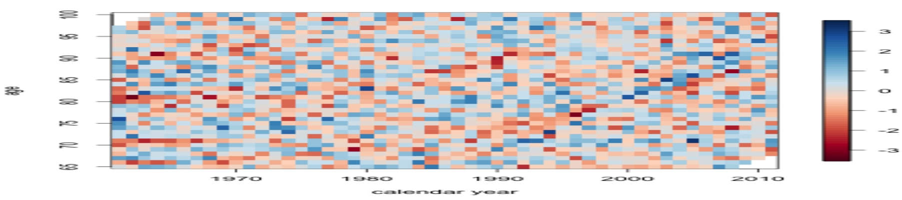

PLAT

Figure 3.4.1: Heat-maps of mortality models. Age range is $0 - 100$. Time period is $1965 - 2011$.

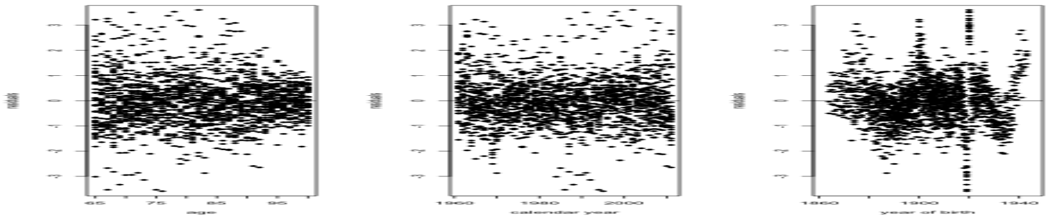

Figure 3.4.2: Scatter plots of deviance residuals for LC model

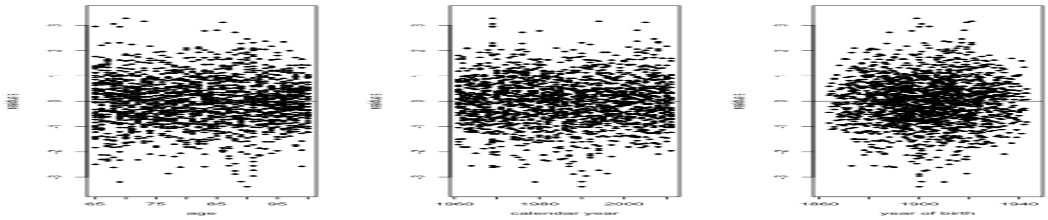

Figure 3.4.3: Scatter plots of deviance residuals for RH model

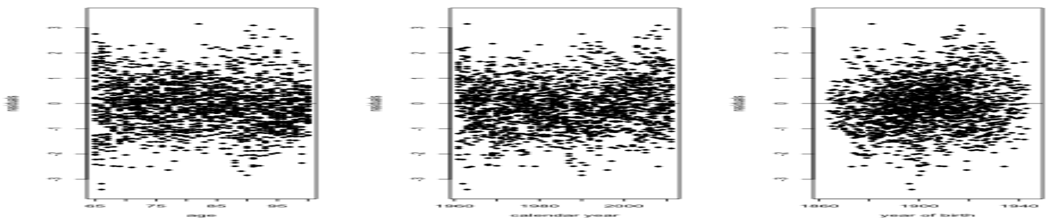

Figure 3.4.4: Scatter plots of deviance residuals for APC model

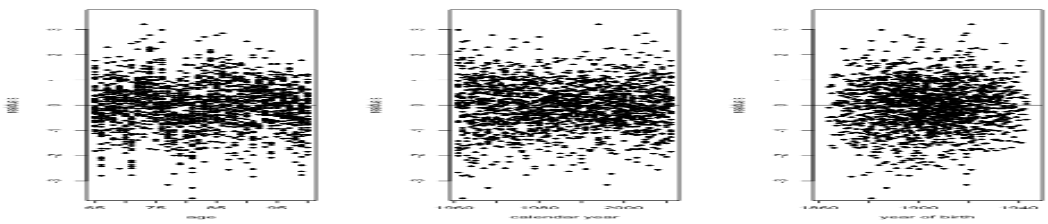

Figure 3.4.5: Scatter plots of deviance residuals for M7 model

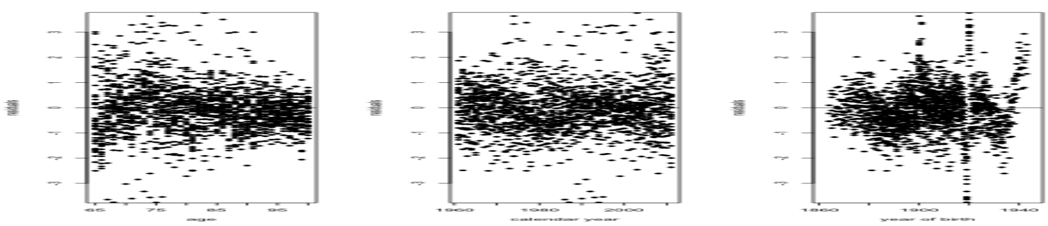

Figure 3.4.6: Scatter plots of deviance residuals for CBD model

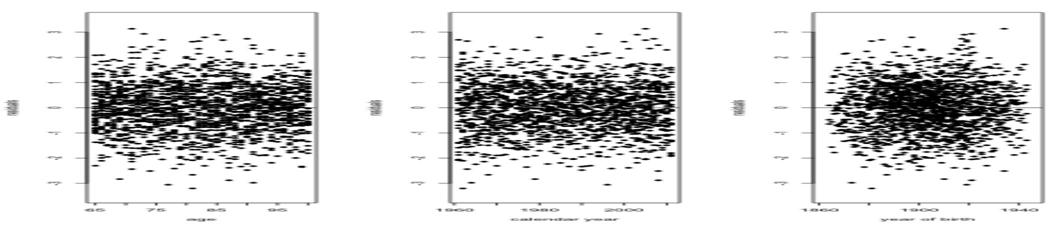

Figure 3.4.7: Scatter plots of deviance residuals for PLAT model

Scatter plots of deviance residuals for different mortality models fitted to England and Wales males population for the period 1965-2011

Now we can proceed to analysing solvency margins for these models allowing for different factors such as the size of portfolio, deferred period, etc.

We apply Monte Carlo simulation technique to generate solvency margins under different scenarios. We first use 100000 runs in order to simulate mortality rates for each stochastic mortality model. This helps us to calculate stochastic reserves and payments to policyholders based on the random number of surviving policyholders, and consequently the random portfolio fund at time t. Then we obtain a matrix of deficits in case no solvency margin is added at the beginning by subtracting reserves at time t from random portfolio fund at time t. Now in order to calculate solvency margin that needs to be added in the beginning in order to ensure solvency at time t we need to calculate the relevant quantiles of these deficit values discounted to time 0. We repeat these steps 100000 times in accordance with a parametric bootstrapping technique in order to find confidence intervals for solvency margins. In other words, we use random sampling with replacement and assign measures of accuracy (95% confidence interval) to sample estimates. The key idea a behind this technique is to resample from the original data obtained via the fitted model to create replicate data sets, from which the variability of the quantities can be assessed (Brouhns et al. [2005]). Figure 3.4.8 illustrates solvency margins with confidence intervals for 6 different models and different portfolio sizes. The figure shows that the solvency margins for all the models start to converge to a certain value for each model when the portfolio size is big enough. The decreasing behaviour of the relative required solvency margins and their confidence intervals with respect to the size of portfolio is due to the pooling effect of random fluctuations; however, the magnitude of solvency margins stabilises quickly and it does not go to zero due to the non-pooling and systematic effect of longevity risk. As far as the size of the portfolio is concerned, Table 3.4.1 also shows that the required margins for all the models decrease as N increases. Table 3.4.1 demonstrates solvency margins for different mortality models and deferred periods when T=n.

The portfolio size vary from $1,000$ to $1,000,000$.

Figure 3.4.9 shows the solvency margins for different models depending on deferred period. As we can see from the figures 3.4.8 and 3.4.9, M7 and CBD models have more extreme values for solvency margins whereas Lee-Carter model has the lowest values. The ranking of the magnitude of the solvency margins and confidence intervals from biggest to smallest is as follows: M7, M5, RH, Plat, APC and LC. These differences in solvency margins can be attributed to the different characteristics of the underlying stochastic mortality models. The ranking of the models according to the solvency margins seems to be based mostly on the number of period terms. The LC model has only one age period term, therefore it does not fully capture the variability associated with these annuities and, therefore, has the lowest solvency margins and smallest confidence intervals among the models. The RH has a cohort term in addition to the age period term and the APC model is a modification of the RH model with the coefficient of the age period term $\beta_x^{(1)} = 1$ being constant, and therefore, it captures less variability than the original RH model. The M5 model has two age-period terms and has one of the highest results for solvency margins. The M7 model has three period terms, including a quadratic age effect, and a cohort term and, therefore, captures more variability. The Plat model is similar to the M7 model, but the definition of the $\beta_x^{(3)}$ is different. This model also introduces an α_x term, which is similar to the LC model. Due to the fact that the Plat model combines the features of the LC and the M7 models the solvency margins results for this model are less extreme than those for M7 model, but are higher than for the LC model. Additionally, there is greater uncertainty associated with greater deferred period, therefore, due to the compounding effect of the model risk and the longevity risk the difference in solvency margin increases significantly for greater deferred periods. This effect is also observed in Richards et al. [2020], where the authors demonstrate that the results for 99.5% VaR capital requirements and conditional tail expectations (CTEs) at 99% for deferred annuities vary considerably with the

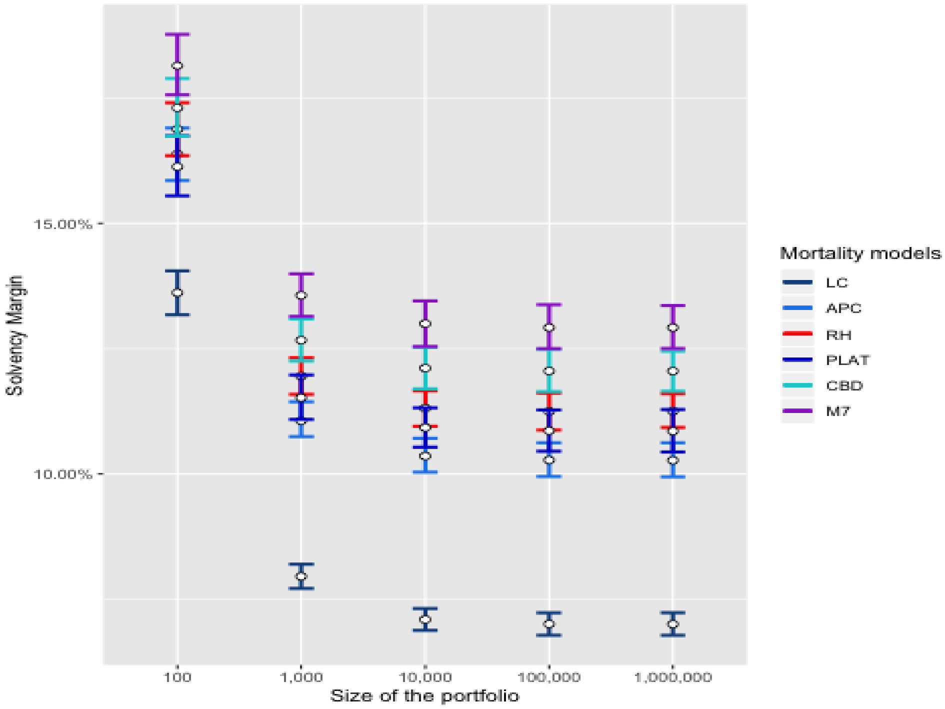

Figure 3.4.8: Solvency margins for different stochastic mortality models for $d = 5$ and $T = n$ with 95% confidence intervals

choice of the model and this effect intensifies with the age.

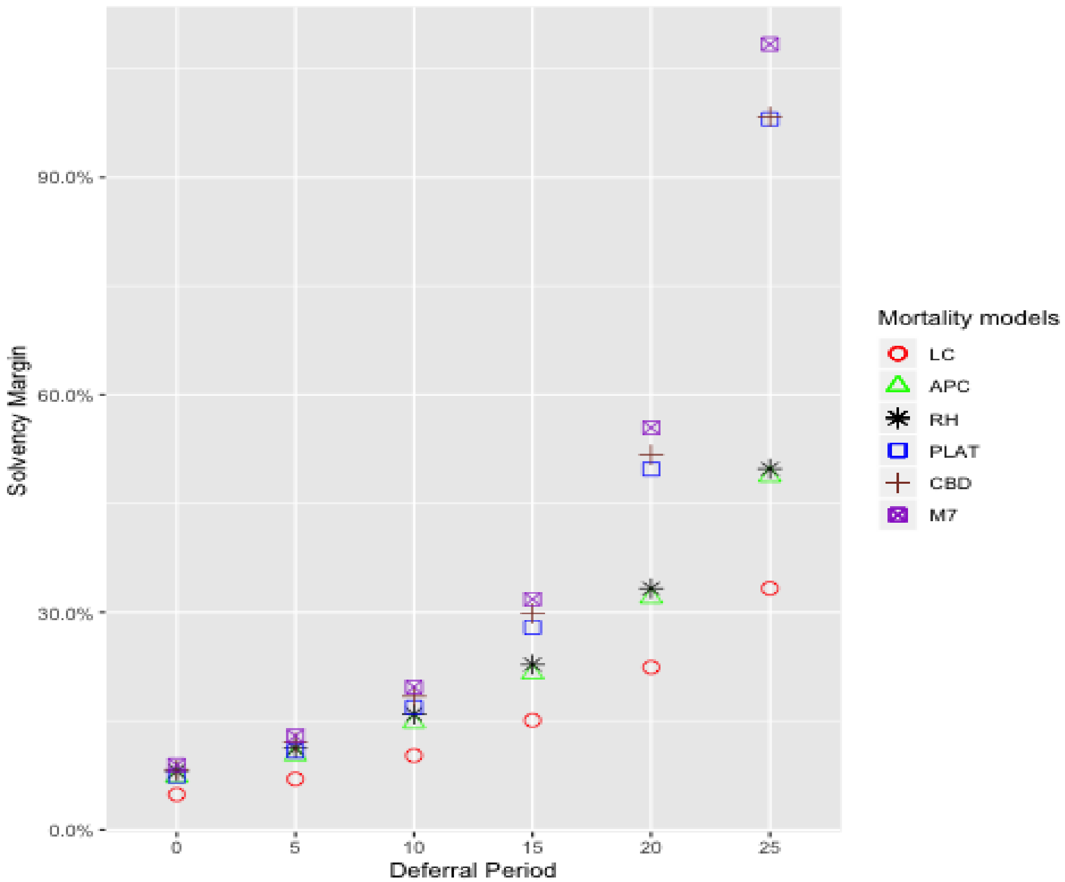

Figure 3.4.9: Solvency margins for different stochastic mortality models and different deferred periods when $T = n$

	deferral=0						deferral=5						deferral=10					
Portfolio size	LC	APC	RH	PLAT	CBD	M7	LC	APC	RH	PLAT	CBD	M7	LC	APC	RH	PLAT	CBD	M7
100	9.79%	11.92%	12.45%	11.34%	12.25%	12.84%	9.79%	16.39%	12.45%	16.14%	17.31%	18.16%	18.84%	22.44%	22.77%	23.57%	25.06%	26.25%
1,000	5.59%	7.88%	8.64%	7.89%	8.77%	9.40%	7.95%	11.06%	11.95%	11.52%	12.67%	13.57%	11.42%	15.72%	16.72%	17.70%	19.19%	20.46%
10,000	4.93%	7.34%	8.13%	7.44%	8.34%	8.97%	7.09%	10.36%	11.31%	10.92%	12.11%	13.00%	10.35%	14.86%	15.97%	16.97%	18.50%	19.78%
100,000	4.86%	7.27%	8.08%	7.39%	8.29%	8.91%	7.00%	10.28%	11.24%	10.86%	12.05%	12.93%	10.24%	14.77%	15.90%	16.89%	18.43%	19.68%
1,000,000	4.86%	7.27%	8.08%	7.39%	8.29%	8.91%	7.00%	10.27%	11.25%	10.85%	12.05%	12.92%	10.24%	14.76%	15.91%	16.88%	18.43%	19.68%

Table 3.4.1: Solvency margins for different mortality models and deferred period when T=n

Tables 3.4.2, 3.4.3, 3.4.4, 3.4.5, 3.4.6 and 3.4.7 demonstrate solvency margins and expected shortfalls for different time horizons and deferred periods for Lee-Carter, Renshaw-Haberman, Age-Period-Cohort, Cairns-Blake-Dowd, M7 and Plat models respectively. Portfolio size used to construct these tables is 1,000,000. Solvency margins increase with greater time horizons reflecting the positive correlation of the uncertainty risk with horizon.

For a given choice of parameters, the comparison between the stochastic approach adopted in section 3.3 and the full stochastic models shows a signifficant difference in required solvency margins and their spreads depending on deferred period and time horizon. This is due to the fact that a full stochastic approach allows us to fully assess the risk of systemic deviations. In order to reach some conclusions about the choice of the full stochastic model for further analysis, we need to compare the models. Results in Tables 3.4.2, 3.4.3, 3.4.4, 3.4.5, 3.4.6 and 3.4.7 have been obtained by performing the valuation for deferred periods $d = 0, 5, ..., 30$, in order to inspect the behaviour of the required margin. In addition, we demonstrate the results for expected shortfall (ES) , as this risk measure is also in use in some countries for solvency purposes. The increase in the relative solvency margin is due to the fact that the size of the portfolio reduces and the age of the annuitants increases with greater deferred periods, which means greater uncertainty. In Tables 3.4.2, 3.4.3, 3.4.4, 3.4.5, 3.4.6 and 3.4.7, the solvency margins required at time 0 for different deferred periods are calculated according to condition 3.6. When the smallest time span (i.e. $T = 5$) is chosen, the results for the RH and APC models are quite similar and higher than the results for other models, whereas the CBD and PLAT models demonstrate lowest values in this case. Although the solvency margins for $T = 5$ are the lowest for the PLAT model, it has one of the highest results when $T = n$. The LC model has the smallest spread between $T = 5$ and $T = n$.

The choice of model often involves significant judgement by the analyst and, as we can see, a change in model can lead to material changes in solvency margins. The M7 and Plat models seem to be reasonable models to use for mortality projections and have in common that they have the highest results for solvency margins when $T = n$. However, when $T = 5$ the Plat model has the lowest result among the 6 models analysed and thus, the speed with which solvency margin changes depending on T is very significant for the Plat model.

The M7 model produces the highest solvency margins under both the VaR and ES approaches to measuring insurer's solvency. As such, it is the model of most interest to regulators and supervisory authorities. In contrast, Lee-Carter and APC models produce the lowest results for solvency margins. Plat model provides a compromise between these models. The Lee-Carter and APC model can be attractive for insurance companies, however, actuaries' duty of prudence would lead them to view the Plat model as one of the suitable models due to the greater spread in uncertainty it captures depending on the time horizon. Furthermore, this model fits historical data well, is applicable to a full age range, and captures the cohort effect. It has a non-trivial correlation structure and has no robustness problems, while the structure of the model remains relatively simple. Therefore, in section 3.5, we further compare these models adopting a stochastic approach to modelling interest rates.

	T=5		T=10		T=n	
deferral	VaR	ES	VaR	ES	VaR	ES
d=0	0.822%	0.932%	1.85%	2.09%	4.86%	5.55%
d=5	1.04%	1.18%	2.56%	2.90%	7.00%	7.99%
d=10	1.04%	1.18%	3.08%	3.49%	10.24%	11.70%
d=20	1.04%	1.18%	3.08%	3.49%	22.41%	25.78%
d=30	1.04%	1.18%	3.08%	3.49%	49.04%	57.44%

Table 3.4.2: VaR and ES for different deferred periods and time horizons for LC model.

	T=5		T=10		T=n	
deferral	VaR	ES	VaR	ES	VaR	ES
d=0	1.02%	1.16%	2.12%	2.40%	8.08%	9.27%
d=5	1.24%	1.40%	2.80%	3.17%	11.25%	12.91%
d=10	1.24%	1.40%	3.24%	3.67%	15.91%	18.25%
d=20	1.24%	1.40%	3.24%	3.67%	33.26%	38.35%
d=30	1.24%	1.40%	3.24%	3.67%	77.18%	90.36%

Table 3.4.3: VaR and ES for different deferred periods and time horizons for RH model.

	T=5		T=10		T=n	
deferral	VaR	ES	VaR	ES	VaR	ES
d=0	1.01%	1.14%	2.14%	2.42%	7.27%	8.35%
d=5	1.24%	1.41%	2.88%	3.26%	10.27%	11.79%
d=10	1.24%	1.41%	3.38%	3.83%	14.76%	16.96%
d=20	1.24%	1.41%	3.38%	3.83%	31.99%	36.97%
d=30	1.24%	1.41%	3.38%	3.83%	76.62%	90.03%

Table 3.4.4: VaR and ES for different deferred periods and time horizons for APC model.

3.5 Stochastic interest rates

As we mentioned before, the results are sensitive to changes in the parameter i and therefore, we investigate the results for the above mortality models considering also stochastic models of interest rates. In order to analyse the effect of stochastic nature of interest rates on solvency margins for deferred annuity policies we use the Vasicek model [Vasicek, 1977] which is often used in actuarial applications (Qiu et al. [2011], Russo et al. [2017], Wu and Liang [2018]) since it satisfactorily represents the long-term development of the rate of return. It is an example of one-factor short rate model as it describes interest rate movements as driven by only one source of market risk. There exist more complex models for interest rate modelling in the literature but for the purposes of this chapter we use the simplest one to illustrate the effect of incorporating stochastic interest rates into our model. Let us assume that r_t is the short interest rate and its behaviour can be described

	T=5		T=10		T=n	
deferral	VaR	ES	VaR	ES	Var	ES
d=0	0.64%	0.73%	1.60%	1.81%	8.29%	9.63%
d=5	0.81%	0.93%	2.23%	2.53%	12.05%	14.00%
d=10	0.81%	0.93%	2.73%	3.09%	18.43%	21.43%
d=20	0.81%	0.93%	2.73%	3.09%	51.71%	60.67%
d=30	0.81%	0.93%	2.73%	3.09%	215.80%	264.13%

Table 3.4.5: VaR and ES for different deferred periods and time horizons for CBD model.

	T=5		T=10		T=n	
deferral	VaR	ES	VaR	ES	VaR	ES
d=0	0.85%	0.96%	1.88%	2.13%	8.91%	10.4%
d=5	1.06%	1.20%	2.59%	2.93%	12.92%	15.03%
d=10	1.06%	1.20%	3.12%	3.52%	19.68%	22.92%
d=20	1.06%	1.20%	3.12%	3.52%	55.45%	65.22%
d=30	1.06%	1.20%	3.12%	3.52%	255.67%	314.91%

Table 3.4.6: VaR and ES for different deferred periods and time horizons for M7 model.

by the Ornstein-Uhlenbeck process. Thus,

$$dr_t = a(\gamma - r_t)d_t + \sigma dW_t \tag{3.21}$$

where W_t is a standard Wiener process and a, γ and σ are positive constants. The long-term mean of the short rate is represented by γ, a is a friction force bringing the process back towards γ and σ the diffusion coefficient. The random portfolio fund in this case is described as follows

$$Z_t = Z_{t-1}(1 + i_t) - R_t \tag{3.22}$$

where $i_t = e^{r_t} - 1$ is the random return, described by the continuous stochastic differential equation in (3.21). The requirements for solvency margins are the same as in the previous sections. As far as mortality in concerned we refer to the M7 and Plat models considered in section 3.4. We adopt the same set of simulations for mortality, but instead of a single rate of 0.03 we use $10,000$ simulations of r and the convert it to i. The parameters for the stochastic interest rate model are given in Table 3.5.1. They are chosen so that they reflect

	T=5		T=10		T=n	
deferral	VaR	ES	VaR	ES	VaR	ES
d=0	0.61%	0.73%	1.50%	1.76%	7.39%	8.74%
d=5	0.78%	0.93%	2.12%	2.48%	10.85%	12.84%
d=10	0.78%	0.93%	2.61%	3.05%	16.88%	19.96%
d=20	0.78%	0.93%	2.61%	3.05%	49.76%	59.24%
d=30	0.78%	0.93%	2.61%	3.05%	225.18%	281.33%

Table 3.4.7: VaR and ES for different deferred periods and time horizons for Plat model.

adequate stochastic fluctuations from the rate 0.03 which we used in the previous sections and match the overall performance of assets, resulting from both market behaviour and the investment strategy of an insurance company. We also modify volatility σ to compare the results. Alternatively, the parameters can be estimated from given data.

r_0	0.03	a	0.3
γ	0.03	σ	0.05, 0.1, 0.2

Table 3.5.1: Parameters for simulations of interest rates for Vasicek model

The greater severity of the solvency margins is due to the fact that the assets, accumulating at a random rate, are compared with the reserve, which is calculated according to a financial hypothesis which could be significantly different from the actual investment performance. The solvency margins in the M7 model combined with Vasicek model are higher and the corresponding confidence intervals are wider than in the Plat model.

As we can see from Figure 3.5.1 the confidence intervals for the M7 and Plat models in the case of stochastic interest rates are wider than in the case when interest rates are deterministic. Although the confidence intervals tend to narrow down as portfolio size increases eliminating the impact of random fluctuations, the effect of stochastic interest rates on the overall width of confidence intervals in comparison with those in section 3.4 is significant due to the non-pooling and systematic nature of interest rate risk. Since we have added an extra source of variability by introducing stochastic interest rates, the results in figures 3.5.1, 3.5.2 and 3.5.3 demonstrate higher solvency margins and wider

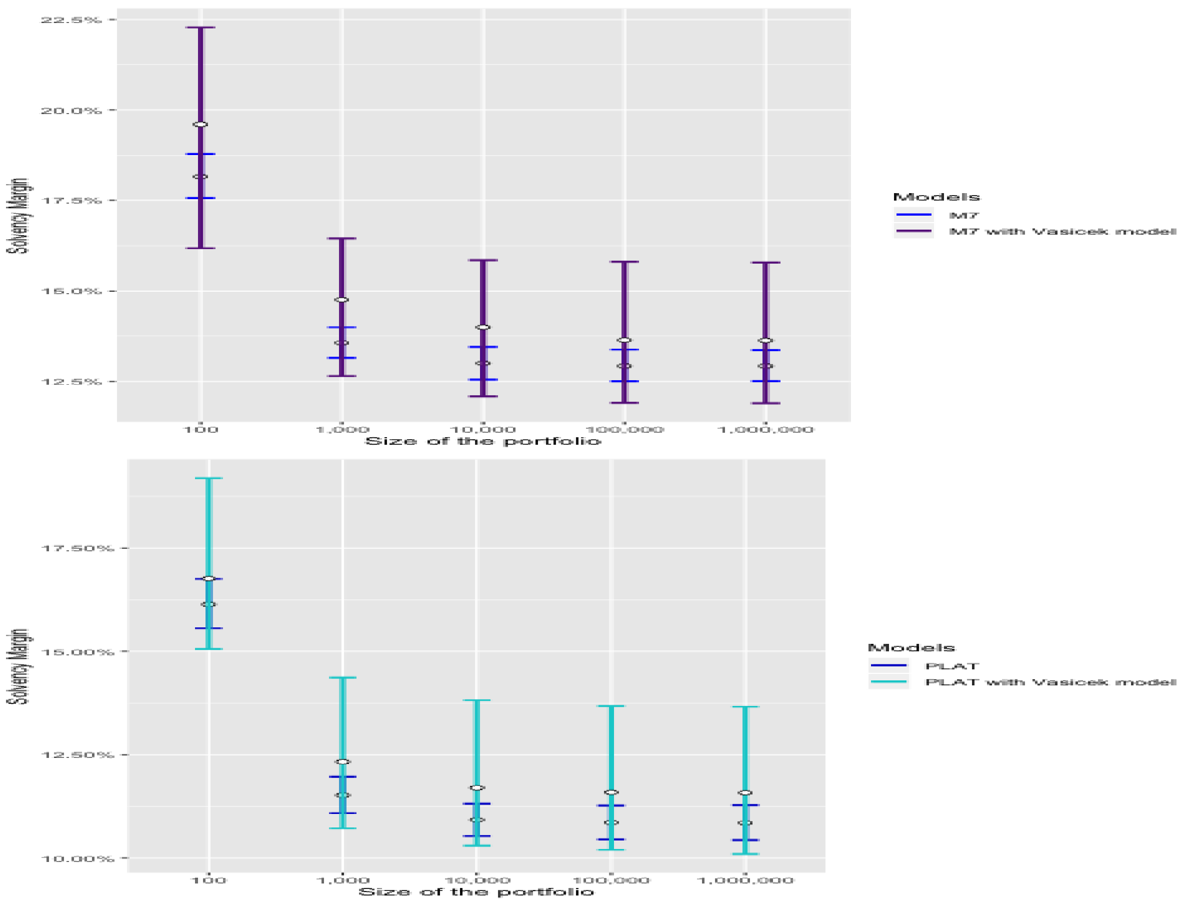

Figure 3.5.1: Solvency margins for different stochastic mortality models combined with Vasicek stochastic interest rate model with $\sigma = 0.05$ for $d = 5$ and $T = n$ with 95% confidence intervals.

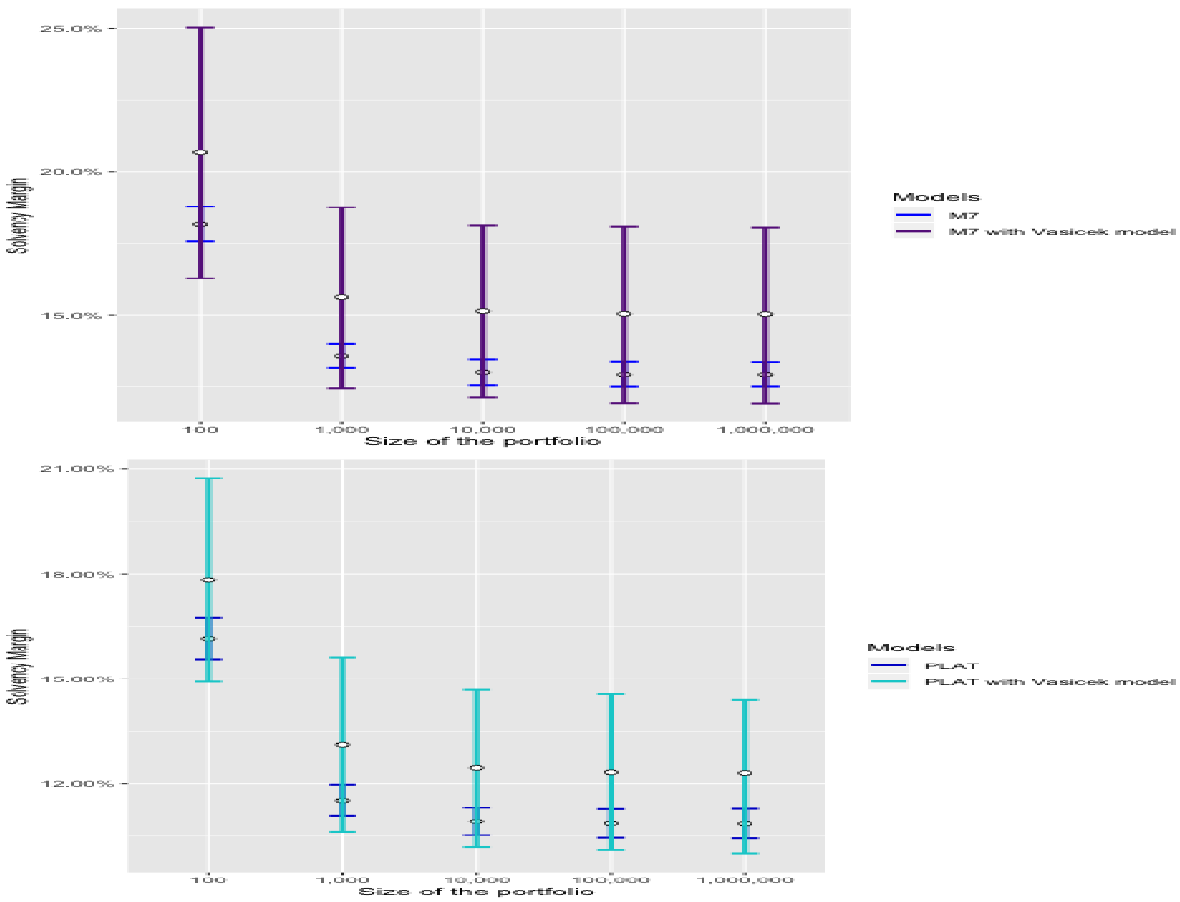

Figure 3.5.2: Solvency margins for different stochastic mortality models combined with Vasicek stochastic interest rate model with $\sigma = 0.1$ for $d = 5$ and $T = n$ with 95% confidence intervals.

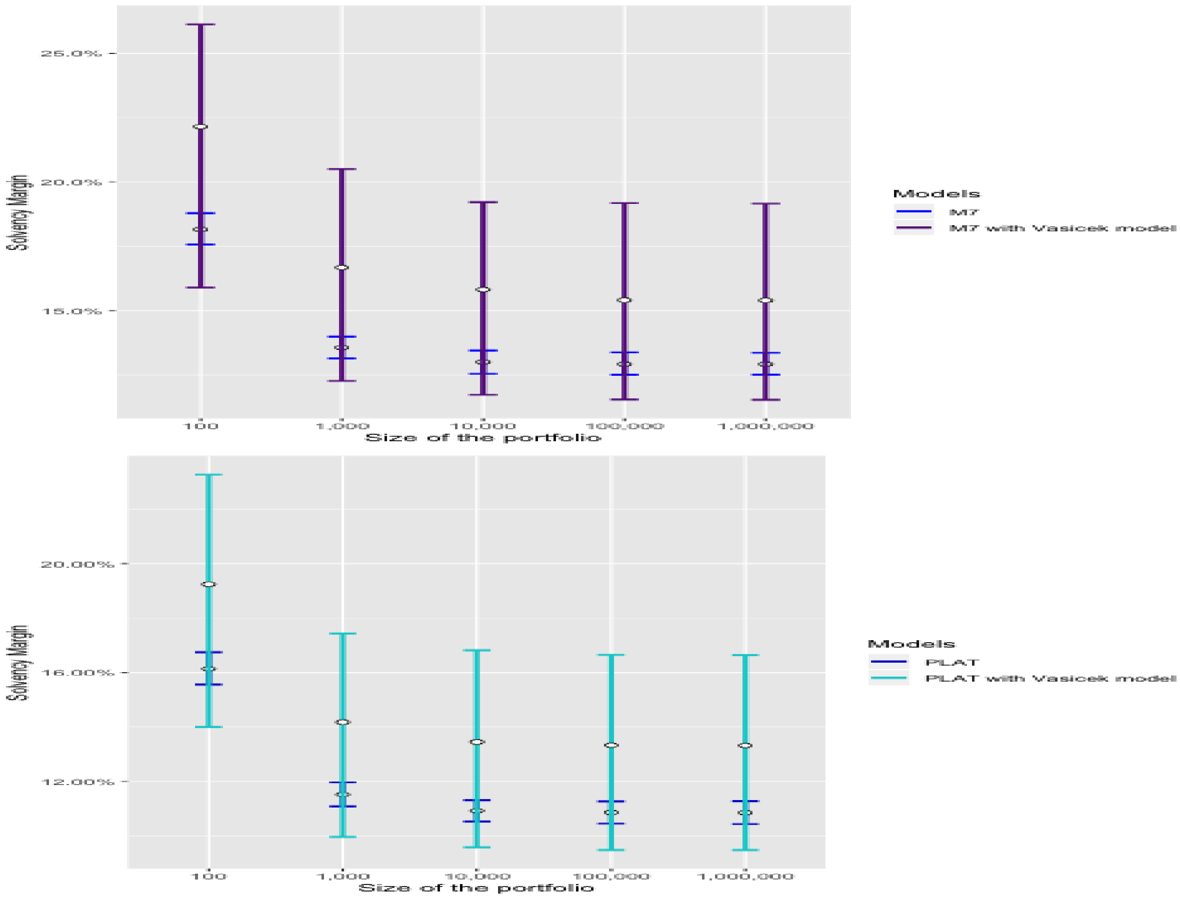

p

Figure 3.5.3: Solvency margins for different stochastic mortality models combined with Vasicek stochastic interest rate model with $\sigma = 0.2$ for $d = 5$ and $T = n$ with 95% confidence intervals.

confidence intervals. Moreover, we can observe that with greater σ, the solvency margins and confidence intervals increase reflecting higher level of uncertainty.

One of the disadvantages of Vasicek model is that its short rates can be negative for certain combinations of model parameters (Liang et al. [2011], Mallier and Deakin [2002]). Moreover, there is no term structure of volatility and it is assumed constant. It is a one factor model. It assumes that short rates are 100% correlated and can only cater for parallel shifts in the yield curve. We use this stochastic interest rate model to generate future simulations over long time horizons and the use of a model based on just the short term interest rate presents some disadvantages, however these disadvantages, are not critical for usefulness of our model. Our main goal is to demonstrate the impact of stochastic interest rates on the magnitude of the solvency margin and we achieve this goal by using the Vasicek model.

3.6 Further extensions

Further research work should concern the effects of various alterations to the insurance contracts on solvency margins. The results in this chapter can be extended to capture the effect of guarantees in the design of annuity contracts. Annual premiums are used in many types of insurance policies so investigation of the effect of annual premiums rather than a single premium can also be of interest of actuaries. Furthermore, the below mentioned metrics which are used in some insurance regulations can be applied

- $CV[X] = \frac{\sqrt{Var[X]}}{E[X]}$ = coefficient of variation (or risk index), where X = random NPV (Net Present Value) of the portfolio outflows for annuity payments

- Relative and absolute solvency margins, i.e. $[\frac{Z_0 - \mathcal{V}_0}{\mathcal{V}_0}]''$ and $[Z_0 - \mathcal{V}_0]''$ according to the stress scenario (Solvency II), consisting in a permanent 20% decrease of all the q_x, with relation to the probabilities adopted in premium and reserve calculations

Another extension can be incorporation of two-factor interest rate models for the analysis of the effect of stochastic interest rates on solvency margins. Examples are the two factor Hull-White model (Hull and White [2001]), Cox–Ingersoll–Ross model (Cox et al. [2005]). The Hull-White model allows for mean reversion of interest rates and the Cox–Ingersoll–Ross uses a square-root diffusion process to ensure that the calculated interest rates are always non-negative which can solve the above mentioned problems with the Vasicek model. Due to the fact that two-factor models assume that more than one stochastic factor affects the future evolution of the interest rates, they are able to capture more uncertainty associated with the interest rates risk, and, therefore, this is likely to increase the solvency margin.

3.7 Conclusions

Solvency requirements for deferred annuities have been analysed and compared to those of immediate annuities. Particular focus has been placed on the longevity risk. This has been incorporated in the analysis using different deterministic and stochastic models, particularly the family of generalized age-period-cohort stochastic mortality models. Several numerical examples illustrate the solvency requirements produced by these different approaches to modelling longevity risk. The results demonstrate the dramatic importance of the mortality models on evaluation of solvency margins for life annuities and the fact that model risk is an important issue when forecasting solvency margins. Another focus of this chapter is the *deferred period* and its effect on solvency requirements. The solvency margins increase with greater deferred periods which is caused by the extra longevity risk and the greater uncertainty about the numbers of future survivors. In essence, deferred annuities are more uncertain than immediate annuities, so as a result they require higher solvency margins. As discussed in section 3.1, retirees are reluctant to convert retirement savings into annuities voluntarily. One of the reasons is that in order to purchase immediate annuities they need to give up significant amount of cash. Deferred annuities require lower premiums as a result of the discounting effect and the possibility that the annuitant may not live until the benefit payments start. The model considered in this chapter could be applied to pension schemes with active members, where deferred benefits naturally arise. While deferred annuities may be difficult for the insurers to sell as stand alone products due to the lack of incentives on the policyholder side, they may be embedded in other products such as variable annuities or guaranteed annuity options. From the insurer's viewpoint, deferred annuities will tipically feature level premiums (and a death benefit, usually in the form of a return of premiums during the deferment period). The presence of level premiums will result in higher solvency margins compared to those obtained in this chapter. In section 3.5 we exploit the impact of stochastic interest rates on solvency margins and corresponding confidence intervals. The results demonstrate higher solvency margins and wider confidence intervals compared to the models with deterministic interest rates used in section 3.4. Comparison of results of these different models demonstrate the importance of model risk and help to assess it. For reserving purposes the models which are more conservative and lead to larger solvency margins on VaR and ES bases should be chosen even if they are not the best fit to the original data. This approach is broadly supported in the actuarial literature (Richards [2008], Melnikov and Romaniuk [2006], Enchev et al. [2017])

Chapter 4

Pricing buy-outs using different stochastic mortality models

4.1 Introduction

Pension buyouts, a pension de-risking strategy, have recently gained more and more attention from both scholars and practitioners. Longevity risk poses significant threat to the provision of retirement income with life expectancy having steadily risen in most of the world's countries. Improvements in mortality rates increase pension liabilities (Cox et al. [2006], Cox et al. [2013], Milidonis et al. [2011]). Increasing life spans make pensions more expensive for employers because they have to pay out fixed pension benefits to participants over a longer period. These pension liabilities are becoming extremely expensive to maintain, so pension plans are considering transferring these risks to insurance companies. As a result, there has been a surge of interest from defined benefit plan sponsors to de-risk their pensions with strategies such as longevity hedges and pension buyouts in recent years (Lin et al. [2015]).

A longevity hedge, such as a longevity swap, allows a pension plan to transfer its tail longevity risk to a third party. In contrast, a pension buyout involves purchasing annuities from an insurance company. According to LCP [2020] 2019 was an unprecedented year for pension buy-out and buy-in deals , with both volume sizes and transaction sizes increasing dramatically.

A buy-in is a policy that covers a proportion of the liabilities of a pension scheme, such as the benefits for the pensioners in-payment. The policy pays an income equal to the benefits of the covered members and therefore removes the risk of insufficient assets to meet future liabilities. A buyout is a type of financial transfer where a pension fund sponsor pays a fixed amount in order to avoid any liabilities relating to that fund. Thus, an insurer receives the payment but takes on responsibility for meeting those liabilities. Therefore, the main difference between pension buy-ins and pension buy-outs is related to credit risk. A buyout allows a firm to offload all pension obligations from its balance sheet and eliminate credit risk. However, the liabilities of buy-in insurers are usually not fully collateralised and guaranteed by third parties, and therefore, counter-party risk arises. Single-premium pension buyouts are the most popular type of pension-risk transfer. Employers transfer their pension assets and obligations to an insurance company by purchasing a group annuity contract for all or a portion of the plan participants. Compared with longevity swaps, pension buyouts are more effective in improving firm value. Longevity hedges retain most of the pension risk transferring only tail longevity risk and, so they prevent a firm from taking full advantage of pension de-risking. Pension buyouts, however, transfer the whole pension risk including longevity risk, interest rate risk and investment risk. Therefore, pension buyouts provide more freedom for a firm, within its risk tolerance, to take on more risky projects with high positive net present values. Consistent with this observation, Lin et al. [2017a] find that in the enterprise risk management framework, buyouts create more value than longevity hedges.

Progress in the area of longevity hedging and calculations of values of pension buyouts was hindered by the lack of closed-form formulae for the valuation of mortality-linked liabilities. Cairns [2011] proposes using a Taylor expansion for the approximation of longevity-contingent values. The paper makes use of the probit function along with a

Taylor expansion in the case of the Cairns-Blake-Dowd model (M5) (Cairns et al. [2006]. Thus, as the second objective of this chapter, we show how computationally expensive nested simulations problem can be avoided by extending the methodology used in Cairns [2011] to the Lee and Carter [1992] and Plat [2009] stochastic mortality models. Developing a sensitivity analysis in this area is important since it will help market participants better understand the effect of mortality trends on different pension risk management instruments and especially pension buy-outs.

The mortality and survival rates are evaluated using a publicly available projected mortality table for England and Wales estimated with the Lee and Carter [1992], Cairns et al. [2006] and Plat [2009] mortality models.

Little attention has been paid to how the price of pension buyouts will change taking into account new mortality trends. In this chapter we use observed age specific mortality rates for males in England and Wales (EW) between 1961 and 2016 and observe that over the period of 1961-2011 mortality rates have been declining at all ages, but since 2012 the mortality trends have reversed. According to Sanders [2018], since 2011 the rate of improvement of mortality rates has slowed for those aged 55-89 and among those aged 15-54 mortality rates have worsened years since 2012 . These phenomena have been analysed further. Thus, Bennett et al. [2018] investigate how much deaths from different diseases and injuries and at different ages have contributed to the increase in life expectancy inequalities. Ho and Hendi [2018] discuss recent trends in life expectancy across high income countries. We therefore, believe that it is important to reflect recent mortality trends in the pricing of pension buyouts and to develop a comparison analysis. Generally, analysis of the sensitivity of the price of pension buyouts to the fitted data, different fitting periods and different mortality models and model risks associated with these is important in assessing this product for insurers.

The chapter is organized as follows: Section 4.2 presents the basic framework for modelling a pension buyout. Section 4.3 describes different stochastic mortality models used in this chapter for estimating longevity risk. Section 4.4 demonstrates the Taylor series expansion approach to mortality models while section 4.5 discusses the Wang transform approach. In section 4.6 we describe formulas for the risk-neutral price of the pension buyout. In section 4.7 we demonstrate some numerical results for the pricing of pension buyout and provide a sensitivity analysis of the prices of pension buy-outs to different mortality models and data. Section 4.8 concludes this chapter.

4.2 Model

Consider a defined benefit pension plan with a cohort of N_0 members of age x_0 at time 0 all receiving the same amount of pension payment. We denote the plan's annual payment received by each member by P. The pension liability at time t, PL_t, is the present value of future obligations,

$$PL_t = N_t \cdot Pa_{x_0+t} \quad t = 0, 1, 2, \ldots, \tag{4.1}$$

where N_t is the number of survivors at time t, and a_{x_0+t} is the value at time t of an immediate life annuity for an individual aged $x_0 + t$, equal to

$$a_{x_0+t} = \sum_{s=1}^{\infty} v^s \, {}_sp_{x,t} \tag{4.2}$$

where $v = \frac{1}{1+r}$, and r is the discount rate used for annuity pricing.

The s-year survival probability for age x conditional on information prevailing at time t,

$${}_sp_{x,t} = E_t\Big[p_{x,t} \times p_{x+1,t+1} \times \ldots \times p_{x+s-1,t+s-1}\Big], \tag{4.3}$$

where E_t denotes expectation conditional on information available at time t.

Calculation of this conditional probability involves calculation of conditional expectations that usually have no closed form. When the probability is simulated out to some future horizon period T, the future time-T probabilities and annuity values contingent on the value of the state variables at time T need to be obtained. If stochastic simulation is applied to solve this, a nested simulations technique, which is very computationally expensive, is required. In the next section we discuss different stochastic mortality models and then show how to calculate the probability (4.3) for these models avoiding the nested simulations problem.

4.3 Longevity Risk Model

Currie [2016] shows that many mortality models can be expressed in terms of generalized linear models or non-linear models. We assume that the numbers of deaths D_{xt} at age x in year t follow Binomial distribution:

$$D_{xt} \sim Bin(E^0_{xt}, q_{x,t}), \tag{4.4}$$

where $q_{x,t}$ and E^0_{xt} are the death rate and the initial exposed to risk at age x in year t. The *systematic component* captures the effects of age x, calendar year t and cohort $c = t - x$ through the *predictor* η_{xt}

$$\eta_{xt} = \alpha_x + \sum_{i=1}^{M} \beta_x^{(i)} k_t^{(i)} + \beta_x^{(0)} \gamma_{t-x}, \tag{4.5}$$

where α_x is the static age function capturing the general shape of mortality by age, $M \geq 0$ an integer indicating the number of age-period terms describing the mortality trends, with each time index $k_t^{(i)}, i = 1, \dots, M$ and the term γ_{t-x} accounting for the cohort effect with $\beta_x^{(0)}$ modulating its effect across ages.

The link function is associating the random component to the systematic component so that

$$logit\left(E\left(\frac{D_{xt}}{E_{xt}}\right)\right) = \eta_{xt}. \tag{4.6}$$

It is convenient to use the canonical link and pair the Binomial distribution with the logit link function given by $log\frac{q_{x,t}}{1-q_{x,t}} = \eta_{xt}$ (Currie [2016]).

Buy-outs involve attempting to quantify future cash flows over a long future time period, where the cashflows involve uncertainty because the number of future survivors at future time points is unknown. One important component of the uncertainty is not knowing the correct mortality model to use for simulating the future numbers of survivors. Therefore, it is important to investigate the sensitivity of the results to the choice of the stochastic mortality model and assess the model risks associated with these products.

In order to investigate the effect of mortality models on pricing of pension buy-out we use three types of mortality models: with one age-period term, with two age-period terms, and a model that also captures the cohort effect. The stochastic mortality model with one age-period term we apply in this chapter is the model developed by Lee and Carter [1992] with predictor

$$\eta_{xt} = \alpha_x + \beta_x^{(1)} k_t^{(1)}. \tag{4.7}$$

The time index $k_t^{(1)}$ is modeled and forecasted using ARIMA processes. Typically, a random walk with drift has been shown to provide a reasonable fit, that is,

$$k_t^{(1)} = \delta + k_{t-1}^{(1)} + \epsilon_t, \tag{4.8}$$

where δ is the drift parameter and ϵ_t is a Gaussian white noise process with variance σ_k^2.

Cairns et al. [2006] (M5) model proposes a predictor structure with two age-period terms with pre-specified age-modulating parameters:

$$\eta_{xt} = k_t^{(1)} + (x - \bar{x}) k_t^{(2)}, \tag{4.9}$$

where $\bar{x}$ is the average age in the data used to fit the model.

The CBD model obtains mortality forecasts by projecting the period effects $k_t^{(1)}$ and $k_t^{(2)}$ using a bivariate random walk with drift:

$$\begin{cases} k_t^{(1)} = \delta^{(1)} + k_{t-1}^{(1)} + \epsilon_t^{(1)} \\ k_t^{(2)} = \delta^{(2)} + k_{t-1}^{(2)} + \epsilon_t^{(2)} \end{cases}, \tag{4.10}$$

where $\epsilon_t^{(1)}$ and $\epsilon_t^{(2)}$ are correlated Gaussian white noises.

Plat [2009] model is suitable for the full age range and also captures the cohort effect. The predictor in this model is given by

$$\eta_{xt} = \alpha_x + k_t^{(1)} + (x - \bar{x})k_t^{(2)} + (x - \bar{x})^+ k_t^{(3)} + \gamma_{t-x}, \tag{4.11}$$

where α_x is a static age function and there are three age period terms with pre-specified age-modulating parameters $\beta_x^{(1)} = 1$, $\beta_x^{(2)} = \bar{x} - x$, $\beta_x^{(3)} = (x - \bar{x})^+ = \max(0, x - \bar{x})$.

We then use these three models to predict future mortality rates and simulate N_t from section 4.2, the random number of survivors at time t.

4.4 Taylor series expansion approach to mortality models

The calculation of the conditional probability in (4.3) using the models introduces in section 4.3 involves calculation of conditional expectations that usually have no closed form. An attempt to use stochastic simulation runs into a problem. When we simulate the probability out to some future horizon period T, we then need to obtain the future time-T probabilities and annuity values contingent on the value of the state variables (time indices $k_t^{(i)}$) at time T. If stochastic simulations are applied to solve this, we will need to implement "simulations within simulations", i.e. nested simulations which is computationally expensive. An alternative method to obtain future probabilities and annuity values contingent on the outcomes of the time-T state variables can be through a Taylor series approximation. In this case, we need to simulate the state variables out to T, and then use the Taylor series approximation to assess probabilities and annuity values at time T as functions of the values of the state variables.

We first demonstrate this method as is described in Cairns [2011] for the two-factor model(M5) in Cairns et al. [2006] and then extend the application of the Taylor expansion method to other stochastic mortality models. In Cairns et al. [2006] model the probability, as measured in time $t+1$, that an individual aged x at time t survives to time $t+1$ is defined as $p_{x,t}$. For the M5 model, this is given by:

$$p_{x,t} = \frac{\exp[k_t^{(1)} + k_t^{(2)}(x - \bar{x})]}{1 + \exp[k_t^{(1)} + k_t^{(2)}(x - \bar{x})]} \tag{4.12}$$

where $k_t = (k_t^{(1)}, k_t^{(2)})$ is a two-dimensional random walk with drift.

It is useful to define the survivor index as

$$S(T, x) = p_{x,0} \cdot p_{x+1,1} \cdot \cdots \cdot p_{x+T-1,T-1}, \tag{4.13}$$

It represents the ex post probability that an individual aged x at time 0 would have survived to time T.

Spot survival probabilities $p(t, s, x, k)$ are non-linear functions of the future path of k_t that need to be computed using simulation. This is the probability that an individual aged $x-t$ at time 0, and still alive at time t (age x), survives until time s, based on the information about aggregate mortality at time t, as summarised by the vector $k_t = k$. This probability can be expressed as

$$_sp_{x,t} = p(t, s, x, k) = E\left[\frac{S(T+s, x-t}{S(T, x-t)}\middle| k_t = k\right] \tag{4.14}$$

For the calculation of pension buyout prices in our problem we need to ask the question: what is the distribution of $p(t, s, x, k)$, the probability that an individual alive and aged

x at time t survives s more years? This depends upon the simulated value of k_t at time t so for each simulated k_t we need to conduct further simulations to establish the value of $p(t, s, x, k)$.

The fact that random walk assumption implies that k_t has Markov and time-homogeneity properties and that $q_{x,t}$ depends on k_t mean that $p(t, s, x, k) = p(0, T, x, k)$. Therefore, although our usual starting point k_0 is known, we can evaluate spot survival probabilities at time 0 using other initial conditions.

The probit transform is applied before making approximations, that is, $f(T, x, k) = \Phi^{-1}(p(0, T, x, k))$, where Φ^{-1} is the inverse of the standard normal distribution function. A probit transformation, in combination with the first and second order Taylor approximations has been found by Cairns [2011] to produce accurate estimates of the spot survival probabilities that compare favourably with alternative transformations such as the log or logistic transforms or no transforms at all. The logit and log transfers were considered by Cairns (2011) as alternatives to the probit transform, however, they were relatively poor compared to the probit transform and as a conclusion the probit was considered to be better suited for these kinds of problems.

Let $\hat{k} = (\hat{k_1}, \hat{k_2})' = E[k_t]$. A linear approximation of the function f based upon the Taylor expansion around $\hat{k}$ is

$$f(T, x, k) \approx D_0(T, x) + D_1(T, x)'(k - \hat{k}) + \frac{1}{2}(k - \hat{k})'D_2(T, x)(k - \hat{k}) \quad , \tag{4.15}$$

where $D_0(T, x)$ is a scalar function of (T, x), $D_1(T, x)$ is a $2 * 1$ vector of first derivatives, and $D_2(T, x)$ is a $2 * 2$ matrix of second derivatives.

We now consider the corresponding results for the other two stochastic mortality models being examined. The probability, as measured in time $t + 1$, that an individual aged x at time t survives to time $t+1$ for the Lee-Carter model is

$$p_{x,t} = \frac{\exp[\alpha_x + \beta_x k_t^{(1)}]}{1 + \exp[\alpha_x + \beta_x k_t^{(1)}]} \tag{4.16}$$

where $k_t = (k_t^{(1)})$ is a one-dimensional random walk with drift.

$D_0(T,x)$ is a scalar function of (T,x), and due to the fact that there is only one period term in LC model, both $D_1(T,x)$ and $D_2(T,x)$ are scalars.

The probability, as measured in time $t+1$, that an individual aged x at time t survives to time $t+1$ for the Plat model is

$$p_{x,t} = \frac{\exp[\alpha_x + k_t^{(1)} + k_t^{(2)}(x-\bar{x}) + k_t^{(3)}(x-\bar{x})^+ + \gamma_{t-x}]}{1 + \exp[\alpha_x + k_t^{(1)} + k_t^{(2)}(x-\bar{x}) + k_t^{(3)}(x-\bar{x})^+ + \gamma_{t-x}]} \tag{4.17}$$

$D_0(T,x)$ is a scalar function of (T,x), $D_1(T,x)$ is a $3*1$ vector of first derivatives, and $D_2(T,x)$ is a $3*2$ matrix of second derivatives.

For our particular problem, we need to use the above technique in order to calculate $a^{(i)}_{65+T,T}$, where $T = 1, 2, \ldots, \omega$ and ω is final age. Thus,

$$a^{(i)}_{65+T,T} = \sum_{s=1}^{55-T} E\left[{}_s p_{65+T,T} | k_T^{(i)}\right] v^s \quad , \tag{4.18}$$

where

$$\begin{aligned} \Phi^{-1}\left(E\left[{}_s p_{65+T,T} | k_T^{(i)}\right]\right) &= f(s, 65+T, k_T^{(i)}) \\ \approx f(s, 65+T, \hat{k}_T) + \frac{\partial f}{\partial k}(s, 65+T, \hat{k}_T)(k_T^{(i)} - \hat{k}_T) &+ \frac{1}{2}\frac{\partial^2 f}{\partial k^2}(s, 65+T, \hat{k}_T)(k_T^{(i)} - \hat{k}_T)^2 \quad . \end{aligned} \tag{4.19}$$

For a general, twice-differentiable function $g(x_1, x_2)$, for small h_1 and h_2:

$$\frac{\partial g}{\partial x_1}(x_1, x_2) \approx (g(x_1 + h_1, x_2) - g(x_1, x_2))/h_1, \tag{4.20}$$

$$\frac{\partial g}{\partial x_2}(x_1, x_2) \approx (g(x_1 +, x_2 h_2) - g(x_1, x_2))/h_2, \tag{4.21}$$

$$\frac{\partial^2 g}{\partial x_1^2}(x_1, x_2) \approx (g(x_1 + h_1, x_2) - 2g(x_1, x_2) + g(x_1 - h_1, x_2))/h_1^2, \tag{4.22}$$

$$\frac{\partial^2 g}{\partial x_2^2}(x_1, x_2) \approx (g(x_1, x_2 + h_2) - 2g(x_1, x_2) + g(x_1, x_2 - h_2))/h_2^2, \tag{4.23}$$

$$\frac{\partial^2 g}{\partial x_1 \partial x_2}(x_1, x_2) \approx (g(x_1 + h_1, x_2 + h_2) - g(x_1 - h_1, x_2 + h_2) \\ -g(x_1 + h_1, x_2 - h_2) + g(x_1 - h_1, x_2 - h_2))/4h_1h_2 \tag{4.24}$$

These approximations are not unique, but they are known to be effective in a variety of circumstances.

4.5 Wang transform

The Wang transform is a market-based equilibrium pricing method that unifies finance and insurance pricing theories. Wang(1996, 2000, 2001, 2002) introduced a method of pricing insurance risks by transforming the underlying distribution. It has been used to price longevity swaps by some authors. Lin et al. [2017a] used the Wang transform method for the pricing of buy-outs. Wanyama [2018] applied the method for hedging longevity risk using longevity swaps. Shiqing [2015] derived an analytical pricing formula of longevity swaps with a trigger mechanism based on the Wang transform. This transform extends the Capital Asset Pricing Model (CAPM) to the pricing of all kinds of assets and liabilities, having any type of probability distribution in finance or insurance. This transform is easily applied to contingent payoffs that are co-monotone with their underlying assets or liabilities. Unlike many other possible transforms including the Proportional Hazard transform also developed in Wang [1996], the simple and more generalized families of the Wang Transform build directly upon CAPM and Black-Scholes Theory. The main parameter in the Wang Transform is the market price of risk which is a familiar concept in financial economics. Furthermore, the market price of risk in the Wang Transform is not subject to the same disadvantages of "underwriting beta" due to the fact that the market price of risk can be easily calibrated from industry capital requirements. This calibration is more robust than historical estimates of the "underwriting beta". The transform is equally applicable to primary insurance business and excess-of-loss reinsurance when calculating fair value of liabilities (Wang [2002]). To apply it for the pricing of pension buy-outs, the observed prices of pure longevity securities can be used to determine the parameter of the Wang transform and the longevity risk premium of a buy-out contract can then be derived [Lin et al., 2017b].

In general, the Wang transform distorts a cumulative distribution function $F_X(x)$ to obtain a transformed distribution $F_X^*(x)$ according to the following equation:

$$F_X^*(x) = \Phi[\Phi^{-1}(F_X(x)) - \lambda], \tag{4.25}$$

where $\Phi(x)$ is the standard normal cdf and λ can be interpreted as the market price of risk. The fair price of X then equals the discounted expected value using the transformed distribution $F_X^*(x)$. We follow Lin et al. [2015], and apply the Wang transform to the death probabilities

$$F_{T(x,0)}^*(s) = \Phi[\Phi^{-1}(F_{T(x,0)}(s)) - \lambda], \tag{4.26}$$

where $T(x,0)$ is the lifetime of a person at age x in time 0 and λ is the market price of longevity risk. In the context of this chapter, the Wang transform can be expressed as

$$q_{x,s}^* = \Phi[\Phi^{-1}(q_{x,s}) - \lambda], \tag{4.27}$$

where $q_{x,s}^*$ is the expected probability that a person aged x at time 0 dies before age $x+s$ and $s = 1, 2, \ldots$

According to Lin and Cox [2008] in bulk annuities the market price of risk in the Wang transform reflects the level of market systematic risk and firm-specific unhedgeable risk. The idea is that, after transformation, the fair price of a claim X should be the discounted expected value using the transformed distribution. Assume an insurer transfers its longevity risk to financial markets by issuing a longevity bond. The market price of risk λ can be derived based on the annuity retail market, and then we can use the same λ to price the longevity bond. If there are no transaction costs between the two markets and annuities were actually traded, this method guarantees no arbitrage opportunity between these markets.

Assume the market price of longevity risk, λ is constant in time. In that case, the transformed s-year survival rate for age x at time 0, $p^*_{x,0}$, is

$$p^*_{x,0} = 1 - q^*_{x,0} = 1 - \Phi[\Phi^{-1}(q_{x,0}) - \lambda] \quad . \tag{4.28}$$

The market price of longevity risk λ can be determined from a longevity security with equation (4.28), so that at time 0 the price of the longevity security is the discounted expected value under the transformed probability ${}_sp^*_{x,0}$ in the case of annuity:

$$\sum_{s=1}^{S} v^s \, {}_sp^*_{x,0} = \sum_{s=1}^{S} v^s \left(1 - \Phi[\Phi^{-1}(q_{x,0}) - \lambda]\right) \quad . \tag{4.29}$$

To apply this in our buy-out pricing we can first set desired values for longevity risk premium P_{lr}

$$P_{lr} = \frac{a^*_{x_0}}{a_{x_0}} - 1 \quad , \tag{4.30}$$

where $a^*_{x_0}$ is the present value of an immediate annuity at time 0 for the cohort cohort aged x_0 calculated using the transformed survival rates, and then work backwards to calculate λ and consequently the transformed s-year survival probabilities.

4.6 Price of a buy-out

In this section we derive the formulas for the risk-neutral price of the funding guarantee option of the pension buy-outs.

Assume that the annual survival payments from the insurer to the retirees are made at the end of each year. Let A_t denote the value of pension assets at time t and L_t the present value of liabilities at time t. We assume that the pension scheme is fully funded at inception with $A_0 = L_0$. At the end of each year, the pension assets are reduced by the annuity (or survival) payments. Furthermore, in the event of pension shortfalls, the bulk annuity insurer has obligations to inject cash to cover up the deficits.

Thus, the option component of the buyout at time t is

$$O_t = \max\{L_t + N_t \cdot P - A_t, 0\}, \tag{4.31}$$

where O_t is the deficit at time t covered by the pension buyout. Denote by A_{t^+} the value of pension assets after the annuity payments are made at time t and the deficit is covered (if any), so that A_{t^+} satisfies the equation

$$A_{t^+} = O_t + A_t - N_t \cdot P = \max\{A_t - N_t P, L_t\} \quad . \tag{4.32}$$

The value of the pension assets between annuity payment dates grows according to a General Brownian Motion dynamics under the risk neutral probability Q used for the pricing of the buy-out:

$$A_{t+1} = A_{t^+} e^{(r-\frac{\sigma^2}{2})+\sigma \Delta z_t} \quad t = 0, 1, 2, \ldots, \tag{4.33}$$

where r is the risk-free rate, σ is volatility and $\Delta z_t \sim N(0,1)$ is standard normal distribution. Investment risk is assumed to be independent of the longevity risk.

Thus, the risk-neutral price of the funding guarantee option of the buy-outs equals

$$B = \sum_{t=1}^{\omega-x} v^t E^Q[O_t] - v^{\omega+1} E^Q[A_{\omega+1}] \quad , \tag{4.34}$$

where v^t is the t-year discount factor based on the risk-free rate r and Q is the risk adjusted probability obtained through the Wang transform. The first component on the right-hand side of (4.34) represents the present value of supplementary contributions whenever an underfunded event occurs and the second component is the released reserve after all the pensioners are deceased.

The relative investment risk premium B_{rel} can then be obtained by dividing (4.34) by the initial pension liabilities L_0,

$$B_{rel} = \frac{B}{L_0} - 1 \quad . \tag{4.35}$$

This is the cost, per pound of pension liability, of the buy-out protection guarantee.

4.7 Numerical illustrations

In this section, we use a numerical example to illustrate how to determine the values of the buy-outs.

We calculate the cost of the buyout for the 3 stochastic mortality models introduced before (Lee Carter, CBD, Plat), using different scenarios and different approaches to fitting and forecasting mortality in order to be able to estimate the sensitivity of key parameters. Namely,

1) Fitting using ages: 65-100, 60-100, 55-100;

2) Fitting using input data: 1960-2000, 1965-2005, 1970-2010, 1975-2015.

Particularly in order to demonstrate the effect of the latest trends in mortality to the pricing of pension buyouts we analyse the data after 2010 separately.

The results for the derivatives D_0, D_1, D_2 for Lee-Carter, M5 and Plat models for age $x = 70$ in 5 years time and the results for D_0,D_1 ,D_2 for Lee-Carter, M5 and Plat models for age $x = 80$ in 15 years time and for age $x = 90$ in 25 years time are demonstrated in the Appendix and we can analyse them in order to see how sensitive are these values to age and period. The first subscript in the D terms demonstrate the order of derivatives, and the second subscript is the κ term. For example, $D_{1,1}$ is the first order derivative for the first κ term. We can comment on these tables as follows:

- $D_0(T,x)$ for all three mortality models become more negative as T increases, reflecting the gradually lower probability of survival to T.
- $D_0(T,x)$ decrease with age x for all three models.
- $D_1(T,x)$ for LC model and $D_{1,1}(T,x)$ for CBD and Plat are all negative, indicating that a lower values of $k(\tau)$ and $k_1(\tau)$ respectively means mortality rates will normally be lower at all future ages and consequently survival rates will be higher. Considering that all future mortality rates will be lower then there will be a proportionately bigger negative impact on survival probabilities to smaller ages.
- D_2 for LC model and $D_{2,11}$ for CBD model are also negative.
- $D_{1,2}$, $D_{2,12}$ for CBD and Plat models and $D_{2,13}$ for Plat model change sign.
- $D_{2,22}$, $D_{2,23}$, $D_{2,33}$ are negative indicating that a lower values of $k_t^{(2)}$ and $k_t^{(3)}$ respectively means mortality rates will normally be lower at all future ages and consequently survival rates will be higher.

The following tables demonstrate values for $a_{65} = a_{60+5}$, conditional on information prevailing at time 5, for different fitting periods and fitting ages for the three models.

Table 4.7.1: a_{65} values for LC model for different fitting periods and ages.

	55-100	60-100	65-100
1960-2000	13.46	13.53	13.62
1965-2005	13.58	13.64	13.78
1970-2010	13.62	13.76	13.85
1975-2015	13.56	13.67	13.78

The method introduced in Lin et al. [2017b] uses the Lee Carter stochastic mortality model in order to assess the value of a_{65}. In Lin et al. [2017b] the value of λ is first calculated which then is used to assess the values of P_{long} of 3.14% and a_{65}. The UK male population mortality tables for ages 65–104 from 1950 to 2013 from the Human Mortality

Table 4.7.2: a_{65} values for CBD model for different fitting periods and ages.

	55-100	60-100	65-100
1960-2000	14.77	14.86	14.96
1965-2005	14.91	14.98	15.13
1970-2010	14.97	15.11	15.21
1975-2015	14.86	14.90	15.01

Table 4.7.3: a_{65} values for Plat model for different fitting periods and ages.

	55-100	60-100	65-100
1960-2000	16.424	16.524	16.64
1965-2005	16.58	16.66	16.825
1970-2010	16.647	16.802	16.914
1975-2015	16.33	16.48	16.57

Database are used in the paper.

The aim of this chapter is to assess the values of a_x for different stochastic mortality models and effect of fitting different ages and periods on those values. We use the method by Lin et al. [2017b] but we set desired values for longevity risk premium P_{long} and then work backwards to calculate λ and consequently the transformed the values of a_x. We also use three different stochastic mortality model in order to perform comparison analysis assess sensitivity to the choice of model.

Further, we undertake a sensitivity analysis. The goal of this analysis is to show how the the values for a_x change as we vary the mortality model, fitting period, and fitting ages. To this end, we consider a Lee Carter model with fitting period $1960 - 2000$ and fitting ages $55 - 100$ as baseline model. We analyse three mortality models with different fitting periods and fitting ages for England and Wales data. We carry out 100000 simulations. We set the risk-free interest rate $r = 3\%$, whilst for the simulation of assets in B (equation 4.34) we use a Geometric Brownian Motion with volatility $\sigma = 30\%$. In order to assess the sensitivity of a_x, we consider the value of a_x for Lee Carter model with fitting period $1960-2000$ and fitting ages $55-100$ as a benchmark and construct a table of the fractions of a_x values. Thus, for example, the sensitivity of a_x value for Plat model would be $\frac{a_x^{Plat}}{a_x^{LC}}$.

Table 4.7.4: Sensitivity of a_{65} value for LC model for different fitting periods and ages.

	55-100	60-100	65-100
1960-2000	1	1.005	1.011
1965-2005	1.009	1.013	1.024
1970-2010	1.012	1.022	1.029
1975-2015	1.007	1.0156	1.024

Table 4.7.5: Sensitivity of a_{65} value for CBD model for different fitting periods and ages.

	55-100	60-100	65-100
1960-2000	1.097	1.104	1.111
1965-2005	1.108	1.113	1.124
1970-2010	1.109	1.123	1.130
1975-2015	1.104	1.107	1.115

The tables demonstrate that the sensitivity of a_x values increase with the length of the fitting periods and as we move shift the age range being fitted to older age. However, the values for fitting period $1975-2015$ are slightly lower that the values for $1970-2010$ which reflects the effect of recent mortality trends. The values for CBD model are about $9\% - 11\%$ higher and the values for Plat model are $22\% - 25\%$ higher than the values for the base Lee Carter model. These differences in the values of a_x come from the different characteristics of the underlying stochastic mortality models. The LC model has only one age period term, therefore it does not fully represent all the characteristics of the data such as changing mortality improvements, therefore, has the lowest values for a_x. The Plat model has also a cohort effect and an additional κ term, and, therefore, is able to better capture recent mortality improvements at different ages. In essence, more elaborate models such as the Plat model with more time trends are capable of capturing more complex patterns in mortality while simpler ones such as the LC model necessarily must achieve a compromise and may result in less accurate projected mortality trends. Model risk is very important and the right model can ultimately only be chosen by actuarial judgement depending on the actuary's objectives. Such judgement should be informed by the results of using several different models. In this particular case, actuaries'

Table 4.7.6: Sensitivity of a_{65} value for Plat model for different fitting periods and ages.

	55-100	60-100	65-100
1960-2000	1.22	1.228	1.236
1965-2005	1.232	1.238	1.25
1970-2010	1.237	1.248	1.257
1975-2015	1.213	1.224	1.231

duty of prudence would lead them to view the Plat model as one of the most suitable due to the fact that this model fits historical data well, is applicable to a full age range, captures the cohort effect and leads to higher a_x values.

In the next few tables we demonstrate the results for B_{rel} for different models. The periods we use for fitting are 1960-2000, 1965-2005, 1970-2010, 1985-2015. The age ranges we use for fitting are 55-100, 60-100, 65-100. The value of P_{long} that we use in order to calculate the transformed survival probabilities are 3%, 4% and 5%. The implied values of λ for these values of P_{long} are given in the Table 4.7.7

Table 4.7.7: λ values for different stochastic mortality values and different P_{long} values.

λ values			
P_{long}	3%	4%	5%
LC	0.083	0.1113	0.14
CBD	0.0804	0.1082	0.1361
Plat	0.0760	0.1035	0.1312

We perform the following analysis using an assumption of a risk free rate of 3% and a volatility for assets of 30%.

Table 4.7.8: Values of investment premium B_{rel} (Buy-out funding cost). Fitting period $1960-2000$. Ages $55-100$.

	3%	4%	5%
Lee Carter	4.23%	5.72%	7.99%
Cairns Blake Dowd	4.39%	6.25%	8.21%
Plat	4.88%	6.58%	9.03%

Table 4.7.9: Values of investment premium B_{rel} (Buy-out funding cost). Fitting period $1960 - 2000$. Ages $60 - 100$.

	3%	4%	5%
Lee Carter	3.85%	5.54%	8.31%
Cairns Blake Dowd	4.41%	6.21%	8.76%
Plat	4.65%	6.93%	9.56%

Table 4.7.10: Values of investment premium B_{rel} (Buy-out funding cost). Fitting period $1960 - 2000$. Ages $65 - 100$.

	3%	4%	5%
Lee Carter	3.88%	5.56%	8.02%
Cairns Blake Dowd	4.07%	5.79%	8.31%
Plat	4.65%	6.34%	9.52%

The tables demonstrate the sensitivity of B_{rel} values to mortality models and P_{long} values. In carrying out these analyses, we explore how the choice of parameter and stochastic mortality models affects buy-out prices. In general, the analyses illustrate intuitive results including how the buy-out prices reflect mortality improvements depending on the fitted age ranges and fitting period. The price of the pension buy-out also increases with increasing longevity risk premium which in its turn depends on the market price of risk λ estimated from the Wang transform. This result makes intuitive sense as a higher risk premium is associated with a higher level of longevity risk and these effects are similar across different mortality models. The values for the Plat model seem to be highest due to the greater spread in uncertainty it captures and the values for the LC model are lowest. However, although we saw a clear effect of fitting period and fitting ages on the values of a_x their effect on the value of B_{rel} seems to be erratic.

Table 4.7.11: Values of investment premium B_{rel} (Buy-out funding cost). Fitting period 1965 – 2005. Ages 55 – 100.

	3%	4%	5%
Lee Carter	4.76%	5.31%	8.67%
Cairns Blake Dowd	4.96%	6.42%	8.78%
Plat	5.01%	6.82%	9.33%

Table 4.7.12: Values of investment premium B_{rel} (Buy-out funding cost). Fitting period 1965 – 2005. Ages 60 – 100.

	3%	4%	5%
Lee Carter	4.04%	5.34%	8.43%
Cairns Blake Dowd	4.34%	6.67%	8.65%
Plat	4.56%	6.92%	9.32%

Table 4.7.13: Values of investment premium B_{rel} (Buy-out funding cost). Fitting period 1965 – 2005. Ages 65 – 100.

	3%	4%	5%
Lee Carter	3.78%	5.34%	8.54%
Cairns Blake Dowd	4.21%	6.21%	8.67%
Plat	4.78%	6.55%	9.32%

Table 4.7.14: Values of investment premium B_{rel} (Buy-out funding cost). Fitting period 1970 – 2010. Ages 55 – 100.

	3%	4%	5%
Lee Carter	4.22%	5.78%	8.43%
Cairns Blake Dowd	4.34%	6.43%	8.56%
Plat	4.86%	6.67%	9.32%

Table 4.7.15: Values of investment premium B_{rel} (Buy-out funding cost). Fitting period 1970 – 2010. Ages 60 – 100.

	3%	4%	5%
Lee Carter	4.34%	5.91%	8.31%
Cairns Blake Dowd	4.37%	6.57%	8.41%
Plat	4.96%	6.86%	9.21%

Table 4.7.16: Values of investment premium B_{rel} (Buy-out funding cost). Fitting period $1970 - 2010$. Ages $65 - 100$.

	3%	4%	5%
Lee Carter	4.20%	5.34%	8.55%
Cairns Blake Dowd	4.21%	6.54%	8.78%
Plat	4.78%	6.77%	9.54%

Table 4.7.17: Values of investment premium B_{rel} (Buy-out funding cost). Fitting period $1975 - 2015$. Ages $55 - 100$.

	3%	4%	5%
Lee Carter	4.23%	5.55%	8.42%
Cairns Blake Dowd	4.43%	6.32%	8.56%
Plat	4.87%	6.89%	9.33%

Table 4.7.18: Values of investment premium B_{rel} (Buy-out funding cost). Fitting period $1975 - 2015$. Ages $60 - 100$.

	3%	4%	5%
Lee Carter	4.67%	5.32%	8.32%
Cairns Blake Dowd	4.96%	6.25%	8.47%
Plat	5.01%	6.68%	9.44%

Table 4.7.19: Values of investment premium B_{rel} (Buy-out funding cost). Fitting period $1975 - 2015$. Ages $65 - 100$.

	3%	4%	5%
Lee Carter	4.88%	5.34%	8.22%
Cairns Blake Dowd	4.96%	6.44%	8.67%
Plat	5.13%	6.78%	9.33%

4.8 Conclusion

Operating defined benefit pensions has become a more and more difficult business for a firm. Unexpected mandatory contributions to defined benefit plans reduce resources available for business investments and adversely affect a firm's business performance. Pension buy-outs can be an important solution to these problems provided by the insurance industry. As a result, pension buyouts have become significant part of pension markets. To help develop this market, in this chapter, we focus on quantifying and pricing risks embedded in the pension buy-out transactions. The price of a buy-out contract depends on the investment risk and longevity risk shifted to an insurer. Developing analytical tools in this direction is important because it will extend traditional annuity market models, and it could be very useful in explaining these pension de-risking instruments to potential pension plan sponsors. Analysis of sensitivity of the price of pension buyouts to the fitted data, different fitting periods and different mortality models and model risks associated with these is important in assessing this product for insurers.

We use different fitting periods, fitting age ranges and three different stochastic mortality models in order to perform sensitivity analysis. Our results demonstrate that sensitivity of a_x values increase with the length of the fitting periods and with a shift of the fitted age range to include older ages. However, the values for fitting period $1975 - 2015$ are lower than the values for earlier fitting period which reflects the effect of recent mortality trends. In general, the price of the pension buy-out increases with increasing longevity risk premium which in its turn depends on the market price of risk λ. This results is intuitive as a higher risk premium is associated with a higher risk and these effects are similar across different mortality models. The values for the Plat model are the highest and the values for the LC models are the lowest amongst the three models. However, although there is a clear effect of fitting period and fitting ages on the values of a_x, their effect on the value of B_{rel} is erratic. Further research can focus on applying stress test scenarios, such as the occurrence of a global pandemics like Covid-19 or the reduction in the historic trend of mortality improvements as seen in many developed countries during the recent period of 2015-2019, and analysis of the effects of these in the pricing of pension buy-outs can be investigated. Separately, the analysis can be extended to capture the sensitivities of the results to the financial parameters, i.e to the changes in risk free rates and volatility parameters and this will likely to have greater effect on the cost of pension buy-outs.

4.9 Appendix

Table 4.9.1: Values for D_0,D_1 ,D_2. LC model for age $x = 70$ in 5 years time.

T	D_0	D_1	D_2
1	2.3365	-0.0104	-0.0011
5	1.5749	-0.0209	-0.0024
10	1.0713	-0.0240	-0.0030
15	0.6268	-0.0260	-0.0035
20	0.1487	-0.0272	-0.0039
25	-0.3985	-0.0278	-0.0042
30	-1.0696	-0.0270	-0.0043
35	-1.8798	-0.0249	-0.0042
40	-2.7553	-0.0246	-0.0044
45	-3.7417	-0.0258	-0.0048
50	-4.9416	-0.0266	-0.0052

Table 4.9.2: Values for D_0,D_1 ,D_2. CBD model $x = 70$ in 5 years time.

T	D_0	$D_{1,1}$	$D_{1,2}$	$D_{2,11}$	$D_{2,12}$	$D_{2,22}$
1	2.6390	-0.3393	7.5643	-0.03401	0.9228	-22.1877
2	2.379	-0.3682	7.932	-0.0423	1.1498	-26.8775
5	1.964	-0.4237	8.3189	-0.0604	1.5622	-34.4612
10	1.5316	-0.4950	8.2022	-0.0867	1.9454	-40.3368
15	1.1676	-0.5667	7.5525	-0.1153	2.1284	-42.9646
20	0.8035	-0.6488	6.3798	-0.1493	2.1278	-44.2590
30	-0.0444	-0.8690	1.5890	-0.2351	1.3453	-50.5535
40	-1.1929	-1.1583	-8.8489	-0.2923	-0.2934	-79.0863
50	-2.6269	-1.3644	-21.8139	-0.2401	-0.4520	-103.8841

Table 4.9.3: Values for D_0,D_1 ,D_2. Plat model $x = 70$ in 5 years time.

T	D_0	$D_{1,1}$	$D_{1,2}$	$D_{1,3}$	$D_{2,11}$	$D_{2,12}$	$D_{2,22}$	$D_{2,13}$	$D_{2,23}$	$D_{2,33}$
1	2.763	-0.355	7.920	4.926	-0.036	0.966	-23.231	0.857	-16.726	-14.449
2	2.491	-0.386	8.305	5.166	-0.044	1.204	-28.141	1.068	-20.261	-17.504
5	2.056	-0.444	8.710	5.418	-0.063	1.636	-36.081	1.451	-25.978	-22.442
10	1.604	-0.518	8.588	5.342	-0.091	2.037	-42.233	1.807	-30.408	-26.269
15	1.223	-0.593	7.908	4.918	-0.121	2.229	-44.984	1.977	-32.388	-27.980
20	0.841	-0.679	6.680	4.155	-0.156	2.228	-46.339	1.976	-33.364	-28.823
30	-0.047	-0.910	1.665	1.035	-0.246	1.409	-52.930	1.249	-38.109	-32.922
40	-1.249	-1.213	-9.265	-5.763	-0.306	-0.307	-82.803	-0.273	-59.618	-51.504
50	-2.750	-1.429	-22.839	-14.206	-0.251	-0.473	-108.767	-0.420	-78.312	-67.653

Table 4.9.4: Values for D_0,D_1 ,D_2. LC model for age $x = 80$ in 15 years time.

T	D_0	D_1	D_2
1	2.1299	-0.0100	-0.0010
5	1.2381	-0.0201	-0.0022
10	0.4972	-0.0229	-0.0026
15	0.3798	-0.0248	-0.0030
20	0.3649	-0.0249	-0.0031
25	-0.6728	-0.0253	-0.0033
30	-1.5384	-0.0256	-0.0032
35	-2.5269	-0.02536	-0.0034
40	-3.6142	-0.0249	-0.0041
45	-5.0439	-0.0245	-0.0047

Table 4.9.5: Values for D_0,D_1 ,D_2. CBD model $x = 80$ in 15 years time.

T	D_0	$D_{1,1}$	$D_{1,2}$	$D_{2,11}$	$D_{2,12}$	$D_{2,22}$
1	2.3491	-0.3291	5.3675	-0.03365	0.9082	-20.6675
2	2.097	-0.3488	5.9765	-0.0415	1.1288	-24.9563
5	1.6466	-0.4173	8.8564	-0.0602	1.4720	-32.9934
10	1.1131	-0.4833	8.6856	-0.0845	1.8545	-37.3304
15	0.9267	-0.5476	7.3495	-0.1001	2.0348	-41.8676
20	0.3245	-0.6289	6.1274	-0.1245	2.0978	-42.9564
30	-0.1338	-0.8599	1.1763	-0.2286	1.2678	-48.8564
40	-1.3992	-1.1397	-6.9784	-0.2700	-0.2744	-77.9754
50	-3.1921	-1.3348	-18.9452	-0.2368	-0.4221	-101.9453

Table 4.9.6: Values for D_0,D_1 ,D_2. Plat model $x = 80$ in 15 years time.

T	D_0	$D_{1,1}$	$D_{1,2}$	$D_{1,3}$	$D_{2,11}$	$D_{2,12}$	$D_{2,22}$	$D_{2,13}$	$D_{2,23}$	$D_{2,33}$
1	2.3764	-0.3345	7.7456	4.7434	-0.0342	0.9236	-20.9567	0.8245	-13.7524	-11.8564
2	2.183	-0.3768	8.006	4.8167	-0.0422	1.1866	-25.8567	0.9847	-17.8673	-14.8673
5	1.9855	-0.4267	8.578	5.1455	-0.0601	1.4522	-36.081	1.157	-21.9678	-20.7564
10	1.4102	-0.4967	8.3785	5.043	-0.0877	1.9845	-36.8646	1.405	-27.7653	-24.8674
15	1.0127	-0.5657	7.7996	4.7656	-0.1031	2.0012	-40.8563	1.6574	-29.3278	-24.8673
20	0.5764	-0.6578	6.4565	3.0815	-0.1345	2.0085	-42.7455	1.7345	-31.8674	-26.8673
30	-0.07976	-0.8876	1.4786	0.9876	-0.2060	1.2114	-49.8556	1.0347	-35.9567	-30.8674
40	-1.5623	-1.1923	-8.9655	-5.4556	-0.2806	-0.6079	-76.4742	-0.2590	-53.8674	-47.9788
50	-2.975	-1.4091	-18.8763	-12.8763	-0.2211	-0.7970	-97.8645	-0.4034	-74.8573	-62.8674

Table 4.9.7: Values for D_0,D_1 ,D_2. LC model for age $x = 90$ in 25 years time.

T	D_0	D_1	D_2
1	1.9721	-0.01002	-0.00098
5	1.0177	-0.0200	-0.0020
10	0.1982	-0.0219	-0.0023
15	0.3176	-0.0234	-0.0027
20	0.2623	-0.0241	-0.0030
25	-0.8786	-0.0249	-0.0031
30	-1.7856	-0.02557	-0.0029
35	-2.9286	-0.02516	-0.0031
40	-4.2166	-0.02327	-0.0037
45	-5.7846	-0.02267	-0.0042

Table 4.9.8: Values for D_0,D_1 ,D_2. CBD model $x = 70$ in 5 years time.

T	D_0	$D_{1,1}$	$D_{1,2}$	$D_{2,11}$	$D_{2,12}$	$D_{2,22}$
1	2.0476	-0.3076	4.7534	-0.03065	0.8756	-17.3465
2	1.9745	-0.31865	4.8564	-0.03956	1.0145	-20.3478
5	1.2436	-0.3976	7.7745	-0.0598	1.2366	-29.2346
10	1.0153	-0.4587	7.6874	-0.0801	1.6434	-32.2376
15	0.8463	-0.5145	6.7645	-0.0956	1.9835	-38.4587
20	0.1244	-0.6065	5.8754	-0.1067	1.9856	-39.3476
30	-0.1587	-0.8256	1.0534	-0.2067	1.0267	-44.3454
40	-1.4566	-1.1165	-5.6745	-0.2566	-0.2489	-72.9243
50	-3.6469	-1.3065	-15.7634	-0.2067	-0.3956	-95.7634

Table 4.9.9: Values for D_0, D_1 ,D_2. Plat model $x = 70$ in 5 years time.

T	D_0	$D_{1,1}$	$D_{1,2}$	$D_{1,3}$	$D_{2,11}$	$D_{2,12}$	$D_{2,22}$	$D_{2,13}$	$D_{2,23}$	$D_{2,33}$
1	2.0776	-0.3134	6.3672	3.8734	-0.0313	0.8723	-18.2352	0.7812	-11.8982	-9.7645
2	1.9833	-0.3434	7.356	4.0198	-0.0402	1.0122	-21.8972	0.8712	-14.8911	-12.8912
5	1.9156	-0.3902	8.0345	4.9834	-0.0589	1.3200	-30.0927	1.0123	-19.9023	-17.0129
10	1.0103	-0.4523	7.8765	4.95763	-0.0801	1.8293	-33.9023	1.3488	-24.8923	-21.8912
15	0.9722	-0.5290	6.9834	4.0122	-0.1002	1.9911	-37.7873	1.5722	-27.1278	-23.8710
20	0.1575	-0.6035	5.0122	2.9780	-0.1134	1.9918	-40.9023	1.6592	-29.1290	-25.1291
30	-0.0487	-0.8178	0.7634	0.8755	-0.1899	1.1789	-47.7823	0.9823	-32.2301	-28.1287
40	-1.1628	-1.0234	-6.8765	-4.7874	-0.2478	-0.4978	-67.9023	-0.1514	-48.1287	-40.1238
50	-2.0656	-1.3509	-16.8764	-10.7645	-0.2012	-0.6873	-88.1310	-0.3290	-69.5622	-57.4367

Chapter 5

Conclusion and Future Research

Two approaches to optimal reinsurance are analysed in chapter 2 of this thesis. The first approach discussed optimal reinsurance model from the insurer's point of view, and the second approach demonstrated a model which uses the Pareto optimality principle. Different premium principles were used for each approach and the optimality problems are solved for each premium principle using Second Order Conic Programming. Numerical illustrations demonstrate that proportional reinsurance is optimal when the risk measure follows the expected value principle. When the standard deviation principle and one-sided moments are used for calculation of the reinsurance premium, optimality is obtained when the model takes the form functional form $\sum R = \sum X \wedge c$, where c is a constant, X is loss amount and R is loss of the reinsurer. This is a special case of capped stop loss reinsurance. Thus, the shape of the optimal ceded loss function can vary for different types of reinsurance premium principles. Our results demonstrate that the functional form of optimal reinsurance contact depends on the adopted reinsurance premium principle and hence emphasize the important role of the premium principle in the determination of the optimal design. Moreover, we observed that the limit on the aggregate losses of reinsurer is considerably smaller when the Pareto optimality principle is in place, provided that all the parameters in the numerical examples are the same for both problems. Similarly, for the expected value premium principle the share of the reinsurer in quota-share reinsurance contract is less for Pareto optimal models. This result is intuitive, due to the fact that the Pareto optimality principle involves the objective function for the reinsurer who aims at minimising its own losses. As a next step this research can be extended to cases when there is a dependence among individual risks, different lines of business or claim sizes and numbers which can be modelled using copula functions. Moreover, other SOCP representable premium principles can be used for this optimisation model, such as the Dutch principle, p-mean value principle, etc. Another potential extension could involve adopting a Solvency II internal stochastic mortality model and illustrate its potential for application in life reinsurance optimisation.

In chapter 3 of this thesis solvency requirements for deferred annuities have been analysed and compared to those of immediate annuities. Particular focus has been placed on the longevity risk. This has been incorporated into the analysis using different deterministic and stochastic models, particularly member of the family of generalized age-period-cohort stochastic mortality models. Several numerical examples illustrate solvency requirements produced by these different approaches to longevity risk. The results demonstrate the dramatic importance of the mortality models on the calculation of solvency margins for immediate and deferred life annuities and the fact that model risk is a prevalent issue when forecasting solvency margins. Another focus of this chapter is the *deferred period* and its effect on solvency requirements for portfolios of deferred annuities. The margins increase with greater deferred periods which is caused by the extra longevity risk and the greater uncertainty about the numbers of future survivors. We also investigate the impact of stochastic interest rates on solvency margins and calculate the corresponding confidence intervals. The results demonstrate higher solvency margins and wider confidence intervals compared to the models with deterministic interest rates. Further research work should take into the account the effects of various alterations to the design insurance contracts on solvency margins. The results in this thesis can be extended to capture the effect of guarantees in annuity period. Annual premiums are used in many types of insurance policies so investigation of the effect of annual premiums rather than single premium can also be of interest of actuaries.

In chapter 4 we focus on quantifying and pricing risks embedded in the pension buy-out transactions. The price of a buy-out contract depends on the investment risk and longevity risk shifted to an insurer. Analysis of sensitivity of the price of pension buyouts to the fitted data, different fitting periods and different mortality models and model risks associated with these is important in assessing this product for insurers. Further research can focus on stress test scenarios for mortality rates, such as global pandemics, and analyse the effects of these in the pricing of pension buyouts.

References

QIS5 technical specifications. Technical report, European Commission, 2010.

LCP pensions de-risking report 2020. Technical report, Lane Clark & Peacock, 2020.

B. Acciaio and G. Svindland. Optimal risk sharing with different reference probabilities. *Insurance: Mathematics and Economics*, 44(3):426–433, 2009.

K. J. Arrow. Uncertainty and the welfare economics of medical care. *American Economic Review,*, 53(5):941–973, 1963.

P. Artzner, F. Delbaen, J.-M. Eber, and D. Heath. Coherent measures of risk. *Mathematical finance*, 9(3):203–228, 1999.

A. V. Asimit, A. M. Badescu, and K. C. Cheung. Optimal reinsurance in the presence of counterparty default risk. *Insurance: Mathematics and Economics*, 53(3):690–697, 2013.

A. V. Asimit, T. Gao, J. Hu, and E.-S. Kim. Optimal risk transfer: a numerical optimization approach. *North American Actuarial Journal*, 22(3):341–364, 2018.

P. Barrieu and N. El Karoui. Inf-convolution of risk measures and optimal risk transfer. *Finance and stochastics*, 9(2):269–298, 2005.

D. Bauer and F. Weber. Assessing investment and longevity risks within immediate annuities. *Asia-Pacific Journal of Risk and Insurance*, 3(1), 2008.

J. E. Bennett, J. Pearson-Stuttard, V. Kontis, S. Capewell, I. Wolfe, and M. Ezzati. Contributions of diseases and injuries to widening life expectancy inequalities in england from 2001 to 2016: a population-based analysis of vital registration data. *The Lancet Public Health*, 3(12):e586–e597, 2018.

C. Bernard and M. Ludkovski. Impact of counterparty risk on the reinsurance market. *North American Actuarial Journal*, 16(1):87–111, 2012.

E. Biffis and P. Millossovich. Optimal insurance with counterparty default risk. *Available at SSRN 1634883*, 2012.

H. Booth and L. Tickle. Mortality modelling and forecasting: A review of methods. *Annals of actuarial science*, 3(1-2):3–43, 2008.

K. Borch. *An attempt to determine the optimum amount of stop loss reinsurance.* 1960.

K. Borch. Equilibrium in a reinsurance market. *Econometrica*, 30:424–444, 1962.

N. Brouhns, M. Denuit*, and I. Van Keilegom. Bootstrapping the poisson log-bilinear model for mortality forecasting. *Scandinavian Actuarial Journal*, 2005(3):212–224, 2005.

J. R. Brown and J. M. Poterba. Joint life annuities and annuity demand by married couples. Technical report, National Bureau of Economic Research, 1999.

J. Cai and C. Weng. Optimal reinsurance with expectile. *Scandinavian Actuarial Journal*, 2016(7):624–645, 2016.

J. Cai, K. S. Tan, C. Weng, and Y. Zhang. Optimal reinsurance under var and cte risk measures. *Insurance: Mathematics and Economics*, 43(1):185–196, 2008.

A. J. Cairns. Modelling and management of longevity risk: Approximations to survivor functions and dynamic hedging. *Insurance: Mathematics and Economics*, 49(3):438–453, 2011.

A. J. Cairns, D. Blake, and K. Dowd. A two-factor model for stochastic mortality with parameter uncertainty: theory and calibration. *Journal of Risk and Insurance*, 73(4): 687–718, 2006.

A. J. G. Cairns, D. Blake, K. Dowd, G. D. Coughlan, D. Epstein, A. Ong, and I. Balevich. A Quantitative Comparison of Stochastic Mortality Models Using Data From England and Wales and the United States. *North American Actuarial Journal*, 2009. ISSN 1092-0277. doi: 10.1080/10920277.2009.10597538.

M. d. L. Centeno and M. Guerra. The optimal reinsurance strategy—the individual claim case. *Insurance: Mathematics and Economics*, 46(3):450–460, 2010.

A. Chen, S. Haberman, and S. Thomas. The implication of the hyperbolic discount model for the annuitisation decisions. *Journal of Pension Economics & Finance*, pages 1–20, 2018.

A. Chen, S. Haberman, and S. Thomas. Cumulative prospect theory and deferred annuities. *Review of Behavioral Finance*, 11(3):277–293, 2019.

K. Cheung, K. Sung, S. Yam, and S. Yung. Optimal reinsurance under general law-invariant risk measures. *Scandinavian Actuarial Journal*, 2014(1):72–91, 2014.

Y. Chi and H. Meng. Optimal reinsurance arrangements in the presence of two reinsurers. *Scandinavian Actuarial Journal*, 2014(5):424–438, 2014.

Y. Chi and K. S. Tan. Optimal reinsurance under var and cvar risk measures: a simplified approach. *ASTIN Bulletin: The Journal of the IAA*, 41(2):487–509, 2011.

M. C. Christiansen and M. Helwich. Some further ideas concerning the interaction between insurance and investment risks. *Blätter der DGVFM*, 29(2):253–266, 2008.

CMI. Mortality projections committee. 2016.

M. Coppola, E. D. Lorenzo, and M. Sibillo. Risk sources in a life annuity portfolio: decomposition and measurement tools. 2000.

M. Coppola, E. D. Lorenzo, and M. Sibillo. Further remarks on risk sources measuring: the case of a life annuity portfolio. 2002.

J. C. Cox, J. E. Ingersoll Jr, and S. A. Ross. A theory of the term structure of interest rates. In *Theory of valuation*, pages 129–164. World Scientific, 2005.

S. H. Cox, Y. Lin, and S. Wang. Multivariate exponential tilting and pricing implications for mortality securitization. *Journal of Risk and Insurance*, 73(4):719–736, 2006.

S. H. Cox, Y. Lin, R. Tian, and L. F. Zuluaga. Mortality portfolio risk management. *Journal of Risk and Insurance*, 80(4):853–890, 2013.

I. D. Currie. On fitting generalized linear and non-linear models of mortality. *Scandinavian Actuarial Journal*, 2016(4):356–383, 2016.

T. Davidoff. Housing, health, and annuities. *Journal of Risk and Insurance*, 76(1):31–52, 2009.

T. Davidoff, J. R. Brown, and P. A. Diamond. Annuities and individual welfare. *American Economic Review*, 95(5):1573–1590, 2005.

P. Dayananda. Optimal reinsurance. *Journal of Applied Probability*, 7(1):134–156, 1970.

A. De Waegenaere, B. Melenberg, and R. Stevens. Longevity Risk. *De Economist*, 158 (2):151–192, jun 2010. ISSN 0013-063X. doi: 10.1007/s10645-010-9143-4. URL http://link.springer.com/10.1007/s10645-010-9143-4.

W. H. DuMouchel. The pareto optimality of an n-company reinsurance treaty. *Scandinavian Actuarial Journal*, 1968(3-4):165–170, 1968.

I. Dushi and A. Webb. Household annuitization decisions: Simulations and empirical analyses. *Journal of Pension Economics & Finance*, 3(2):109, 2004.

V. Enchev, T. Kleinow, and A. J. Cairns. Multi-population mortality models: fitting, forecasting and comparisons. *Scandinavian Actuarial Journal*, 2017(4):319–342, 2017.

T. Fischer. Risk capital allocation by coherent risk measures based on one-sided moments. *insurance: Mathematics and Economics*, 32(1):135–146, 2003.

E. W. Frees and E. A. Valdez. Understanding relationships using copulas. *North American actuarial journal*, 2(1):1–25, 1998.

M. Guerra and M. d. L. Centeno. Optimal reinsurance policy: The adjustment coefficient and the expected utility criteria. *Insurance: Mathematics and Economics*, 42(2):529–539, 2008.

S. Haberman and A. Renshaw. A comparative study of parametric mortality projection models. *Insurance: Mathematics and Economics*, 48(1):35–55, 2011.

N. Hari, A. De Waegenaere, B. Melenberg, and T. E. Nijman. Longevity risk in portfolios of pension annuities. *Insurance: Mathematics and Economics*, 42(2):505–519, 2008.

O. Hesselager. Some results on optimal reinsurance in terms of the adjustment coefficient. *Scandinavian Actuarial Journal*, 1990(1):80–95, 1990.

J. Y. Ho and A. S. Hendi. Recent trends in life expectancy across high income countries: retrospective observational study. *bmj*, 362, 2018.

W.-Y. Hu and J. S. Scott. Behavioral obstacles in the annuity market. *Financial Analysts Journal*, pages 71–82, 2007.

J. Hull and A. White. The general hull–white model and supercalibration. *Financial Analysts Journal*, 57(6):34–43, 2001.

A. Hunt and D. Blake. On the structure and classification of mortality models. *North American Actuarial Journal*, pages 1–20, 2020.

M. Kaluszka. Mean-variance optimal reinsurance arrangements. *Scandinavian Actuarial Journal*, 2004(1):28–41, 2004.

M. Kaluszka and A. Okolewski. An extension of arrow's result on optimal reinsurance contract. *Journal of Risk and Insurance*, 75(2):275–288, 2008.

N. Krämer, E. C. Brechmann, D. Silvestrini, and C. Czado. Total loss estimation using copula-based regression models. *Insurance: Mathematics and Economics*, 53(3):829–839, 2013.

R. D. Lee and L. R. Carter. Modeling and forecasting us mortality. *Journal of the American statistical association*, 87(419):659–671, 1992.

J. Liang, J. M. Ma, T. Wang, and Q. Ji. Valuation of portfolio credit derivatives with default intensities using the vasicek model. *Asia-Pacific Financial Markets*, 18(1):33–54, 2011.

Y. Lin and S. H. Cox. Securitization of catastrophe mortality risks. *Insurance: Mathematics and Economics*, 42(2):628–637, 2008.

Y. Lin, R. D. MacMinn, and R. Tian. De-risking defined benefit plans. *Insurance: Mathematics and Economics*, 63:52–65, 2015.

Y. Lin, R. D. MacMinn, R. Tian, and J. Yu. Pension risk management in the enterprise risk management framework. *Journal of Risk and Insurance*, 84(S1):345–365, 2017a.

Y. Lin, T. Shi, and A. Arik. Pricing buy-ins and buy-outs. *Journal of Risk and Insurance*, 84(S1):367–392, 2017b.

Z.-Y. Lu, L.-P. Liu, Q.-J. Shen, and L.-L. Meng. Optimal reinsurance under var and cte risk measures when ceded loss function is concave. *Communications in Statistics-Theory and Methods*, 43(15):3223–3247, 2014.

M. Ludkovski and V. R. Young. Optimal risk sharing under distorted probabilities. *Mathematics and Financial Economics*, 2(2):87–105, 2009.

R. Mallier and A. Deakin. A green s function for a convertible bond using the vasicek model. *Journal of applied mathematics*, 2, 2002.

A. J. McNeil, R. Frey, P. Embrechts, et al. *Quantitative risk management: Concepts, techniques and tools*, volume 3. Princeton university press Princeton, 2005.

A. Melnikov and Y. Romaniuk. Evaluating the performance of gompertz, makeham and lee–carter mortality models for risk management with unit-linked contracts. *Insurance: Mathematics and Economics*, 39(3):310–329, 2006.

A. Milidonis, Y. Lin, and S. H. Cox. Mortality regimes and pricing. *North American Actuarial Journal*, 15(2):266–289, 2011.

P. Millossovich, A. M. Villegas, and V. K. Kaishev. Stmomo: An R package for stochastic mortality modelling. *Journal of Statistical Software*, 2015.

A. Olivieri. Uncertainty in mortality projections: an actuarial perspective. *Insurance: mathematics and economics*, 29(2):231–245, 2001.

A. Olivieri and E. Pitacco. Solvency requirements for pension annuities. *Journal of Pension Economics & Finance*, 2(2):127–157, 2003.

E. Pitacco. Longevity risk in living benefits. developing an annuity market in europe, fornero, e. and luciano, e. eds, 2004.

R. Plat. On stochastic mortality modeling. *Insurance: Mathematics and Economics*, 45 (3):393–404, 2009.

D. Qiu, Y. Hu, and L. Wang. The application of option pricing theory in participating life insurance pricing based on vasicek model. In *Quantitative Financial Risk Management*, pages 39–46. Springer, 2011.

A. E. Renshaw and S. Haberman. A cohort-based extension to the lee–carter model for mortality reduction factors. *Insurance: Mathematics and economics*, 38(3):556–570, 2006.

S. Richards. Applying survival models to pensioner mortality data. *British Actuarial Journal*, 14(2):257–303, 2008.

S. Richards and I. Currie. Longevity risk and annuity pricing with the lee-carter model. *British Actuarial Journal*, 15(2):317–343, 2009.

S. J. Richards, I. D. Currie, T. Kleinow, and G. P. Ritchie. Longevity trend risk over limited time horizons. *Annals of Actuarial Science*, 14(2):262–277, 2020.

V. Russo, R. Giacometti, and F. J. Fabozzi. Intensity-based framework for surrender modeling in life insurance. *Insurance: Mathematics and Economics*, 72:189–196, 2017.

S. Sanders. Changing trends in mortality: a cross-uk comparison, 1981 to 2016. Technical report, Office for National Statistics, 2018.

P. Shi, X. Feng, and A. Ivantsova. Dependent frequency–severity modeling of insurance claims. *Insurance: Mathematics and Economics*, 64:417–428, 2015.

X. Shiqing. The working mechanism and pricing formula for longevity swap. *Securities Market Herald*, page 02, 2015.

K. S. Tan and C. Weng. Empirical approach for optimal reinsurance design. *North American Actuarial Journal*, 18(2):315–342, 2014.

O. Vasicek. An equilibrium characterization of the term structure. *Journal of financial economics*, 5(2):177–188, 1977.

R. Verlaak and J. Beirlant. Optimal reinsurance programs: an optimal combination of several reinsurance protections on a heterogeneous insurance portfolio. *Insurance: Mathematics and Economics*, 33(2):381–403, 2003.

S. Wang. Ordering of risks under ph-transforms. *Insurance: Mathematics and Economics*, 18(2):109–114, 1996.

S. S. Wang. A universal framework for pricing financial and insurance risks. *ASTIN Bulletin: The Journal of the IAA*, 32(2):213–234, 2002.

A. A. Wanyama. Hedging longevity risk using longevity swaps. 2018.

Y. Wu and X. Liang. Vasicek model with mixed-exponential jumps and its applications in finance and insurance. *Advances in Difference Equations*, 2018(1):1–15, 2018.

M. E. Yaari. Uncertain lifetime, life insurance, and the theory of the consumer. *The Review of Economic Studies*, 32(2):137–150, 1965.

X. Zeng and S. Luo. Stochastic pareto-optimal reinsurance policies. *Insurance: Mathematics and Economics*, 53(3):671–677, 2013.